Compositional studies of cartilage matrix using NMR spectroscopy

by

Leann Marie Lesperance

B.S.E. Marquette University (1985)
M.S.E.E. Marquette University (1987)

SUBMITTED TO
THE HARVARD - MASSACHUSETTS INSTITUTE OF TECHNOLOGY
DIVISION OF HEALTH SCIENCES AND TECHNOLOGY
IN PARTIAL FULFILLMENT OF THE REQUIREMENTS FOR THE DEGREE OF

DOCTOR OF PHILOSOPHY

at the

Massachusetts Institute of Technology

September 1993

Signature of Author_____
Harvard-Massachusetts Institute of Technology
Division of Health Sciences and Technology
July 29, 1993

Certified by_____
Martha Gray
Thesis Supervisor

Certified by_____
Deborah Burstein
Thesis Supervisor

Accepted by_____
Roger G. Mark
Chairperson, Graduate Committee

Compositional studies of cartilage matrix using NMR spectroscopy

by
Leann Marie Lesperance

Submitted to the Harvard-Massachusetts Institute of Technology Division of Health Sciences and Technology on July 29, 1993 in partial fulfillment of the requirements for the degree of Doctor of Philosophy in Medical Engineering

ABSTRACT

Cartilage is a dense connective tissue which functions as a load bearing material in synovial joints and provides a smooth surface for joint articulation. It is composed of a highly charged solid phase (the extracellular matrix), an electrolyte fluid, and relatively few cells. Many of the structural and functional properties of cartilage are dependent on the two major constituents of the extracellular matrix: glycosaminoglycans and collagen.

The goal of this project was to develop NMR spectroscopy techniques to provide nondestructive and noninvasive determinations of cartilage structural and functional integrity. As described below, sodium NMR was used to measure sodium content of cartilage from which fixed charge density (FCD) was calculated, giving an estimate of glycosaminoglycan content. Magnetization transfer NMR was used to evaluate collagen content and structure. These techniques were verified and then used to study changes in matrix composition following perturbations which mimic physiologic and pathophysiologic states.

Because glycosaminoglycans (GAGs) have a net charge under physiological conditions, GAG concentration in the tissue is directly related to tissue fixed charge density (FCD). In turn, FCD is a determinant of the concentration of sodium in tissue water. The NMR method of determining GAG concentration involves detection of the NMR signal from sodium nuclei (the magnitude of this signal is directly proportional to the number of sodium ions in the sample). Sodium concentration is calculated from sodium and water content. GAG concentration can then be calculated using Donnan equilibrium theory. We have verified the NMR visibility of sodium in cartilage by comparison of sodium measured by NMR to sodium measured by inductively coupled plasma emission spectroscopy. Using NMR sodium measurements in calf articular cartilage, we have calculated FCD on the order of that measured using other techniques. For calf epiphyseal cartilage, FCD varied with the position of the sample within the tissue, in a manner consistent with tissue GAG content determined using a biochemical assay. Preliminary NMR images of intact ulnar epiphyseal cartilage demonstrated similar variations in sodium content. NMR measurements for cartilage exposed to baths of differing salt composition, pH, or ionic strength demonstrated the ability of this technique to track changes in tissue sodium content. FCD was also observed to decrease when cartilage was depleted of GAGs by exposure to trypsin. These results demonstrate the ability of sodium NMR to nondestructively measure FCD in cartilage and to follow changes in FCD with changes in matrix charge and composition.

To examine collagen, an NMR experiment known as magnetization transfer (MT) was performed. With a type of MT known as saturation transfer, the protons on macromolecules are perturbed with a radiofrequency pulse until the magnetic moments are randomized. These protons are then given time to exchange magnetization with bulk

water protons, leading to a randomization of the magnetic moments in the water. Observation of the water signal at this point results in less signal relative to the case without MT. The amount of relative signal decrease, expressed as Ms/Mo, provides an indication of the amount of macromolecules present and of the interaction between macromolecular and water protons. MT experimental parameters were characterized for collagen suspensions and cartilage. Based on these results, the saturation pulse length in subsequent experiments was chosen to be at least 5T1 (typically 12 sec for cartilage, 16 sec for collagen model systems), saturation pulse power was 12 μT (set with 1 msec 180 degree pulse), and frequency offset was 6 kHz. Ms/Mo did not change significantly in samples after freezing. Repeated measurements of Ms/Mo on the same sample varied by less than 5% (SD/mean). We have shown that the MT effect is dependent on collagen concentration in collagen suspensions, collagen gels, soluble collagen suspensions, and cartilage, with an approximately logarithmic relationship. However, at concentrations on the order of those seen *in vivo*, MT is relatively insensitive to changes in concentration. In addition, we have demonstrated that factors other than concentration affect the MT signal in collagen suspensions and cartilage. For example, Ms/Mo was ~20% greater for highly crosslinked insoluble collagen suspensions than for soluble suspensions of equal collagen content. Ms/Mo also varied among cartilage from different sources with similar collagen content. We have shown that an intact triple helix is important for MT; loss of the triple helix with thermal denaturation of soluble collagen suspensions resulted in substantially increased Ms/Mo. Furthermore, treatment with enzymes or low pH led to measurable differences in Ms/Mo which were not explained by differences in collagen concentration. They may be attributable to changes in matrix charge, structure and/or collagen fibril hydration (although changes in fibril hydration with trypsin and low pH produced conflicting results). These data demonstrate the ability of MT to detect changes in collagen concentration and collagen structure.

Osteoarthritis is a degenerative disease of cartilage, particularly common among the aging population, which results in diarthrodial joint failure. The ability to fully understand the disease and formulate sensible preventive and therapeutic strategies has been hampered by the inability to assess the *in vivo* functional status of cartilage. Clinical diagnosis of degenerative diseases like osteoarthritis is typically only possible once the disease has progressed to some advanced state in which gross structural changes have occurred. We have shown that sodium and magnetization transfer NMR can be used to study cartilage matrix composition, specifically the glycosaminoglycan and collagen constituents. In the future, these techniques should be applicable in a clinical setting for early diagnosis and monitoring progression of degenerative diseases.

Thesis Supervisors:

Martha L. Gray, Ph.D.
J.W. Kieckhefer Associate Professor of Electrical and Medical Engineering
Department of Electrical Engineering and Computer Science
MIT and Harvard-MIT Division of Health Sciences and Technology

Deborah Burstein, Ph.D.
Associate Professor of Radiology
Beth Israel Hospital
Harvard Medical School

Members of Thesis Committee

Martha L. Gray (chairperson)
J.W. Kieckhefer Associate Professor of Electrical and Medical Engineering
Department of Electrical Engineering and Computer Science, MIT
Harvard-MIT Division of Health Sciences and Technology

Deborah Burstein
Associate Professor of Radiology
Department of Radiology,
Beth Israel Hospital and Harvard Medical School
Harvard-MIT Division of Health Sciences and Technology

Alan J. Grodzinsky
Professor of Electrical, Mechanical, and Bioengineering
Department of Electrical Engineering and Computer Science, MIT
Harvard-MIT Division of Health Sciences and Technology

Solomon R. Eisenberg
Associate Professor of Biomedical and Electrical Engineering
Department of Biomedical Engineering,
Boston University

ACKNOWLEDGMENTS

I left these pages until the end because the experimental details seemed more urgent. Yet in the final analysis, nothing is more important. None of this work would have been possible without the support of all the people mentioned below and the others whom I'll forget to thank in my haste to turn this document over to the proper authorities.

First I would like to thank my advisors, Martha and Debbie, for years of support and encouragement. They taught me about NMR and about cartilage, but more importantly they taught me to believe in myself. They have been incredibly enthusiastic about this project and about my role in it. But they have also been positive role models for me, getting engaged, married, having children, and keeping a sense of humor, all while juggling the rigorous demands of academic life. Yet they managed to save more than a few hours to talk with me about work or life or whatever. In addition, I should thank Dickie, Drew, Mark, and Aviva for the hours I kept Martha and Debbie from them. Although my six year tenure as a graduate student at MIT has been filled with ups and downs, the overall experience has been fruitful, educational, and enjoyable, in large part due to Martha and Debbie, and for them I am truly thankful.

I would also like to thank the other members of my committee, Al and Sol, for their assistance with this project. They have been generous with helpful ideas and comments, participated in many long committee meetings, read many drafts of abstracts, papers, and this thesis, and are also positive role models in balancing family and career.

Numerous other individuals contributed to the experiments discussed in this thesis. Lee Gehrke provided the IL-1 for the degradation experiments. Jill Urban and Alice Maroudas gave us many helpful comments over the years and analyzed some of our samples for comparison of fixed charge density. Lou Gerstenfeld helped set up the hydroxyproline analysis. David Eyre listened to my naive questions about collagen and provided excellent feedback on the magnetization transfer experiments. Many of his suggestions will appear in future theses from this lab! Bill Landis also eagerly listened to a discussion of the MT data and shared his thoughts on collagen. Olena Jacenko and Jim San Antonio spent a few hours giving me their thoughts on collagen, too. Dr. Donald Reilly from the Beth Israel Hospital provided the post-operative pathologic human samples and several pathology residents dealt with my efforts at procuring those samples.

My introduction to laboratory life at MIT came from the Continuum Electromechanics Group. Paul Grimshaw and Eliot Frank probably answered more questions during my years at MIT than anyone; correctly, too! One of the three bikes in my basement is due to an infection with their particular brand of cycle-mania. I don't think I've ridden that bike since my ride to the cape! Minerva Garcia shared the office with me but she also shared her friendship. Young-Jo Kim and Bob Sah gave me a similar mix of advice and friendship.

Brent Foy taught me much of what I know about NMR and spent many hours teaching me the tricks of the trade. Recently, PV Prasad has helped me learn more about magnetization transfer. Finishing up this thesis would not have been half as fun if I hadn't been going through it with Kathleen Donahue. Whenever either of us said we would "never finish," the other would jump and say "yes, you will!"

Eric Fossel answered many questions and asked a few unanswerable ones himself. Lunches were never long enough when shared with Chris Brosnihan, Nishan Mahendran, Cathy Sanders, and Christine Zanella. I also spent many enjoyable hours with Audrey Hartman, Rob Gipe, and Chitra Raman.

Ann Black and Steve Gladstone gave me technical assistance whenever I needed it. Steve also helped motivate me to finish this thesis with his reverse "you'll never finish" psychology. It was well worth the five dollar bet I lost to him. Administrative tasks were made easier by Linda Bragmann, Jackie Solberg, and Christine Holbrook. They were also more fun because Linda, Jackie and Christine were always willing to share a joke or listen to my latest story.

Everyone in HST has been helpful from day one. The friendliness and cheerfulness all began with Almena Palombo who remembered my name after meeting me once and then continued with Roger Mark, Gloria McAlvenia and her never-empty candy jar, Barbara Jaskela, Keiko Oh, Carol Campbell, Sally Mokalled, and Ron Smith.

I can not thank Patty Cunningham enough for everything! We have talked, listened, laughed and cried. I am so glad to be continuing my education in HST because it means another two years to hang out in Patty's office!

I would like to thank my roommate Jon Come who took the EM photos of collagen, answered my chemistry questions, gave me tons of late night rides home and worried about me a lot. I also thank my other roommates, Scott Jaynes, King Taft, Mike Strange, Alexe Page, and Sandy Gould for meals and conversations shared.

My life has been richer by far because of the friends I have made. Tom Mullen has kept me laughing (and singing) for years. Steve Blacker understands me perhaps better than anyone in this world. Michelle Guyton, Brian Benda, and Tobi Nagel have "been there" for me time and time again. And then there are the friends I have made through the Paulist Center 6pm music group who have given me love and encouragement, especially this last year: Cathy Ford, John and Janet Moreland, Joe Richard and Rene Morrissette, Pat Wilkinson and Annie Foley, Diane and Paul Morruzzi, Julie and Jim Buras Zigo, Maggie McCarthy and Gordon Woode, Jim Haungs and Joe Cambone, Jacqui Paradis and Joe Haungs, David and Carolyn Ward, Bob Siefert and Maureen Shea, and Mark and Jane Widzinski. I have to thank Richard Davis and Viki Vasquez (the thesis police) separately because it would make them too nervous to be included with that big Catholic bunch!

Most of all, I thank my family and my friend Drew, for their love and support. My parents have always encouraged me to follow my dreams. They have been supportive of my academic endeavors even though none of my degrees has yet resulted in gainful employment. My step-parents, Len and Jackie, my sister Kelly and her family, and my grandma Charlotte have been equally encouraging. Drew had the courage to enter into a relationship with me during the last six months of this thesis, which was no easy task. Whenever I called, he always had a smile or cheery word to brighten my day. He also provided technical (Mac) support in addition to the emotional support. I owe him my deepest gratitude.

I would like to express my gratitude for fellowships received from the National Science Foundation, the Fred M. Roddy Foundation, and Clement Vaturi. This project was funded in part by grants from NIH, the JW Kieckhefer Foundation, Procter and Gamble Company, DePuy Company, and the Johnson and Johnson Research Fund.

In loving memory of Ed Gaudiano,
Trudy Paradis and Zachary Deskur

Table of Contents

List of Figures

List of Tables

INTRODUCTION

Cartilage is a dense connective tissue which performs several functions in the human body. For example, epiphyseal cartilage serves as the primordial tissue of long bones while articular cartilage acts as a load bearing material in synovial joints and between vertebral bodies. Cartilage is composed of a highly charged solid phase known as the extracellular matrix (ECM), electrolyte fluid, and relatively few cells (Stockwell and Meachim 1979). The major constituents of cartilage ECM include collagen type II fibrils (50-60% of dry weight), large aggregating proteoglycans, small proteoglycans, and a variety of noncollagenous proteins (Heinegard and Oldberg 1989, Meachim and Stockwell 1979). The collagen and proteoglycan molecules contain sulfate, carboxyl, and amino groups which are ionized under physiologic conditions. With nearly equal numbers of anionic and cationic groups, collagen contributes little to the net matrix charge. In contrast, the glycosaminoglycan (GAG) side chains of the proteoglycans contain up to two anionic groups per disaccharide subunit and thus provide a net negative charge to the matrix. This net matrix charge, referred to as fixed charge density (FCD), in adult articular cartilage has been reported to be on the order of 0.2 moles of negative charge per liter tissue water (Maroudas 1979, Grodzinsky 1983).

Many of the biomechanical and chemical properties of cartilage are dependent on the constituents of the ECM (Grodzinsky 1983, Frank 1990). Proteoglycans provide elasticity and stiffness on compression due to electrostatic repulsion of their abundant negative charges. FCD may be important to cartilage for its cellular activity. The ionic composition of the intratissue fluid surrounding the chondrocytes is determined in part by the FCD in a manner consistent with electroneutrality and Donnan equilibrium. Furthermore, compression-induced changes in mobile ion composition provide one mechanism by which cells may sense and respond to an applied load. Collagen is believed to help immobilize proteoglycans within the tissue and provides tensile and shear strength to the tissue.

Osteoarthritis (OA) is a degenerative disease of cartilage, particularly common among the aging population, in which diarthrodial (movable, synovial-lined) joints fail (Grushko 1989, Brandt and Kovalov 1991). The ability to fully understand the disease and to formulate sensible preventive and therapeutic strategies has been hampered by the inability to assess the functional status of cartilage *in vivo*. Advances in image resolution

for magnetic resonance imaging, computed tomography, and arthroscopy now make possible the diagnosis of many cartilage lesions and structural abnormalities. However, for degenerative cartilage diseases like OA, diagnosis is typically only possible once the disease has progressed to some advanced state in which gross structural changes have occurred. In fact, for most degenerative diseases there is not a definitive diagnostic test, but rather a list of clinical criteria. The diagnosis of osteoarthritis is made from a combination of clinical, radiologic, and laboratory findings.

Advanced degenerative joint disease is routinely evaluated using weight-bearing radiography of the knee. Joint space narrowing (JSN) generally, but not always, reflects loss of articular cartilage. In a recent study of 161 patients at a sports medicine clinic who complained of chronic knee pain, weight-bearing radiographic evidence of JSN was not a confident predictor of the condition of the articular cartilage as assessed by arthroscopy (Fife 1991). In this study, Fife et al concluded that in patients with radiologically mild OA, serial measurement of joint space width could not confidently be used to assess the efficacy of a therapeutic intervention. Despite the uncertainties, conventional radiography remains the mainstay for examination of patients with arthritis when combined with a physical examination, careful history, and laboratory data (Kaye 1990). The staging or progression of the disease is often followed by comparing recent with previous radiographs; however, small changes are difficult to detect.

Efforts are now being made to use magnetic resonance imaging (MRI) for the diagnosis of degenerative diseases such as osteoarthritis, particularly for the assessment of early degenerative changes. One group of investigators performed *in vitro* NMR studies on aspirated synovial fluid and minced joint tissues to investigate possible differences in proton relaxation times and mobile proton content between inflamed and noninflamed articular tissue (Baker 1985). They were unable to predict the amount of inflammation present or correlate values obtained for T1, T2, and proton content with a direct diagnosis but suggested that with further refinement, MRI might provide "superb images of articular soft tissue structures."

In the last several years, many studies have been performed on the clinical use of MRI in the evaluation of the knee. MRI has proven useful for characterizing meniscal tears and evaluating the articular surface (Burk 1986, Mink 1988) and for detecting surface lesions (Gylys-Morin 1987) and anterior cruciate ligament tears (Mink 1988).

Using an experimental model of surgically induced OA, one group obtained MR images of dog knees (Sabiston 1987). Meniscal changes, osteophytes, and capsular fibrosis were visualized; changes seen on MR images correlated positively and significantly with changes seen on gross pathological examination. Furthermore, these changes were detected on MR images up to eight weeks earlier than initial radiologic evidence of disease. The authors conclude that MRI offers improved visibility of earlier pathologic changes with OA that traditional radiography. This study, however, did not address the issue of detection of the earliest changes seen with OA, such as collagen structural damage, increased hydration, and proteoglycan loss.

While the etiologic event or agent for primary osteoarthritis has not been clearly defined, one major theory is based on biomechanical failure of the cartilage matrix. Much of the current research in the area of osteoarthritis pathogenesis involves animal models which alter the normal loading pattern of a joint and result in osteoarthritic changes to the cartilage. It has been hypothesized that the inciting event for osteoarthritis is structural damage to the collagen network (due to abnormal joint loading) which reduces its restraining force. The decrease in tensile strength allows increased swelling by the proteoglycans and thus, increased hydration (Maroudas 1973). Proteoglycans are then lost into the surrounding synovial fluid. Ultimately, both proteoglycan and collagen concentrations decrease. The resulting decrease in charge density (due to decreased proteoglycan concentration) further compromises the functional integrity of the tissue, leading to further loss of proteoglycans and eventual matrix degeneration.

Chemical analysis of osteoarthritic cartilage has shown reduction in total proteoglycan content and fixed charge density compared with normal cartilage (e.g. Matthews 1953, Mankin and Lippiello 1971, Venn and Maroudas 1977, Heinegård 1987, Inerot 1991). Additionally, the structure of the remaining proteoglycans has been shown to vary from those found in normal tissue. In a surgically-induced model of hip OA in dogs, proteoglycans in OA tissue were smaller than normal and had lost the ability to aggregate with hyaluronic acid (Inerot 1991). McDevitt and Muir (1976) found that proteoglycans were more easily extracted from osteoarthritic cartilage. Several studies have shown changes in the relative amounts of GAG constituents (chondroitin sulfate, keratan sulfate) in osteoarthritic cartilage compared to normal (Mankin and Lippiello 1971, McDevitt and Muir 1976, Venn and Maroudas 1977, Heinegård 1987). The GAG composition of OA tissue resembles that of immature cartilage. Thus, it has been suggested that the chondrocyte responds to excessive matrix degeneration by reverting to a more immature

form, effectively altering its pattern of matrix synthesis to resemble that of immature tissue. A comparison of aged versus osteoarthritic human tissue revealed that the changes which are observed with osteoarthritis are opposite those which occur during the normal aging process; fixed charge density increased in normal, aged samples but decreased in cartilage from osteoarthritic joints (Grushko 1989).

Increased water content has also been observed in osteoarthritic tissue. In one study of experimental dog OA (McDevitt and Muir 1976), water content was 73.0 ± 4.8% for osteoarthritic samples versus 68.0 ± 5.0% in the contralateral samples. In studies of the human femoral head, the mean water content for normals was around 70% while that for fibrillated specimens increased to around 80% (Venn and Maroudas 1977, Grushko 1989).

Since it is the charges on the GAGs which account for swelling of the tissue, it might seem that loss of proteoglycans would result in decreased water content, rather than the observed increased water content. However, in osteoarthritic tissue, the swelling forces exerted by the proteoglycans are not adequately restrained by the damaged collagen network. Proteoglycans are therefore free to imbibe greater amounts of water. Eventually, the decreased charge density seen with increased hydration (and loss of proteoglycans) will decrease the tendency to swell. After a large fraction of proteoglycans is lost from the matrix, swelling would be expected to decrease. Therefore, as cartilage degeneration progresses, water content would first increase and then decrease. In fact, severely fibrillated cartilage has been shown to have a decreased water content when compared with cartilage from less severe stages of arthritis (McDevitt and Muir 1976).

Because proteoglycans are depleted and water content is increased in osteoarthritic tissue, one would expect to observe a decrease in the overall net matrix charge when expressed per tissue water. Studies conducted with radiotracers showed a significant reduction in fixed charge density of osteoarthritic tissue compared to normal (Maroudas 1973, Venn and Maroudas 1977, Grushko 1989). Maroudas et al (1973) further observed that the difference in fixed charge density between normal and osteoarthritic tissue was greater when expressed as charge per wet weight than as charge per dry weight.

Venn and Maroudas (1977) measured collagen content in normal and osteoarthritic femoral head cartilage; osteoarthritic samples had less collagen than normal cartilage

when expressed per wet weight. However, no significant difference in the collagen content was observed when normalized to dry weight. This suggests that total collagen as a proportion of total solid material is not decreasing but hydration is increasing. These authors note that one might not expect to see much change in collagen content since it is the predominant solid in cartilage, i.e. a small change may be difficult to detect biochemically.

In summary, the degeneration of cartilage is presumed to begin with alterations to the collagen structure resulting in decreased collagen structural integrity. In addition, osteoarthritic tissue has lower total proteoglycan content than normal tissue. Osteoarthritic tissue also has higher water content than normal, resulting in decreased proteoglycan and collagen concentrations. Therefore, early degenerative changes in cartilage may be detected by determination of collagen structural integrity or measurement of proteoglycan or collagen concentration, well before radiologic or other anatomic evidence is available.

Nuclear magnetic resonance (NMR) spectroscopy and magnetic resonance imaging (MRI) have the potential to evaluate cartilage integrity nondestructively and noninvasively. Specifically, sodium NMR may be used to estimate proteoglycan content and magnetization transfer NMR may be used to evaluate collagen content and structure.

Sodium NMR spectroscopy can be used to measure sodium content in isolated cartilage samples. With knowledge of tissue water content (determined from proton NMR spectroscopy or from the difference between wet and dry weights), sodium content can be converted to sodium concentration. Donnan equilibrium theory can then be used to calculate FCD from intratissue sodium concentrations. Since proteoglycans provide the dominant source of charge in cartilage, FCD is an indicator of proteoglycan content. Thus, sodium NMR can provide an estimate of proteoglycan content.

The magnetization transfer (MT) technique has been used to improve contrast in MR images of the knee (Wolff and Balaban 1989) and has recently been proposed as an NMR method for staging cartilage degeneration (Kim 1993). Kim et al had shown that the phenomenon of MT is specifically related to the collagen component of cartilage. This technique may provide an indication of the amount of collagen present and of its structural integrity.

The general aim of this project was to develop techniques using NMR spectroscopy which provide noninvasive and nondestructive *in vitro* determinations of cartilage structural and functional integrity. The work was divided into two parts: sodium experiments measuring proteoglycan content and magnetization transfer experiments evaluating collagen content and structure.

The first half of this thesis involves determination of proteoglycan content using sodium NMR. Specifically, we (1) verify the determination of FCD using sodium NMR, (2) investigate the influence of changing bath ionic composition, ionic strength, and pH on intratissue ion measurements and subsequent FCD calculations, (3) determine the degree to which the sodium measurement can be used to evaluate intact cartilage degradation and (4) extend this technique to an imaging mode.

The second half of this thesis involves the evaluation of the magnetization transfer technique for the determination of collagen content and/or structure. Specifically, we (1) characterize the MT experimental parameters, (2) examine the dependence of MT on collagen concentration or content, (3) examine the dependence of MT on collagen structure, and (4) determine the specificity with which MT can be used to evaluate cartilage degradation in intact cartilage samples.

The ability to fully understand degenerative joint diseases and formulate sensible preventive and therapeutic strategies has been hampered by the inability to assess the *in vivo* functional status of cartilage. Clinical diagnosis of degenerative diseases like osteoarthritis is typically only possible once the disease has progressed to some advanced state in which gross structural changes have occurred. We show that sodium and magnetization transfer NMR can be used to study cartilage matrix composition, specifically the glycosaminoglycan and collagen constituents. In the future, these techniques should be applicable to the clinical setting for early diagnosis and monitoring of degenerative diseases like osteoarthritis.

PART I SODIUM

SODIUM NMR

TO CALCULATE FCD AND

ESTIMATE PROTEOGLYCAN CONTENT

BACKGROUND

A. PROTEOGLYCANS

Proteoglycans are composed of glycosaminoglycan (GAG) side chains (chondroitin sulfate and keratan sulfate) covalently linked to a core protein (Rosenberg and Buckwalter 1986). Proteoglycan monomers are then assembled into large aggregates by association of the core protein and a link protein with a large hyaluronate backbone. It is the GAG side chains which contribute the large negative charge, containing up to two anionic groups per disaccharide subunit (one sulfate, or one carboxyl and one sulfate). Since the ionic charge groups are "fixed" to the solid matrix, the net charge per volume is referred to as the fixed charge density (FCD). FCD in adult articular cartilage and intervertebral disc has been reported to be on the order of 0.2 moles of negative charge per liter tissue water, ranging from -0.05 M to -0.35 M, depending on age and anatomical site (Grushko 1989, Maroudas 1969, Maroudas 1979, Maroudas and Thomas 1970, Phillips 1984, Urban and Maroudas 1979).

B. PROTEOGLYCANS IN CARTILAGE

For its function as a load-bearing material, articular cartilage relies heavily on the extracellular matrix (ECM). Many of the biomechanical properties of cartilage are dependent on the ECM charge. Proteoglycans provide elasticity and stiffness on compression (Kuettner and Kimura 1985). The high negative charge density of the proteoglycans exerts a swelling pressure of several atmospheres inside the tissue. When the tissue is compressed, as for example during walking, the charge density increases, therefore increasing the swelling pressure and resisting further compression. When the load is removed, the tissue imbibes water, restoring its original shape. Both direct and indirect evidence suggests that the equilibrium and dynamic compressive moduli decrease with decreasing FCD (Eisenberg and Grodzinksy 1985, Frank 1987). In adult bovine articular cartilage, electrostatic interactions between fixed charge groups provide 50% of the tissue equilibrium compressive stiffness (Eisenberg 1983).

Proteoglycans also affect solute concentrations within the tissue. The ionic composition of the intratissue fluid is determined, in part, by tissue FCD in a manner consistent with Donnan equilibrium (Maroudas 1979). Because of the net negative charge on the matrix,

cations (e.g. Na^+, H^+, Ca^{2+}) are at higher concentrations within the tissue relative to surrounding solutions (e.g. synovial fluid or blood), while anions (e.g. Cl^-, HCO_3^-) are relatively dilute. The high concentration of proteoglycans may also retard the diffusion of larger molecules (Kuettner and Kimura 1985). Diffusion effects are significant for cartilage since it is relatively avascular and relies on diffusion for nutrition and waste removal.

The influence of proteoglycans and thus, tissue FCD on intratissue fluid flow and ion content may have important biochemical and cellular consequences. For instance, hyaluronate binding properties of proteoglycans are dependent on intratissue pH (Sah 1990), and cell synthesis of matrix macromolecules is sensitive to pH (Gray 1988), sodium concentration (Urban and Bayliss 1989), and water content (Schneiderman 1986). Experimental evidence suggests that changes in intratissue fluid ionic composition resulting from compression-induced changes in FCD may provide a mechanism by which cells sense and respond to mechanical load (Gray 1988, Schneiderman 1986, Urban and Bayliss 1989). In addition, when cartilage is compressed, as would occur during walking, the intratissue fluid is expelled from the tissue. The separation of mobile counterions from the fixed matrix charge then results in the establishment of an electric potential referred to as an electrical streaming potential. The streaming potential has also been suggested as a possible mechanism for connective tissue growth and remodeling (Grodzinsky 1983).

Tissue hydration is also affected primarily by proteoglycans via bath (and therefore, intratissue fluid) pH and ionic strength (Grodzinsky 1983). The net charge on the ECM is a function of intratissue pH. Matrix carboxyl and sulfate groups become protonated at low pH, with intrinsic pK values reported to be around 3.5 for carboxyl and 2.0 for sulfate groups. Amino groups are affected at extremely basic pH; their pK is reported to be around 11 (Bowes and Kenten 1948a). Ultimately proteoglycans lose their charge (i.e. become less net negative) as pH decreases and collagen acquires a net positive charge. As the net matrix charge decreases at lower pH, intratissue swelling pressure and tissue hydration decrease. Ionic strength affects the electrostatic repulsion felt by adjacent negative charges. At low ionic strength, this repulsive force is greater since there are few counterions present to shield the charges. The tissue swells slightly, being constrained by the collagen fibrils. Although such extremes in bath pH and ionic strength are not seen *in vivo*, they are frequently used in research studies to provide information about matrix composition and structural interactions. Since it is related to matrix composition, tissue hydration can be considered to be an indicator of tissue health and is often measured in studies on degenerative disease (e.g. Maroudas 1969).

C. TECHNIQUES FOR MEASURING PROTEOGLYCAN CONTENT

Proteoglycan content is typically measured in the laboratory using biochemical techniques. Cartilage samples are isolated, digested, and then analyzed using an appropriate assay. Indirect assessments of proteoglycan content have also been established using nondestructive techniques which determine fixed charge density, since the matrix charge is determined predominantly by proteoglycans.

1. CHEMICAL DETERMINATION

Chemical analysis of solubilized tissue provides a destructive means of quantifying proteoglycan content by estimating the total number of available ionizable groups. For cartilage, the focus has been on determining GAG content through measures of total hexosamine (Antonopoulas 1964), uronic acid (Bitter and Muir 1962), or sulfated GAG (Farndale 1986). FCD is calculated from these measurements using estimates of molecular weight and charge of the measured species and independent measurements of tissue water content (e.g. Maroudas 1970).

2. NONDESTRUCTIVE TECHNIQUES

Several nondestructive techniques have been reported for quantifying proteoglycan content by measuring tissue FCD, including titration, radiotracer, and streaming potential methods. Phillips (Phillips 1984, Frank 1990) estimated the FCD of adult bovine articular cartilage using a titration method wherein thin (200 μm) slices of tissue were bathed in NaCl solutions and allowed to equilibrate after each of several quantitative additions of HCl or NaOH to the bathing medium. Using measurements of the resulting equilibrium bath pH, the known titration behavior of water, an independent measure of tissue isoelectric point, and Donnan theory, tissue FCD at physiological pH was computed to be in the range of -0.2 to -0.25 M.

Using ion exchange theory, Maroudas (Maroudas 1970, Maroudas 1969) described a means for computing FCD from independent measurements of streaming potential, specific conductivity, and hydraulic permeability. FCDs thus computed for adult articular cartilage specimens were found to agree within 10% to estimates based on chemical measures of hexosamine and hexuronic acid content (Maroudas 1969).

Perhaps the most technically straightforward of the techniques for measuring the FCD of intact tissue is the radiotracer method. Here the tissue is equilibrated in an electrolyte solution (typically NaCl) containing trace quantities of radioactive ion(s) such as ^{22}Na or ^{36}Cl. Intratissue sodium and/or chloride content is determined from ^{22}Na and/or ^{36}Cl measurements. Using Donnan theory and a separate measure of water content, tissue FCD can be calculated (see Theory section). Maroudas and Thomas (1970) found that the FCDs estimated using radiotracer techniques were within 9% of chemical determinations.

While the above techniques have contributed greatly to *in vitro* studies of the ionic properties of cartilage, none is applicable to the study of intact heterogeneous specimens or *in vivo* systems. Nuclear magnetic resonance (NMR) spectroscopy and imaging have the potential to enable nondestructive determinations of FCD. Several ions, including sodium, lithium, potassium, and chloride, have net magnetic moments and are observable by NMR. Therefore, intratissue ion concentrations can be determined with this technique. Sodium NMR spectroscopy may be used to measure sodium content in isolated cartilage samples. With knowledge of tissue water content (determined from proton NMR spectroscopy or from wet and dry weights), sodium content can be converted to sodium concentration. FCD can then be calculated from these ion concentrations using electroneutrality and ideal Donnan theory.

The basic technique is applicable to heterogeneous samples, living tissue, and *in vivo* systems. The objective of the studies reported here were to verify the use of sodium NMR for determination of FCD in cartilage and to use this technique to study changes in matrix composition in response to various interventions which mimic physiologic and pathophysiologic states.

THEORY

A. GENERAL NMR THEORY

The following introduction to NMR theory is taken primarily from Carrington and McLachlan (1967), Farrar (1989), and Edelman and Hesselink (1990). For further details, the reader is referred directly to these texts or to more advanced texts such as Slichter (1980).

All nuclei which have either an odd number of protons or an odd number of neutrons (or both) possess the property of spin. Spin angular momentum is represented as a vector with magnitude $\mathbf{I}\hbar$, where $\hbar$ is Planck's constant divided by 2π. $\mathbf{I} = 0$ corresponds to nuclei with even mass numbers (sum of the number of protons and neutrons) and even numbers of protons; nuclei with even mass numbers but odd numbers of protons have **I** values which are integral multiples of 1. For nuclei with an odd mass number, **I** takes on values which are odd integral multiples of 1/2 (1/2, 3/2, etc.). Because these nuclei possess both spin and charge, they have a nuclear magnetic moment μ_N which is proportional to the magnitude of the spin with the constant of proportionality called the gyromagnetic (or magnetogyric) ratio, γ:

$$\mu_N = \gamma \hbar \mathbf{I} \tag{1}$$

The gyromagnetic ratio is measured in units of radians sec^{-1} $gauss^{-1}$ or MHz $tesla^{-1}$.

According to the theory of quantum mechanics, the allowable nuclear spin states are quantized such that the nuclear spin vector in any one direction (referred to as the nuclear spin quantum number, m) may have only one of a discrete set of values, namely $m = +\mathbf{I}$, $(\mathbf{I}\text{-}1)$, ..., $-(\mathbf{I}\text{-}1)$, $-\mathbf{I}$. Therefore when the nuclear magnetic moment interacts with the an applied magnetic field, the nucleus has $(2\mathbf{I} + 1)$ equally spaced energy levels where the spacing between energy levels is given by:

$$\Delta E = \frac{\mu B_0}{\mathbf{I}} \tag{2}$$

with B_0 being the applied magnetic field. For a spin 1/2 nucleus such as proton, m takes on values of +1/2 and -1/2.

The state m = +1/2 corresponds to a situation in which the spins and an applied magnetic field are parallel. The state m = -1/2 represents the situation in which the spins and applied magnetic field are antiparallel. Thus the state m = +1/2 has a lower energy than the state m = -1/2. For an ensemble of protons interacting with a magnetic field B_0 at temperature T, the distribution of protons between the +1/2 and -1/2 spin states is governed by Boltzmann's law:

$$\frac{N_{+1/2}}{N_{-1/2}} = e^{-\Delta E/kT} \tag{3}$$

where N represents the number of spins in each state and ΔE is a function of B_0 (see equation 2). At ordinary room temperature and for typical applied fields on the order of 1-10 tesla, there is only a slight excess of protons aligned in the lower energy state ($\sim 1:10^6$). Further discussion will deal only with these excess nuclei since we are interested in the net magnetic moment to which the others do not contribute.

In addition to aligning with or against the field, the individual magnetic moments also precess about the applied field with random phase at a frequency proportional to the strength of the magnetic field according to the following equation:

$$\omega_0 = \gamma B_0 \tag{4}$$

where ω_0 is called the Larmor or resonant frequency. Since the phases of the spins are randomized in the xy plane, the net magnetization from this population of magnetic moments is along the z axis (where z is defined as the direction of the magnetic field).

B. SPECIFIC NMR EXPERIMENTS

1. ONE PULSE

In the presence of a static magnetic field, a net magnetization is developed along the direction of the field, defined here as z. There is no net magnetization in the xy plane due to the random phase of the individual precessing magnetic moments. In the one pulse

NMR experiment, a radiofrequency (rf) magnetic field is applied perpendicular to the static field for a short period of time (an rf "pulse"). This rf pulse is oscillating at the Larmor frequency. At this frequency, stimulated transitions occur (the resonance condition) and some nuclei change their orientation with respect to the applied static field. In addition, the perpendicularly applied rf pulse will induce a phase coherence. In other words, the projections of the individual magnetic moments onto the xy plane will be aligned (but still spinning with angular frequency ω_0). The net magnetization vector (the sum of the individual magnetic moments) is therefore tipped off the z axis and precesses around the z axis with frequency ω_0.

The angle by which the net magnetization vector is rotated off the z axis is referred to as the flip angle. The flip angle increases with the strength and duration of the rf pulse. The relationship between the duration of the rf pulse and the angle by which the net magnetization vector is tipped from the z axis is described by:

$$\theta = \omega_1 t_p = \gamma B_1 t_p \qquad (5)$$

where B_1 is the strength of the field of the rf pulse and t_p is the pulse duration. If the rf pulse has the appropriate strength and duration to tip the net magnetization vector entirely into the xy plane, it is referred to as a 90 degree pulse. In this case, an equal number of nuclei will be precessing parallel as are precessing antiparallel to the applied static field.

The time varying magnetization in the xy plane as the nuclei return to their steady state conditions induces a signal in a pickup coil (Figure 1A). This signal is referred to as a free induction decay (FID). The initial intensity of the FID is proportional to the number of nuclei in the sample. In practice, the number of nuclei is determined by integrating the area under the curve of the Fourier transform of the FID which is equal to the initial FID intensity (Figure 1B) and calibrating the system to a known standard. The time constant for the return to random phase and consequently for the decay of the xy magnetization (and hence the detected signal) is referred to as T2. The time constant for total recovery of the magnetization vector along the z axis is referred to as T1.

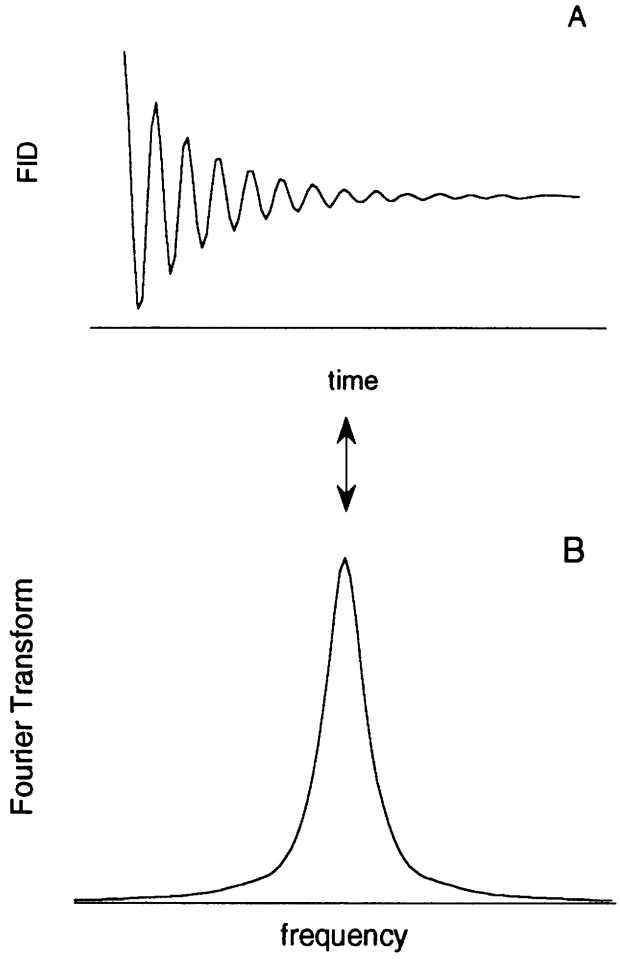

FIGURE 1 A) Free induction decay (FID) and B) Fourier transform of FID. Area under transform curve (B) is equal to initial intensity of FID.

2. T1 RELAXATION

T1, the spin-lattice relaxation time, describes the recovery of the net magnetization vector along the z axis after being tipped into the xy plane. The inversion recovery sequence is most commonly used to measure T1:

$$180^\circ - \tau - 90^\circ - \text{acquire} \tag{6}$$

The return to equilibrium after the 180 degree pulse is described by the following equation with time constant T1:

$$I(\tau) = I(0)\,(1 - 2\,e^{-\tau/T1}) \tag{7}$$

At equilibrium, the net magnetization vector lies along the +z axis; after a 180 degree rf pulse, it is rotated 180 degrees so that it lies along the -z axis. The z component of the magnetization will gradually return to equilibrium, passing through zero along the way. At time τ, a 90 degree pulse is applied which tips whatever z component is present so that it lies in the xy plane. At this point the signal is acquired. This sequence is repeated for various values of τ. T1 is determined by fitting the data to equation 7.

3. T2 RELAXATION

T2, the spin-spin relaxation time, describes the loss of magnetization in the xy plane by the return of the individual magnetic moments to random phase. This relaxation process is characterized by the following equation:

$$I(\tau) = I(0)\,e^{-\tau/T2} \tag{8}$$

Ideally, T2 relaxation would be reflected in the decay of the FID by its exponential envelope. However, the time constant which describes the actual observed decay of the FID is referred to as $T2^*$. This constant takes into account relaxation which occurs due to magnet inhomogeneities: slight variations in field strength result in the precession of the nuclei at slightly different Larmor frequencies. The individual magnetic moment vectors can be pictured as dephasing in the xy plane with some precessing faster, some slower than others. Thus, the phase coherence established by the rf pulse is lost.

The value of T2 is typically measured using a Hahn spin-echo experiment:

$$90^\circ - TE/2 - 180^\circ - TE/2 - \text{acquire} \qquad (9)$$

In this experiment, two pulses are given separated by some time TE/2 where TE stands for echo time. The first 90 degree pulse flips the net magnetization vector into the xy plane. During the ensuing interval of time, TE/2, the spins lose some of their phase coherence due to local field inhomogeneities as described above and some due to inherent T2 relaxation processes. A 180 degree pulse then inverts the spins about the x or y axis so that after another delay of TE/2, an echo is detected as the spins refocus. Any decay in the magnitude of the net magnetization vector at the time of this echo is due to inherent relaxation processes in the system and not to static magnet inhomogeneities. It is assumed that the spatial distribution of inhomogeneities is such that diffusive motion of nuclei is not sufficient to alter the field experienced by an individual nucleus over the time TE. The experiment is repeated for multiple values of TE to determine a value for T2 using equation 8.

4. IMAGING

In NMR imaging experiments, magnetic field gradients are used to encode the signal as a function of spatial position in the sample. Therefore, the local concentration of a given nucleus can be obtained.

C. FCD CALCULATION

For a homogeneous tissue, FCD can be calculated from measurements of intratissue ion concentrations. Whether ion concentrations are measured using NMR, radiotracers (Maroudas and Evans 1972, Maroudas and Thomas 1970), or some other technique, the theory used for calculation of FCD is equivalent. It is reviewed briefly here.

Consider first the simple system of tissue bathed in NaCl. Let the subscript **t** represent the tissue and the subscript **b** represent the bath.

Electroneutrality requires that:

$$[Na^+]_t - [Cl^-]_t + FCD = 0 \quad (10)$$

$$[Na^+]_b - [Cl^-]_b = 0 \quad (11)$$

In situations where both $[Na^+]_t$ and $[Cl^-]_t$ can be determined and bath concentrations are known, FCD can be computed directly from equation 10.

The assumption of electrochemical or Donnan equilibrium across the tissue/bath interface requires that:

$$(\gamma_t)^2 [Na^+]_t [Cl^-]_t = (\gamma_b)^2 [Na^+]_b [Cl^-]_b \quad (12)$$

where γ is the mean ionic activity coefficient.

In the case of ideal Donnan equilibrium, $\gamma_t = \gamma_b$ such that:

$$[Na^+]_t [Cl^-]_t = [Na^+]_b [Cl^-]_b \quad (13)$$

Equations 10, 11, and 13 can then be solved for FCD:

$$FCD = \frac{[Na^+]_b^2}{[Na^+]_t} - [Na^+]_t \quad (14)$$

$$FCD = [Cl^-]_t - \frac{[Cl^-]_b^2}{[Cl^-]_t} \quad (15)$$

With the assumption that ideal Donnan theory holds, equation 14 or 15 can be used to calculate FCD from a single measurement of tissue sodium or chloride concentration.

The theory can be extended to include multiple ions and multiple compartments. Equations used for the experiments described in this thesis are presented here for completeness.

In cases where bath contains NaCl and LiCl and either $[Na^+]_t$ or $[Li^+]_t$ is measured:

$$FCD = \frac{[Na^+]_b[Cl^-]_b}{[Na^+]_t} - [Na^+]_t\left(1 + \frac{[Li^+]_b}{[Na^+]_b}\right) \tag{16}$$

$$FCD = \frac{[Li^+]_b[Cl^-]_b}{[Li^+]_t} - [Li^+]_t\left(1 + \frac{[Na^+]_b}{[Li^+]_b}\right) \tag{17}$$

In cases where bath contains NaCl at low pH, such that $[H^+]$ is significant and $[Na^+]_t$ is measured:

$$FCD = \frac{[Na^+]_b[Cl^-]_b}{[Na^+]_t} - [Na^+]_t\left(1 + \frac{[H^+]_b}{[Na^+]_b}\right) \tag{18}$$

METHODS

A. NMR METHODS

The intensity of the NMR signal or the area under the resonance curve is proportional to the number of nuclei in the sample. With proper system calibration and sample volume determination, the concentration of the nucleus under study can be determined. NMR calibration curves were made from measurements of ionic solutions of known concentration and volume. Resonance areas obtained from ions in tissue were compared to calibration curves to obtain absolute ionic content. After completion of all measurements, the cartilage was lyophilized and weighed. Water content was computed as the difference between wet and dry weights (1 g = 1 mL). The ionic content was then normalized to tissue water content to yield intratissue ion concentrations:

$$[\text{ion}] = \frac{\text{ion content determined by NMR}}{\text{tissue water content}} \qquad (19)$$

Preliminary experiments (Figure 2) confirm that, under the conditions of these experiments, water content can also be determined nondestructively by measuring the water proton peak in the proton NMR spectrum. Henceforth, the computation of ion concentration from two measurements (equation 19) will be referred to as the NMR measurement of an ion concentration.

NMR spectroscopy experiments were performed on an 8.45 tesla Bruker AM spectrometer (Bruker Instruments, Inc., Billerica, MA). A standard broadbanded probe was used for all experiments, with a radiofrequency coil diameter of 10 mm. Spectra were obtained with a 90° pulse sequence with 5T1 (where T1 is the longitudinal NMR relaxation time) between successive excitations to ensure total equilibration of the nuclei before the next pulse. T1 was measured in one cartilage sample using the standard inversion recovery pulse sequence and agreed with previous results (Foy 1989). The experimental parameters are given in Table 1. All experiments were performed at room temperature.

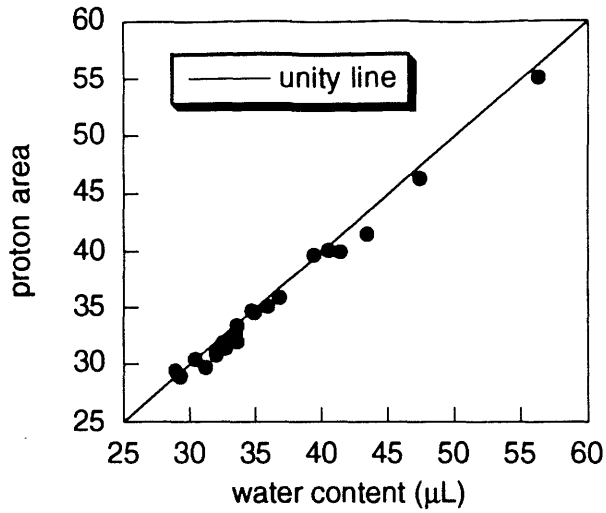

FIGURE 2 Cartilage water content determined from area of proton NMR spectra compared to water content determined from measurements of wet and dry weights.

In MR imaging experiments, magnetic field gradients are used to encode the signal as a function of spatial position in the sample to obtain the local concentration of a given nucleus. Imaging experiments were performed on a 4.7 tesla Bruker BIOSPEC, operating at 200.26 MHz for proton and 52.97 MHz for sodium. All images were obtained with the standard microimaging accessory with gradient coils of 5 cm diameter and dual H and Na radiofrequency coils with diameters of 25 and 20 mm, respectively. Specific imaging parameters are described later in Experimental Protocols.

Table 1 Parameters utilized for the NMR experiments. For each nucleus, the NMR resonant frequency is given, along with the measured T1, number of scans for signal averaging, and the total acquisition time (AQ) for a spectrum.

Nucleus	Freq (MHz)	Solution			Cartilage		
		T1 (sec)	number of scans	AQ (min)	T1 (sec)	number of scans	AQ (min)
H-1	360.13	3.38	8	2	1.76	8	1.5
Li-7	139.96	17.0	8	14	7.5	16	12
Na-23	95.26	0.056	2000	10	0.020	4000	7
Cl-35	35.29	0.030	2000	7	0.002	20000	7

B. CARTILAGE PREPARATION:

The types of cartilage used in these studies were: adult bovine articular cartilage (adult AC), calf (1-2 week old) articular cartilage (calf AC), and calf epiphyseal cartilage (EC). Intact foreleg (EC) and hindleg (calf AC) knee joints were obtained immediately after slaughter (A. Arena, Hopkinton, MA) or frozen (adult AC; City Packing, Boston, MA). Tissue was harvested from the femoropatellar groove (AC) or distal ulna (EC) according to previously established techniques to yield plane-parallel disks 0.8 to 1.0 mm thick and 6.4 to 9.6 mm in diameter (Eisenberg and Grodzinsky 1985, Gray 1988). In all cases tissue was stored at -20°C until later use.

At least 4 hr before an experiment, disks were thawed and equilibrated at 4°C in the desired bathing solution (>100 mL/disk). Unless otherwise indicated, solutions were pH 8 with 5 mM Tris buffer. After equilibration, each disk was taken out of its bathing solution, blotted dry, weighed and placed in a capped 10 mm NMR tube.

Cartilage samples used for compression studies were typically 5 mm in diameter and 2 mm in thickness. Samples were placed in a specially designed NMR-compatible device which allowed radially unconfined compression between two impermeable platens (Hartman 1991). The degree of compression was established by adjusting the spacing between the platens. Control studies confirmed that insignificant NMR signal was obtained from the compression device. After a new compressive load was applied, the sample holder (constraining the sample) was placed in a stirred bath for at least 90 min. Before NMR measurements were made, the sample holder was removed from the bath and thoroughly blotted dry, including the edges of the sample.

C. FCD CALCULATIONS

For most experiments, FCD was calculated from intratissue ion concentrations as measured by NMR using electroneutrality (equation 10) or from intratissue sodium concentrations using ideal Donnan theory (equation 14). Equations for experiments in which additional ions had to be considered are discussed in the Theory section.

EXPERIMENTAL PROTOCOLS

A. CONTROL STUDIES

1. CALIBRATION

To confirm the linear relationship between NMR signal and ion content, spectra were obtained for small volumes (30 - 100 μL) of 0 to 0.5 M NaCl or LiCl solutions. In order to verify that the NMR measurement of sodium content could be made in the presence of GAGs, 5% (w/w) chondroitin sulfate solutions were prepared with NaCl added to yield increases in $[Na^+]$ from 0 to 0.3 M. A 50 μL volume of each solution was placed in a pre-weighed NMR tube, weighed (to confirm volume measurement), and sodium content determined by NMR.

Several studies were conducted in order to determine whether measurements of ion content in tissue were equivalent to measurements of ion content in free solution (i.e. to determine if ions in cartilage are totally "visible" by NMR). Calf AC was equilibrated in 0.15 M or 0.2 M NaCl. Intratissue sodium and chloride content were measured by NMR. 400 - 600 μL of deionized distilled water was added directly to the NMR tube containing the cartilage sample so that the intratissue sodium and chloride would diffuse out of the tissue (ratio of tissue water to added water was approximately 1:10). (Small desorbing volumes were used in order that the total sample volume remain in the sensitive region of the NMR coil.) After 3 hr, sodium and chloride content were measured for the cartilage/water ensemble. Finally, the cartilage was removed from the water, blotted dry, and measured for remaining intratissue sodium and chloride content. Additional calf AC was initially equilibrated in 0.015 to 0.050 M NaCl and then desorbed with 0.15 M KCl. KCl was used as a desorbant rather than water in order to more effectively desorb the sodium. (For these samples $[Cl^-]$ was not determined.)

2. ICP ANALYSIS

Because complete desorption of sodium was not possible with the small volumes used in the desorption experiments described above, an independent technique was used to determine whether all the sodium in tissue is observable by NMR. Calf and adult AC samples were analyzed by NMR for sodium content. These samples were then sent to an

analytical laboratory (IEA-MA, North Billerica, MA) for sodium analysis by inductively coupled plasma emission spectroscopy (ICP) (Skoog and West 1980).

3. SENSITIVITY AND PRECISION

To assess measurement repeatability (precision), calf AC was equilibrated in 0.2 M NaCl. Samples were blotted dry, weighed and placed in the NMR tube. Three independent measurements of $[Na^+]$ and $[Cl^-]$ were made while the sample remained in the NMR tube. The sample was then returned to the bathing solution for at least 30 min. The entire sequence (bath, weigh, NMR x3) was conducted a total of three times covering a total bathing period of 2 hr. (The loss of tissue GAG during a 24 hr equilibration in 0.2 M NaCl had been determined in independent studies to be less than 2% of total GAG content.)

B. TISSUE ION CONCENTRATION AND FCD:

To initially evaluate the technique, calf AC samples were equilibrated in 0.2 M NaCl. Intratissue $[Na^+]$ and $[Cl^-]$ were measured, and the FCD computed by equations 10, 14, and 15.

C. CHANGING TISSUE FCD WITH COMPRESSION

To investigate the effects of compressive loads on intratissue ion measurements, cartilage disks were equilibrated in baths of 0.15 M to 0.3 M NaCl (concentrations higher than physiologic were used to improved signal to noise ratios for these experiments). Intratissue sodium and proton (for water content) were measured in each free swelling sample. The tissue was then re-equilibrated in the original bath while under compression. The entire sample holder was removed from the bath and blotted dry. Sodium and proton content were measured after each compression.

D. VARYING BATH COMPOSITION

The following series of experiments were conducted to investigate how ion concentration, as measured by NMR, and subsequent calculations of FCD were affected by changes in bath ionic composition, ionic strength, and pH.

1. EQUILIBRATION KINETICS

To observe the kinetics of equilibration, one cartilage sample was bathed in 0.2 M LiCl (pH 8) overnight. Intratissue [Na^+] was measured and then the sample was placed in an unstirred 0.2 M NaCl (pH 8) bath. After several minutes, the cartilage was removed from the bath solution; [Na^+] was measured. The sample was returned to the bath and the sequence repeated until three measurements varied by less than 5%. In two other experiments the procedure was essentially identical except the cartilage was initially equilibrated in 0.2 M NaCl (pH 8) and then placed in either 0.015 M NaCl (pH 8) or 0.2 M NaCl (pH 2).

2. INTRATISSUE VERSUS BATH [Na^+], [Li^+], AND [Cl^-] AT CONSTANT IONIC STRENGTH

Calf AC specimens were equilibrated sequentially in a series of constant ionic strength (0.2 M) NaCl/LiCl bathing solutions. For one sample, bath NaCl was increased (bath LiCl decreased) in 0.05 M steps; for the other, bath NaCl was decreased (bath LiCl increased). Intratissue [Na^+], [Li^+], and [Cl^-] were measured following each 90 min equilibration. FCDs were computed according to equations 16 and 17.

3. INTRATISSUE [Na^+] VERSUS BATH PH

Calf and adult AC samples were sequentially equilibrated for 90 min in 0.15 M NaCl solutions of varying pH. (Small volumes from an unbuffered 0.15 M NaCl, pH 6 stock solution were titrated with 1 N HCl; pH 8 solution was buffered with 5 mM Tris.) Intratissue [Na^+] was measured after each equilibration, and FCD was computed using equation 18.

4. INTRATISSUE [Na^+] VERSUS BATH IONIC STRENGTH

Calf AC samples were sequentially equilibrated (90 min) in buffered solutions of 0.015, 0.05, 0.1, 0.15, 0.2, and 0.3 M NaCl (50 μM Tris, pH>6.3). The initial overnight equilibration was at 0.015 M ($n = 3$) or 0.3 M ($n = 3$) NaCl. Intratissue [Na^+] was measured after each equilibration. This series was repeated twice for similar conditions. Equation 14 was used to compute FCDs.

E. TISSUE ION CONCENTRATION VERSUS ANATOMIC POSITION

In unrelated studies, we have consistently observed a substantial spatial variation of [GAG] in distal ulnar epiphyseal cartilage (Boustany 1991). Thus, we would predict a parallel variation in FCD. To test this, cartilage disks from sequential slices of epiphyseal cartilage were equilibrated in 0.15 M NaCl solutions. Intratissue [Na^+] by NMR was determined; FCD was computed using equation 14. Samples were also analyzed for sulfated GAG content after papain digestion (Handley and Lowther 1977) using the dimethylmethylene blue (DMB) assay. Absorbances were obtained at 525 nm with a Lambda 3B spectrophotometer (Perkin-Elmer, Norwalk, CT). Since chondroitin sulfate (CS) is the major GAG constituent in calf cartilage, absorbances were converted to sulfated GAG content by comparison with commercially available CS standards (C4384 from shark and C8529 from bovine trachea; Sigma, St. Louis, MO). Finally, FCD was estimated from sulfated GAG content by assuming each mole of CS salt had two moles of charge (one carboxyl and one sulfate) and 502.5 MW.

F. FCD WITH LOSS OF PROTEOGLYCANS

To verify the ability of this NMR method to measure changes in FCD with depletion of GAGs over time, cartilage samples were enzymatically degraded and FCD was followed. Several samples were initially bathed in 150 mM NaCl; sodium and proton signals were measured and FCD was calculated. Samples were then placed in small volume baths (500 μL) which contained trypsin (25 mg/mL). Exposure of cartilage to the protease trypsin results in the removal of proteoglycans and noncollagenous proteins from cartilage. After several minutes, each sample was removed from its bath at which point sodium and proton were again measured. Samples were then returned to a different bath of the same composition and the sequence was repeated until the measured sodium content remained constant (i.e. varied by less than 5%). The digested samples were analyzed for remaining GAG content using the DMB assay, as were aliquots of each bath solution.

G. IMAGING STUDIES

To confirm that these techniques can be extended to imaging modalities and hence allow the determination of FCD as a function of spatial location in heterogeneous samples or *in vivo*, the spatial variation of intratissue sodium in an intact distal ulna was examined. An intact ulnar segment, extending from the bony epiphysis to metaphysis with the periosteum

intact, was dissected from the distal ulna and equilibrated overnight in 0.15 M NaCl. The segment was then placed in a 20 mm NMR tube filled with 0.15 M NaCl for imaging studies.

A proton image with an echo time (time from excitation to signal acquisition) of 15 msec was first obtained. With this long echo time, a significant amount of relaxation of the magnetization has occurred (due to T2 or transverse NMR relaxation) before signal acquisition, and thus the image intensities of the different tissues are strongly influenced by their T2 time constants. This image accentuates differences between tissues, and is used for anatomic orientation. The image plane was set to run longitudinally through the joint, from epiphysis to metaphysis. The in-plane resolution was 120 μm and the slice thickness was 2 mm.

Proton and sodium images were then obtained with echo times of 2 msec, in-plane resolutions of 120 μm (proton) and 700 μm (sodium), and slice thicknesses of 5 mm. This short echo time minimizes the effects of T2 relaxation before image acquisition. The repetition time between image encoding steps was 5 sec for proton (2 averages of 64 encoding steps, 10 min image time) and 100 msec for sodium (800 averages of 64 encoding steps, 90 min image time).

RESULTS

In the following analyses, all averaged data are presented as mean ± SD.

A. CONTROL STUDIES

1. CALIBRATION

Calibration curves of sodium content in NaCl solutions, both with and without added GAG, were linear over the range relevant to these studies ($r > 0.999$). Subsequent calibrations were performed with two or more solutions.

Studies to establish that calibration with ions in solution was suitable for ions in tissue involved adding "desorbant" solution to the tissue in the NMR tube, so that the ion of interest would diffuse out of the tissue. The ratio of sodium content measured after addition of water to sodium measured before was 0.97 ± 0.03 ($n = 12$); the chloride signal, however, increased by a factor of 2.57 ± 0.36 ($n = 12$) after desorption. After the tissue had been removed from the water, approximately 60% of the original sodium signal and essentially no chloride signal remained, demonstrating that water was effective in desorbing chloride. When KCl was used as the desorbant to more effectively desorb sodium, less than 20% of the original sodium signal remained in the tissue after desorption. Sodium measurements in tissue and in solution were again essentially identical (1.00 ± 0.02, $n = 6$).

2. ICP ANALYSIS

For calf samples, the ratio of sodium content determined by NMR to that determined by ICP was 1.02 ± 0.04 ($n = 7$), for adult it was 1.04 ± 0.11 ($n = 8$). These data serve to validate the total NMR visibility of sodium in cartilage.

3. SENSITIVITY AND PRECISION

Independent control experiments showed that 1 μmole of sodium (the lowest quantity attempted) could be detected under the experimental conditions reported here. Repeated measurements of $[Na^+]$ in calf AC ($n = 2$) varied by less than 2% (SD/mean) when the

sample remained in a capped NMR tube and by less than 4% when the sample was returned to its bath between data acquisitions. Measurements of [Cl^-] varied by less than 6% under both conditions. The wet weights varied by less than 1% for samples returned to the bath.

B. TISSUE ION CONCENTRATION AND FCD

For ten cartilage samples equilibrated in 0.2 M NaCl, the percent water content (determined from (wet weight - dry weight) / wet weight) was 80.3 ± 1.0 %; [Na^+] measured by NMR was 0.38 ± 0.02 M. [Cl^-] measured by NMR was 0.15 ± 0.02 M, where the correction factor determined from desorption studies (2.57) was applied to account for the intratissue fraction invisible to NMR. Calculated FCD was -0.24 ± 0.04 M based on electroneutrality, -0.28 ± 0.03 M based on Donnan partitioning of sodium, and -0.13 ± 0.06 M based on Donnan partitioning of chloride. (It should be noted that if the correction factor was 2.21 or 2.93 (mean ± 1 SD), the corrected mean chloride concentration would be 0.13 or 0.17 M, resulting in chloride-based FCD calculation of -0.18 or -0.07 M.)

C. CHANGING TISSUE FCD WITH COMPRESSION

Compression of cartilage leads to a decrease in tissue water content and a concomitant increase in the concentration of solid matrix constituents. When cartilage was compressed such that water content decreased, the sodium concentration as measured by NMR increased, consistent with the expected increase in GAG concentration, or more precisely, the increase in tissue FCD (Figure 3). The validity of the NMR measurements was assessed independently by calculating the total amount of fixed charge (as the product of FCD and water content) under compressed and uncompressed conditions.

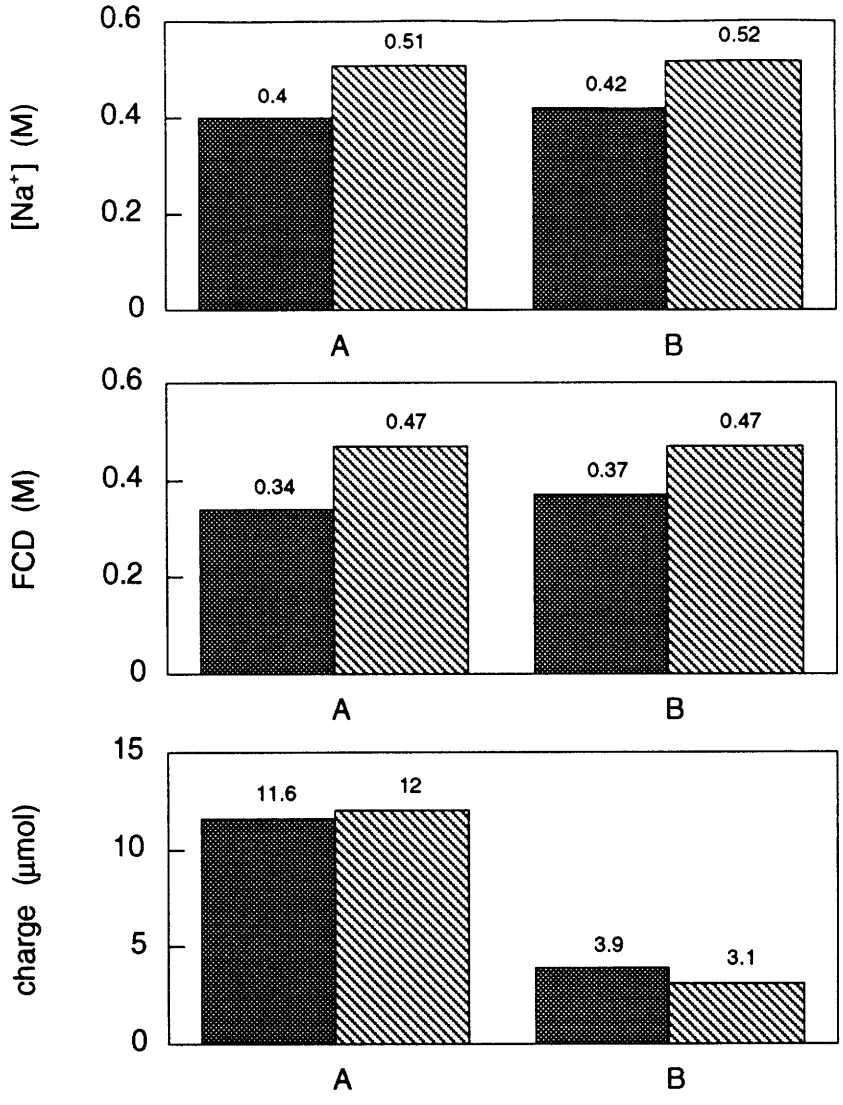

FIGURE 3 [Na^+], FCD, and total charge for each of two samples (A & B), before and after compression by 39% (A) and 25% (B). FCD was calculated using Donnan theory (equation 14). Total charge was the product of FCD and water content.

D. VARYING BATH COMPOSITION

1. EQUILIBRATION KINETICS

Figure 4 shows the time course of intratissue [Na^+] for three individual samples as they re-equilibrate to adjustments in bath pH, composition, or ionic strength. In all cases, greater than 90% equilibration occurred within 30 min. Subsequent equilibrations were at least 90 min.

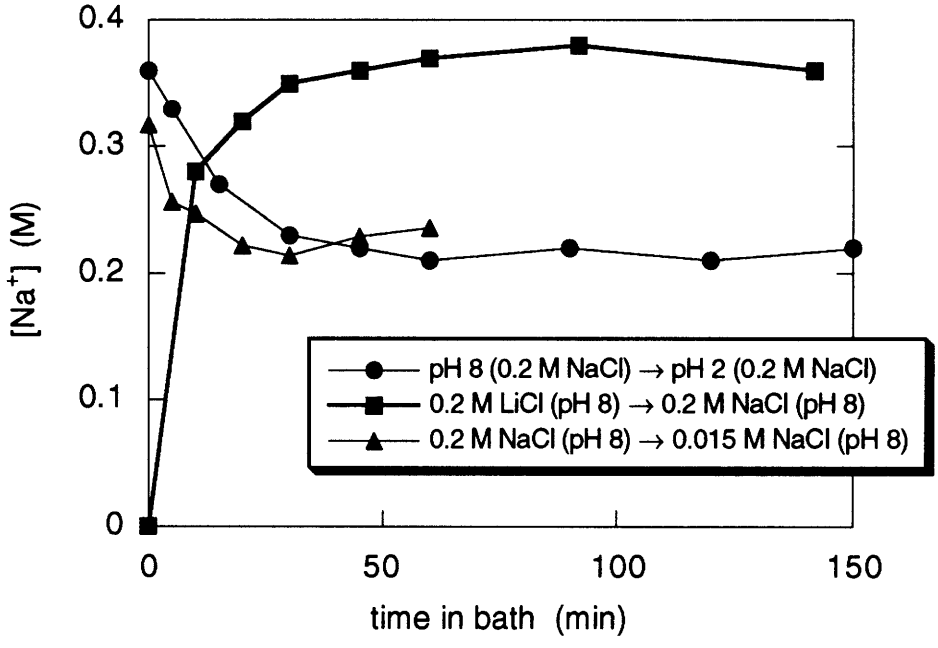

FIGURE 4 Intratissue sodium concentrations versus time for a calf AC sample pre-equilibrated in one solution and at time zero placed in a different solution. The sample was removed from the bath for each NMR measurement. The time axis indicates the cumulative time the sample was in the bathing solution.

2. INTRATISSUE VERSUS BATH $[Na^+]$, $[Li^+]$, AND $[Cl^-]$ AT CONSTANT IONIC STRENGTH

The results in Figure 5 demonstrate that as bath $[Na^+]$ and $[Li^+]$ varied, the intratissue ion concentrations were observed to change accordingly, while measured $[Cl^-]$ was relatively constant (9% variation). Figure 5 also shows that FCDs computed from Donnan partitioning of $[Na^+]$ or $[Li^+]$ appear to be independent of relative bath [NaCl]/[LiCl]. A second identical study yielded equivalent results.

3. INTRATISSUE $[Na^+]$ VERSUS BATH pH

In Figure 6, intratissue $[Na^+]$ and corresponding FCD are plotted as a function of bath pH for calf AC samples (n = 6). Between pH 8 and 4 there was a 3% decrease in intratissue $[Na^+]$; FCD dropped from -0.27 to -0.25 M. Between pH 3 and 2, intratissue $[Na^+]$ decreased dramatically to approximately 20 mM above bath $[Na^+]$, corresponding to an FCD of -0.06 M. Tissue hydration exhibited parallel behavior, dropping approximately 2% between pH 3 and 2. Results for a similar experiment with adult AC samples (n = 2) are also shown.

4. INTRATISSUE $[Na^+]$ VERSUS BATH IONIC STRENGTH

For each of six samples, intratissue $[Na^+]$ decreased with decreasing bath NaCl, while hydration increased slightly (approximately 1%) at the lowest ionic strengths (Figure 7). Figure 7 also shows that FCD calculated from the sodium data using ideal Donnan theory decreased monotonically with decreasing ionic strength. Each data point is presented here rather than mean values to illustrate the consistent trends for samples chosen to have a wide range of FCDs. Sample variation in FCD is commonly observed with varying anatomic position and from animal to animal (Grushko 1989). Similar trends were seen in repeated experiments.

E. TISSUE ION CONCENTRATION VERSUS ANATOMIC POSITION:

Intratissue $[Na^+]$ measured by NMR and absorbance measured from DMB showed the same trend as a function of the anatomic position of origin (Figure 8). Calculated FCD was more negative for samples near the epiphysis than for samples near the growth plate.

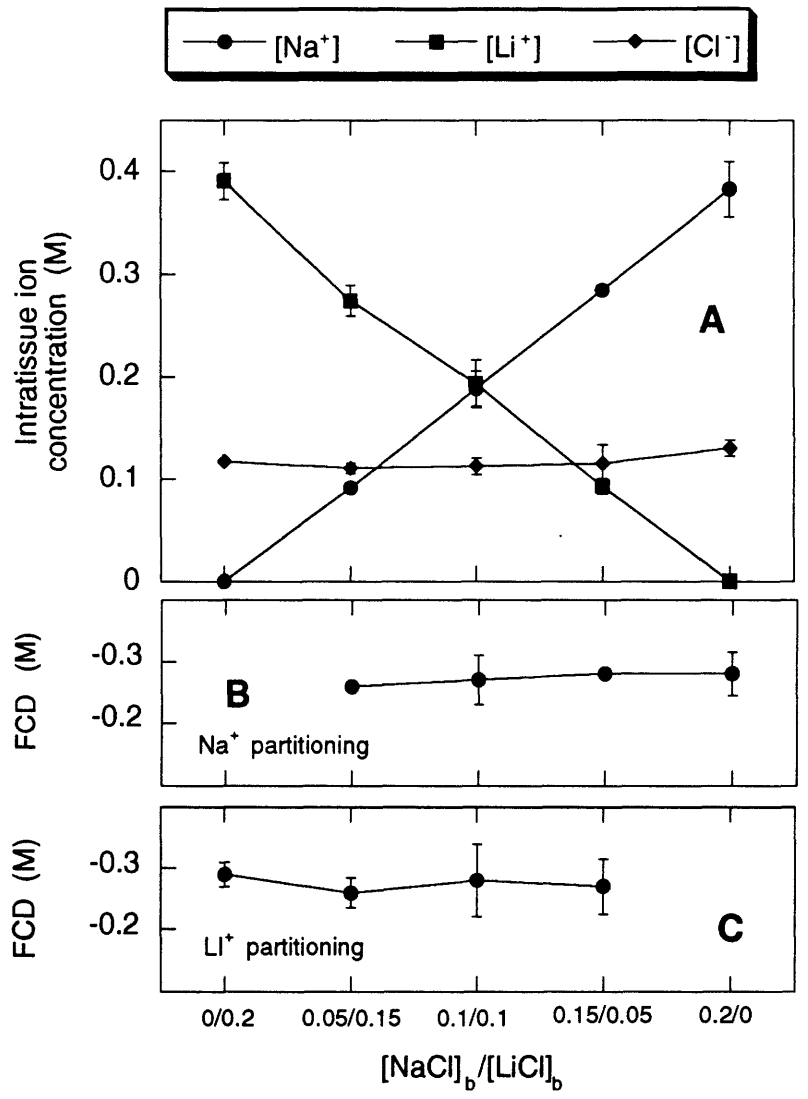

FIGURE 5 A) Intratissue sodium, lithium, and chloride concentration for cartilage samples (n = 2) equilibrated in constant ionic strength baths of varying sodium/lithium concentration. B, C) FCD calculated according to ideal Donnan from the sodium and lithium data. The Cl^- measurements were scaled by 2.57 before calculation of $[Cl^-]$ to account for the fraction invisible to NMR.

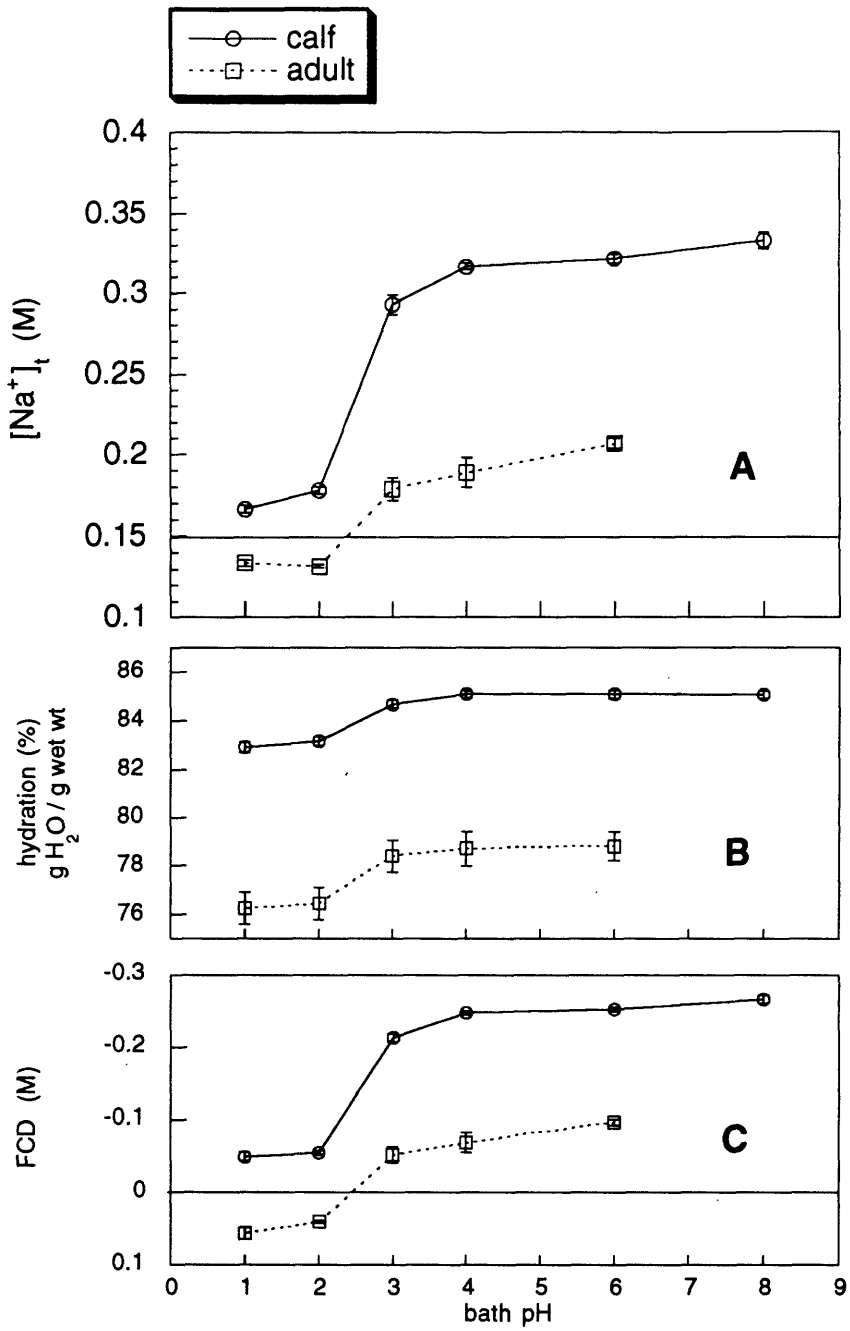

FIGURE 6 A) Intratissue sodium concentration, B) hydration, and C) FCD (calculated from sodium data and ideal Donnan theory) for calf (n = 6) and adult (n = 2) AC samples sequentially equilibrated in 0.15 M NaCl of varying pH. Solid horizontal lines indicate values associated with zero FCD.

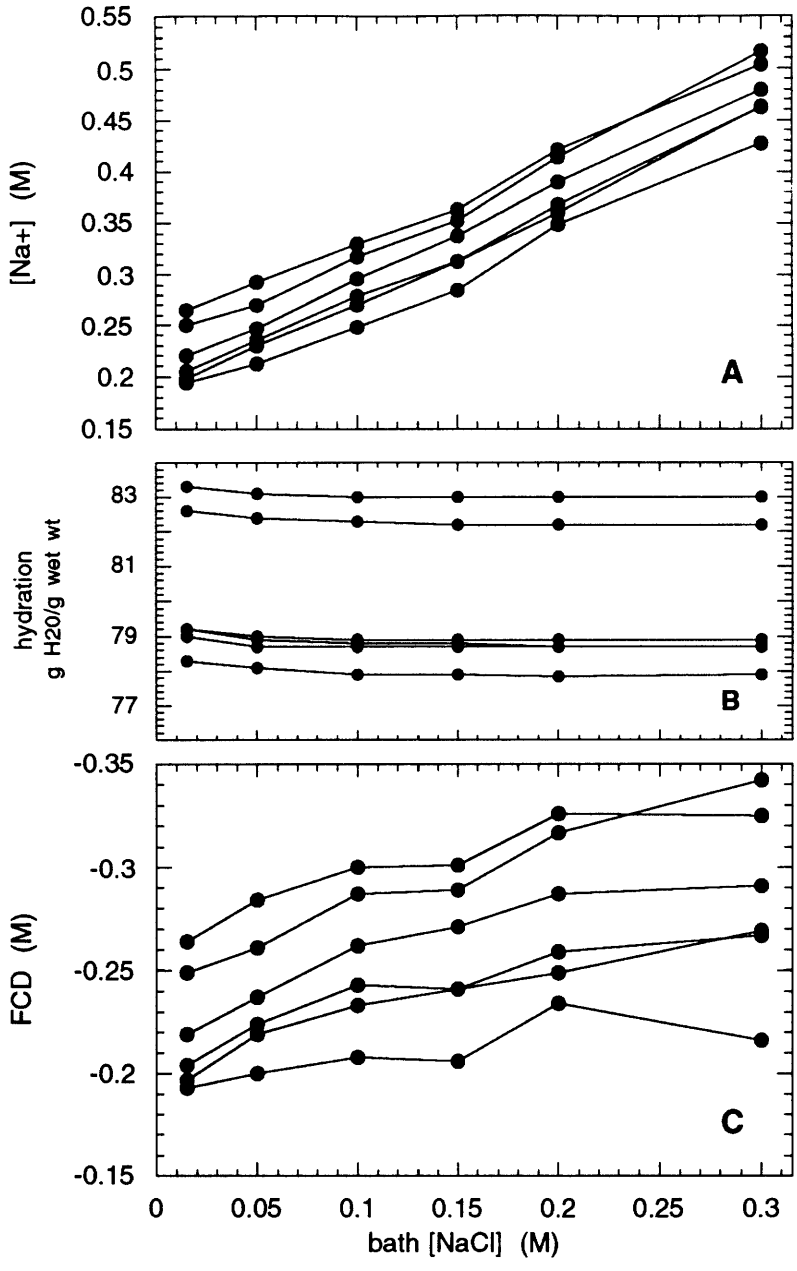

FIGURE 7 A) Intratissue sodium concentration, B) hydration, and C) FCD (calculated from sodium data and ideal Donnan theory) for calf AC samples (n = 6) equilibrated in baths of varying ionic strength at pH > 6.3.

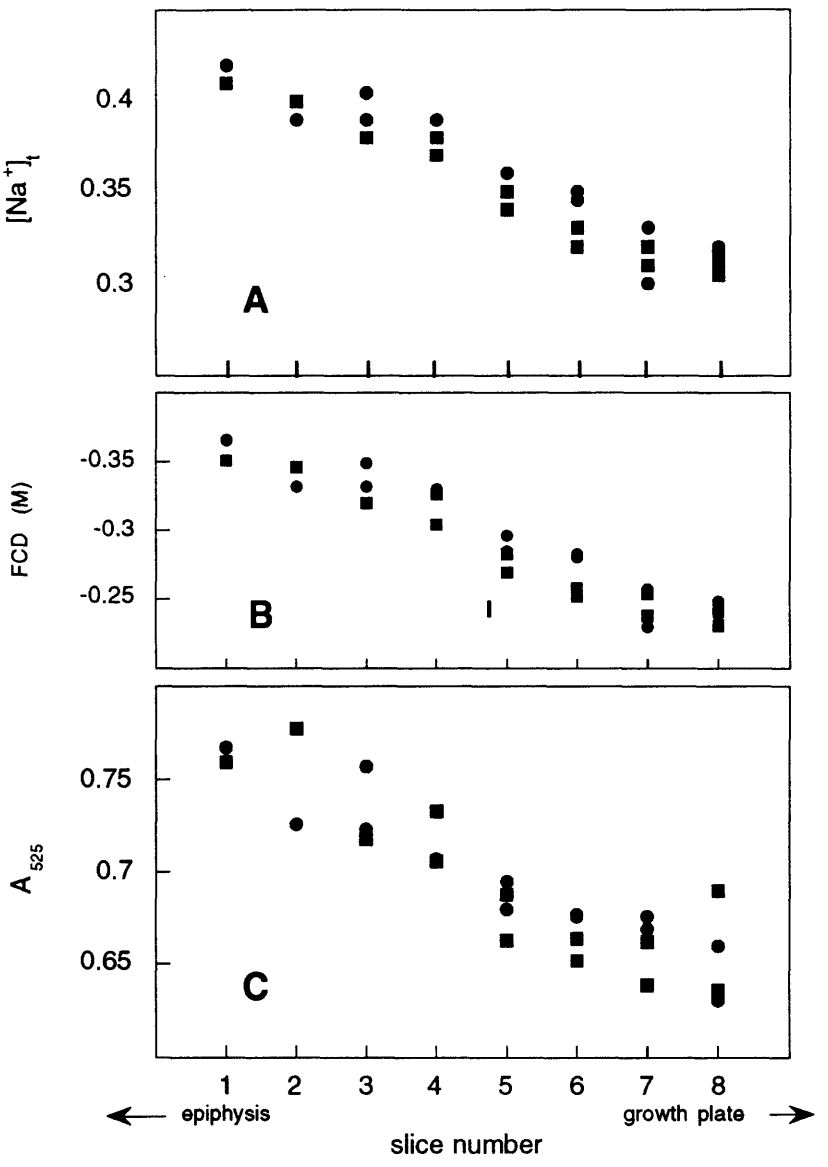

FIGURE 8 A) Intratissue sodium concentration, B) FCD (calculated from NMR sodium data and ideal Donnan theory), and C) DMB absorbance at 525 nm for 27 samples obtained from sequential depths within calf distal ulnar chondroepiphysis and equilibrated in 0.15 M NaCl. The circles and squares represent data from contralateral joints. Slice 1 is closest to the epiphysis; slice 8 is closest to the growth plate.

F. FCD WITH LOSS OF PROTEOGLYCANS

When tissue was progressively depleted of GAG by exposure to trypsin, sodium content and FCD calculated from the sodium content progressively decreased (Figure 9). FCD estimated from biochemical measurements of GAG released into the medium showed a close correlation to the NMR-based estimates (Figure 9). Biochemical determination of tissue GAG content was made using the DMB assay to measure GAG released into the trypsin medium during the study and that remaining in the cartilage samples at the conclusion of the study. FCD was calculated from GAG content assuming 2 moles of charge per mole (502.5 g) of GAG.

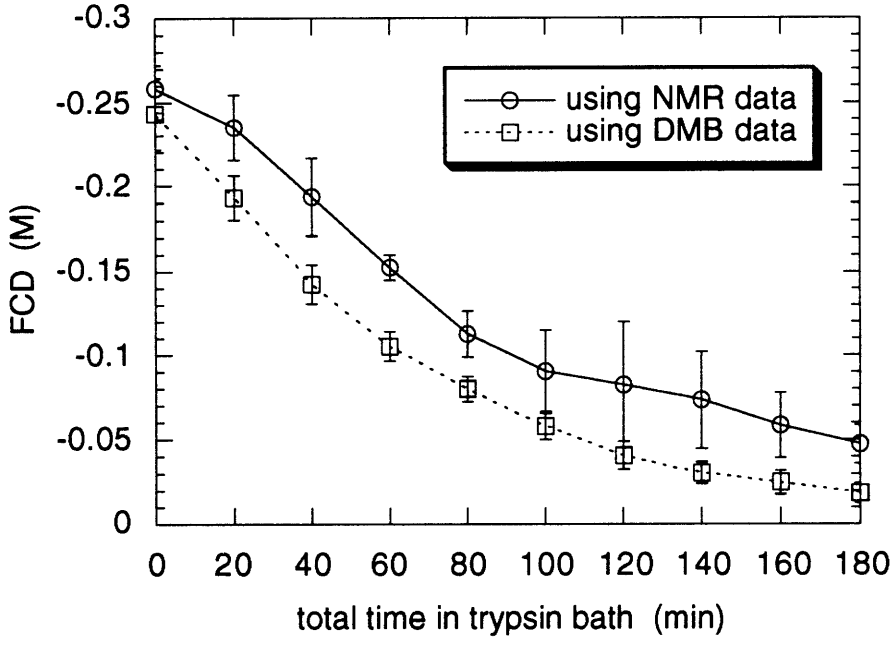

FIGURE 9 FCD calculated for cartilage samples (mean ± SD, n = 3) during exposure to the protease trypsin. FCD was calculated using NMR sodium measurements on the samples and using DMB assay to measure GAG released into the bathing solution and remaining in the sample.

The above study was repeated in order to compare the NMR results with histologic evidence of proteoglycan depletion. Sodium was measured for ten cartilage samples which were initially bathed in 0.15 M NaCl. One of the samples was set aside for later histology and the remaining nine samples were placed in 0.15 M NaCl containing trypsin. After 20 min, samples were again measured for sodium content. Again, one sample was set aside for histology and the remaining samples were returned to trypsin baths. This sequence was repeated until all samples were set aside. A plot of FCD calculated from sodium measurements looks similar to Figure 9. Figure 10 shows histologic sections of each cartilage sample with total time in trypsin indicated beneath each photo. Samples are stained for GAG with toluidine blue.

G. IMAGING STUDIES:

For anatomic orientation, a proton image with an echo time of 15 msec of an intact ulna is shown in Figure 11a. The cartilage can be seen between the bony epiphysis and metaphysis. Figures 11b and 11c show the proton and sodium images (2 msec echo time) and corresponding voxel intensities along a centrally located line from the epiphysis to the metaphysis (Figures 11d and 11e). The proton intensity (hydration) was relatively constant along the length of the cartilage, while the sodium intensity decreased substantially, in general agreement with the results of Figure 8 (obtained from a different joint).

FIGURE 10 (next page) Histologic sections of different cartilage samples, each exposed to trypsin for the indicated length of time (min). Cartilage was fixed using RHT and then stained for GAG using toluidine blue, where purple/blue color indicates the presence of GAG.

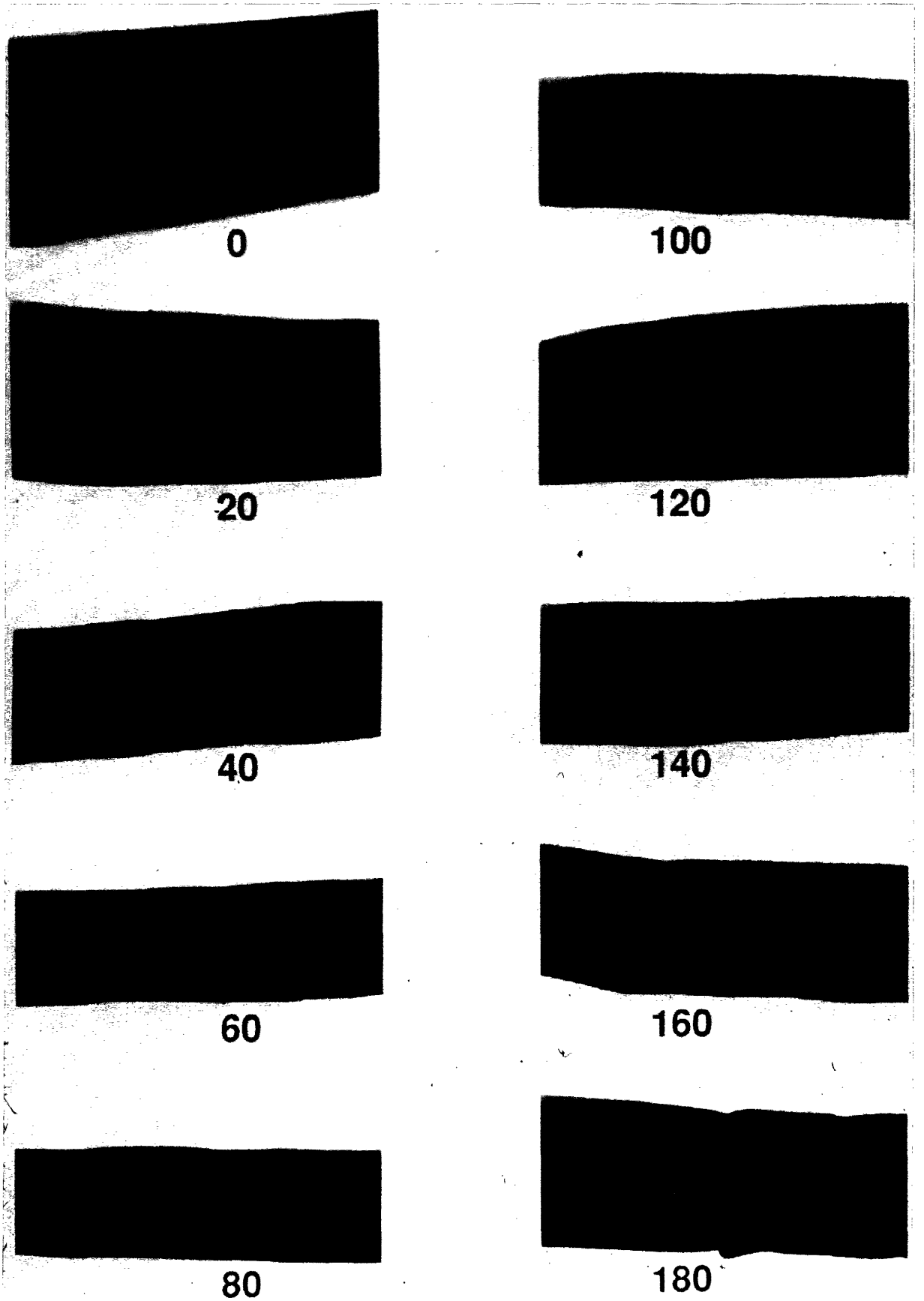
0
100
20
120
40
140
60
160
80
180

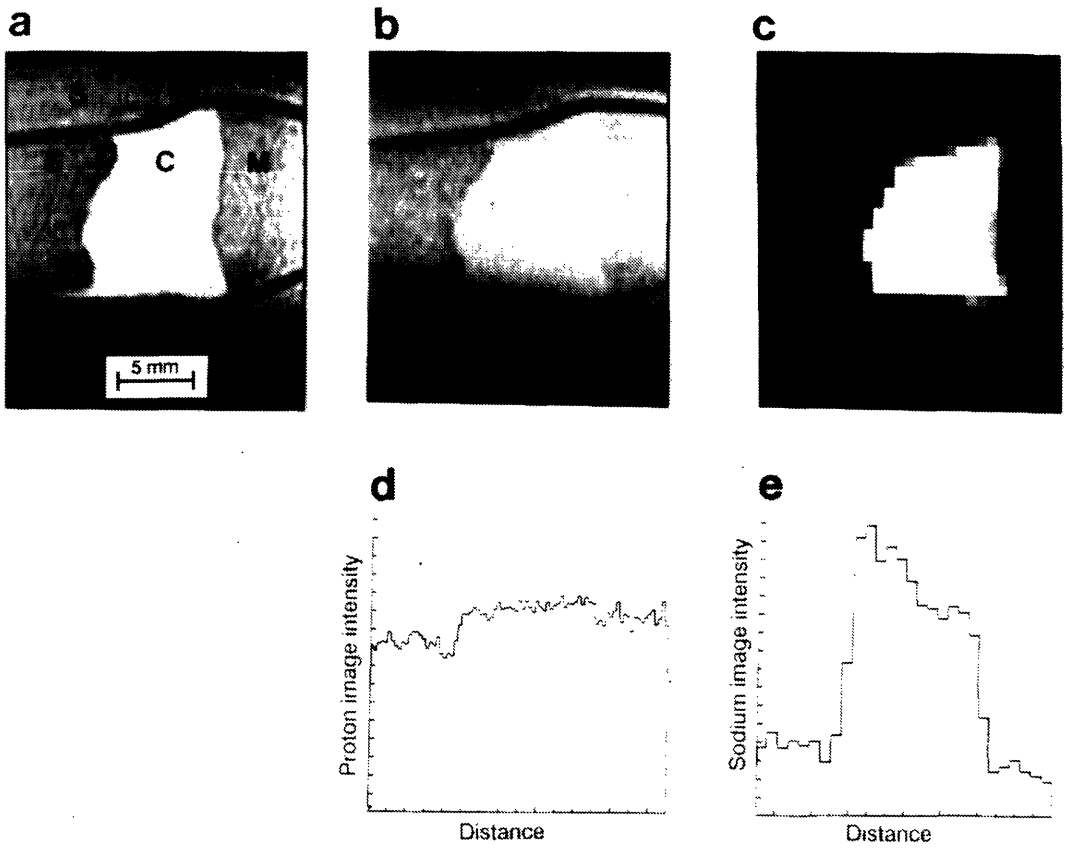

FIGURE 11 a) Proton image (echo time = 15 msec) of a distal ulnar joint immersed in saline (S). The cartilage (C) can be identified between the bony epiphysis (E) and metaphysis (M). b) Proton and c) sodium images (both 2 msec echo times) of the same joint. Imaging parameters are given in Experimental Protocols. The saline has a relatively low signal intensity since, with its long T1 time constant, the repetition time between successive NMR excitations was considerably less than 5T1. d) and e) Corresponding image intensities along a centrally located line from epiphysis to metaphysis. Note the constant hydration along the cartilage with a corresponding decrease in sodium intensity.

DISCUSSION

These experiments demonstrate the feasibility of using NMR to nondestructively measure intratissue ion concentrations, thus providing data for computing tissue FCD. For our experimental configuration (with commercially available NMR equipment), repeatability for $[Na^+]$ and $[Cl^-]$ were within 4% and 8%, respectively, with a sodium sensitivity of at least 1 μmole. Each measurement was obtained in under 12 min (Table 1). This time could be significantly shortened and/or the sensitivity could be increased by designing a radiofrequency coil with dimensions more comparable to the cartilage sample under study.

The validity of calibrating tissue measurements to standard NaCl solutions was demonstrated by comparing measurements of ions in tissue to measurements of ions after a desorbant solution had been added to the tissue in the NMR tube. Sodium measurements for tissue and tissue/desorbant composite were equivalent, suggesting that the desorbed tissue sodium is 100% visible by NMR. Subsequent analysis of total tissue sodium content in additional samples by ICP demonstrated that all tissue sodium is essentially 100% visible by NMR.

However for chloride, the desorption studies showed that only approximately 40% of the intratissue chloride was visible by NMR. The fraction of intratissue chloride undetected by NMR is presumably due to the very fast T2 of intratissue chloride which results in a significant amount of signal decay during the "dead time" of the receiver, i.e. when the receiver is disabled during transmitter ring down (approximately 100 μsec for these experimental conditions). More studies are needed to determine if the percent visibility is constant over a range of bathing conditions and tissue composition, in which case a general correction factor could be applied to the calibration.

With the details of chloride calibration as yet unresolved, for the remainder of this report we focus primarily on the use of sodium measurements alone in combination with ideal Donnan theory to compute tissue FCD. Given 5% variation in the NMR measurement of $[Na^+]$, one can estimate the error inherently associated with using ideal Donnan (equation 14) to calculate FCD. The error, dependent on FCD relative to bath [NaCl], is summarized in Table 2 for relevant experimental conditions. While no error analysis has been reported for FCD calculated from radiotracer ^{22}Na measurements, it would be expected to be comparable to that found here.

Table 2 Estimation of the error inherent in the FCD calculation, given a 5% variation in NMR $[Na^+]$ measurement. For a given combination of FCD and bath $[Na^+]$, the expected intratissue $[Na^+]_{exp}$ was computed according to ideal Donnan theory. FCD $\pm$ ΔFCD were then calculated assuming measurement of $[Na^+]_{exp} \pm 5\%$.

Experimental Condition	FCD (M)	$[Na^+]_b$ (M)	$\frac{-FCD}{[Na^+]_b}$	FCD $\pm$ ΔFCD (M)	$\frac{\Delta FCD}{FCD}$
Normal adult AC	-0.15	0.150	1	-0.15 $\pm$ 0.02	11%
Normal young AC	-0.30	0.150	2	-0.30 $\pm$ 0.02	7%
Low ionic strength	-0.15	0.015	10	-0.15 $\pm$ 0.03	5%
High ionic strength	-0.15	0.300	0.5	-0.15 $\pm$ 0.03	20%
Low pH or low [GAG]	-0.03	0.150	0.2	-0.03 $\pm$ 0.01	49%

Results of several experiments demonstrated the ability of NMR to follow changes in sodium content under a variety of bath conditions. The study using LiCl/NaCl solutions (Figure 5), showed that calculated FCDs were independent of bath composition. This study and additional experiments (data not shown) in which cartilage was equilibrated in tissue culture media, demonstrated the general applicability of intratissue sodium measurements in predicting tissue FCD to situations where the tissue is equilibrated in baths with multiple ions. In the context of *in vivo* applications of this technique, these data suggest that the NMR measured sodium concentration in synovial fluid and tissue may provide a sufficient basis for computing intratissue FCD.

By equilibrating the tissue in solutions of varying pH, one can titrate the ionic moieties, and thereby change the tissue FCD. For both calf and adult AC, FCD computed from sodium NMR measurements fell steeply at around pH 3 (Figure 6). This is consistent with previous reports that the pK of intratissue COO^- and SO_4^{2-} are near 3.5 and 2.0, respectively (Frank 1990). The decreased hydration which occurs at low pH reflects the lower intratissue swelling pressure. These data show an interesting difference between calf and adult tissues: Adult tissue becomes positively charged for bath pH $\leq$ 2 (as has been reported previously (Frank 1990, Maroudas 1968)); however, calf tissue still retains an apparent net negative charge at the lowest pH tested, even after a 24 hr equilibration. A partial explanation for this is that, since calf specimens had more than twice the [GAG] of adult (data not shown), calf FCD would be expected to be more negative (less positive) than adult FCD at every bath pH (assuming comparable collagen compositions).

In a separate series of experiments, we sequentially equilibrated several specimens in NaCl baths of various ionic strengths while maintaining the pH above 6.3. In Figure 7, FCD calculated from sodium data using ideal Donnan decreases with decreasing bath ionic strength. The desorption and ICP experiments demonstrate that this trend is not due to an artifact of the NMR measurement of sodium. Since intratissue pH drops with decreasing bath ionic strength, there is an accompanying titration of the carboxyl and sulfate groups. Previous reports (Frank 1990, Maroudas 1968, Phillips 1984) indicated that for adult (human and bovine) cartilage, titration would be minimal for NaCl concentrations over 0.015 M. For a relatively high tissue FCD of -0.3 M, the pH inside the tissue would be expected to be 6.1, 5.9, 5.5, and 5.0 for 0.3, 0.15, 0.05, and 0.015 M NaCl baths, respectively. With reference to the FCD curve of Figure 6, while pH may affect the 0.015 M data points, it would be expected that the net charge remains constant for bath NaCl between 0.05 and 0.3 M.

The observed dependence of calculated FCD on ionic strength may likely result from the one compartment and/or ideal Donnan assumptions made when calculating FCD. It is generally recognized that, from the point of view of solute distribution, intrafibrillar collagen and extrafibrillar GAG constitute different compartments (Maroudas 1968). For a sample equilibrated in 0.15 M NaCl, an FCD of -0.3 M calculated from intratissue sodium for one compartment would be -0.28 M when the calculation considers the average FCD of two compartments (assuming 30% of the water is in an uncharged "collagen" compartment). Frank et al. (1990) used theoretical models to demonstrate that while absolute magnitudes of FCD are higher when calculated using a one rather than two compartment model, the two models are qualitatively similar for predictions of average intratissue ion concentrations and FCD over a range of bath pH.

Although the ideal Donnan assumption that tissue and bath activity coefficients are equal is commonly used when computing FCD from intratissue ion measurements (Frank 1990, Grushko 1989, Maroudas and Evans 1972, Schneiderman 1986), the effect of this assumption is negligible only at very low ionic strengths. For sodium data obtained from cartilage bathed in 0.05 to 0.3 M NaCl (Figure 7), the apparent dependence of calculated FCD on bath ionic strength would be eliminated if tissue activity coefficients were 0.65 ± 0.06 ($n = 24$). This value for γ_t was calculated by solving the following equation (derived from equations 10 and 12 in Theory section) for each of the six samples from Figure 7 in bath 0.1 - 0.3 M NaCl baths:

$$FCD = \frac{\gamma_b^2 [Na^+]_b^2}{\gamma_t^2 [Na^+]_t} - [Na^+]_t \qquad (20)$$

These activity coefficients are on the order of those measured by Maroudas et al. (1988) (0.67 ± 0.04, n = 4) for GAG solutions with FCD similar to that of our tissue. Simultaneous measurements of sodium and chloride concentrations are necessary to directly quantify the effect of ionic strength on average FCD since they would allow determination of FCD from electroneutrality (equation 10 from Theory section) without the added assumption of ideal Donnan equilibrium..

The one compartment and ideal Donnan assumptions affect the calculation of FCD not only in the varying ionic strength experiment, but throughout this paper, as these assumptions affect any method which calculates FCD from measurements of one intratissue ion. However, while it is true that for any one sample the magnitude of FCD calculated using one compartment and ideal Donnan exhibits a dependence on bath ionic strength (Figure 7), it is also true that at each bath ionic strength the trend in FCD among samples remains essentially the same. Therefore, while the absolute magnitude of FCD reported in these studies may be offset by the one compartment and Donnan assumption, relative trends in calculated FCD are valid for samples studied in the same bathing conditions.

The ability to observe natural variations in tissue FCD was demonstrated by the study of calf epiphyseal cartilage (Figure 8). As suggested by the parallel trends in calculated FCD and in DMB absorbance, this variation is presumably due to differences in tissue [GAG]. FCD may also be estimated from the absorbance data by calibrating absorbance with CS standards to yield [GAG] for each sample and then converting [GAG] to FCD (see Methods). The FCD estimates from the absorbance data of Figure 8 using shark CS standards were 84 ± 0.06% (n = 27) of those calculated from NMR; estimates using bovine trachea CS were 100 ± 0.07% of those obtained from NMR.

The ability to observe changes in FCD due to perturbations which mimic tissue pathology was also demonstrated. Decreases in FCD were observed when proteoglycans were removed from cartilage by exposure to trypsin (Figure 9). FCD determined from sodium measurements were comparable to estimates based on DMB analysis of GAG released into the trypsin bath (Figure 9). The loss of proteoglycans was further confirmed in a separate experiment with a series of histologic sections through cartilage exposed to trypsin for varying lengths of time (Figure 10).

While the ratio of NMR and DMB based FCD estimates are of the same order, consistent with the general belief that GAGs provide the dominant source of cartilage charge (Maroudas 1968), caution must be used when interpreting absolute estimates of FCD based on DMB results. Dye-binding properties of calibration standards may be different than those of tissue CS. Indeed, as suggested above, dye-binding of purified CS standards from two different sources were different - perhaps due to variations in chondroitin-4- and chondroitin-6-sulfate content. (Exhaustive dialysis of standards did not eliminate any of the difference in absorbance.) Furthermore, MW and charge content (i.e. degree of sulfation) for the CS standard are not precisely known. Finally, tissue constituents other than CS may contribute to net charge (e.g. collagen, hyaluronate). Thus, while absolute comparison of FCD determined by NMR and DMB is not possible, DMB estimates do provide an order of magnitude estimate of FCD. Moreover, it is expected that trends are preserved so that DMB estimates are useful for relative comparisons.

Sodium NMR images of an intact distal ulna (Figure 11) exhibited a gradient in sodium intensity that correlates with the spectroscopy results of Figure 8. In order to quantify sodium density in an imaging experiment, care must be taken to utilize an echo time short relative to the T2 of the intratissue sodium (Foy 1989). In an earlier study which investigated spatial variation of intervertebral disc proteoglycan concentration, sodium density was found not to correlate with image intensity (Pollak 1990). With the relatively long echo time (8 msec) used in that study, T2 differences in the tissue are accentuated in the image intensity. In the study described here, the sodium image intensity was found to qualitatively correlate with the sodium density found in the parallel spectroscopy studies, thus suggesting that T2 differences are probably not significant at this very short echo time (2 msec). Current investigations in this laboratory are aimed at further reducing imaging echo times to enable better quantification of sodium density and thus, calculation of the spatially varying FCD for *in vitro* and *in vivo* intact, heterogeneous specimens. Measurements of FCD in intact samples may differ from those in isolated specimens due to changes which may occur during the cutting and re-equilibration process (for example, swelling). The practical spatial resolution and obtainable imaging times necessary for future *in vivo* studies are highly dependent on the location (i.e. depth within the body) of the cartilage under study and the hardware capabilities of the instrumentation.

In comparison to other methods for measuring FCD, NMR has the distinct advantage of being at once nondestructive, rapid, applicable to living tissue both *in vitro* and *in vivo*, and

capable of providing spatial information. The inability to nondestructively examine functionally relevant features of cartilage *in vivo* has undoubtedly been an impediment to understanding cartilage physiology in health and disease. Localized measurements of proton and sodium content should provide a powerful means for observing the progressive development, degeneration, or regeneration of functional cartilage tissue, representing a major advance over current capabilities.

PART II MT

MAGNETIZATION TRANSFER TO DETERMINE COLLAGEN CONTENT AND STRUCTURE

BACKGROUND

A. COLLAGEN

Collagen is thought to be the most common protein in the animal world (Eyre 1980, Gross 1961). At least 14 different types of collagen molecules have been identified to date (Eyre 1991). The different collagens are subdivided into classes based on their structure and function. Type I collagen, the predominant collagen in tendon and bone, and type II collagen, the predominant collagen in cartilage, belong to class I: collagens which form banded fibers (Burgeson and Nimni 1992). Regardless of type, the collagen molecule contains both globular and triple-helical domains. Some collagen molecules also contain noncollagenous domains (e.g. type IX collagen has a covalently attached glycosaminoglycan chain).

The triple-helical domain is composed of three polypeptide chains. Each of the three chains forms a left-handed helix with approximately three residues per turn. The chains are then coiled around each other into a right-handed superhelix (Miller 1984). In both type I and type II collagen, each polypeptide chain has a length of just over 1000 amino acids which are arranged in a repetitive sequence where every third residue is glycine (Gly-X-Y). Every third residue of this twisted structure must be glycine since the chains are in such close proximity when they twist that glycine, with no side chain, is the only amino acid small enough. Approximately one third of the remaining X and Y residues are proline. Many of the proline and lysine residues found in the Y position are post-translationally hydroxylated; the Gly-Pro-Hyp sequence makes up about 10% of the molecule (Burgeson and Nimni 1992, Creighton 1984).

The triple helix is stabilized by close atomic packing, hydrogen bonding between the three chains, and the high content of imino acids, namely, proline and hydroxyproline (Brodsky 1990). While the exact number of hydrogen bonds has not been determined, models exist which propose either one or two hydrogen bonds for every three residues (Burgeson and Nimni 1992). Hydrogen bonds involve the carbonyl group of glycine and the amide groups of adjacent residues on neighboring chains (Byers 1990). The hydroxyl groups on the hydroxyproline residues are involved in these interchain hydrogen bonds (Bornstein and Traub 1979). In addition, proline and hydroxyproline contribute to the stability and

rigidity of the triple helix by preventing easy rotation of the regions in which they are located (Gross 1961).

The different types of collagen vary in the composition of the constituent helical chains. Type I collagen contains two identical chains, referred to as $\alpha 1$(I), and one non-identical $\alpha 2$ chain. Type II collagen contains three identical chains, which are similar to the $\alpha 1$ chains found in type I collagen and are referred to as $\alpha 1$(II) chains.

Cellular synthesis of collagen begins with the synthesis of the specific polypeptide chains. After necessary post-translational modifications are complete, the three chains are assembled into a precursor molecule known as procollagen. Upon exiting the cell, the nonhelical ends of procollagen are enzymatically cleaved, leaving the helical collagen molecule plus telopeptides (small nonhelical regions) on both ends (Figure 12). In the extracellular space, the collagen molecules spontaneously form macromolecular aggregates known as fibrils.

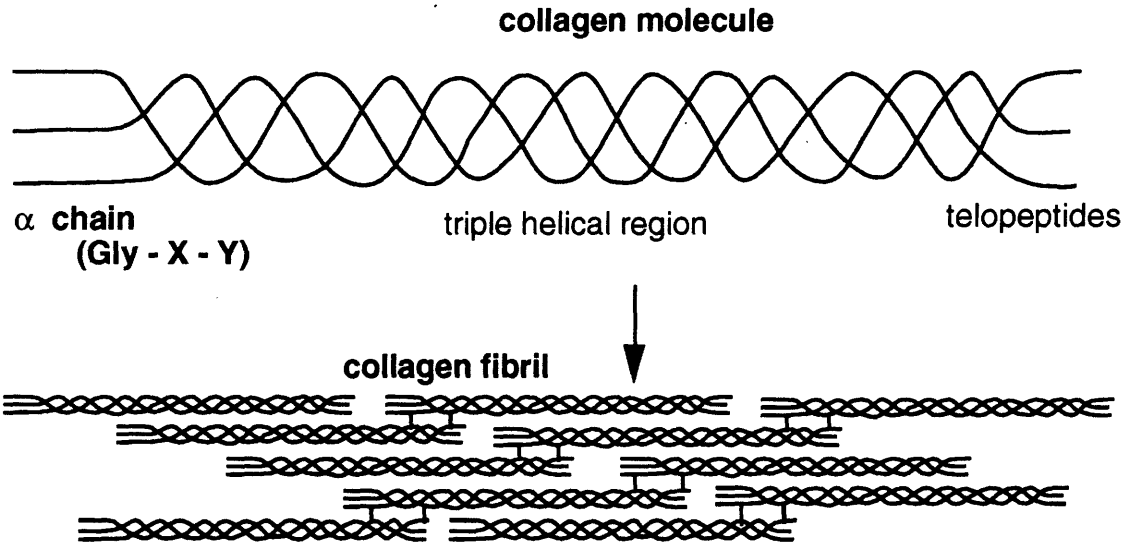

FIGURE 12 The basic form of the collagen molecule and collagen fibril. Within the fibril, molecules are periodically staggered and are covalently crosslinked between triple helical and telopeptide regions.

The regulation of fibril formation is incompletely understood and is an area of active research. The smallest subunit proposed is the five stranded microfibril in which five molecules are aligned in the same direction with a one-quarter length overlap (Smith 1968). Exclusion of water from nonpolar regions along the collagen molecule results in hydrophobic bonds which enhance fibril stability (Burgeson and Nimni 1992). The overlapping creates the characteristic banded pattern seen with electron microscopy. These microfibrils then aggregate laterally and end-to-end to form fibrils. The diameter and length of collagen fibrils vary greatly, depending on the type and age of tissue (Eyre 1980). The words fibril and fiber are often used interchangeably when describing the aggregated collagen molecules; collagen fiber typically refers to large fibrillar aggregates seen on light microscopy (Eyre 1980). The term fibril will be used throughout this discussion.

Once assembled, fibrils are stabilized by a variety of covalent crosslinks between triple helical molecules; these crosslinks primarily involve the lysine and hydroxylysine residues. The enzyme lysyl oxidase converts some of these residues to aldehydes which then undergo an aldol condensation to form the crosslinks. Four crosslinking sites are evident in types I, II, and III collagen molecules, two near each end of the molecule (Eyre 1984). These crosslinks are essential for the strength and normal function of collagen fibrils and are thought to be responsible for the insolubility of collagen fibrils (Tanzer 1973). The extent and type of crosslinking vary with the physiological function and age of the tissue (Bornstein and Traub 1979). Collagen in rat tail tendon is relatively soluble in dilute acid or after heating in water beyond its denaturation temperature because the aldimine crosslink is cleaved easily under these conditions (Light and Bailey 1980). Insoluble collagen, such as that found in cartilage, contains the stable keto imine crosslink which is resistant to acids or thermal denaturation (Light and Bailey 1980). With aging, reducible crosslinks are converted to stable, non-reducible crosslinks which decrease the solubility and swelling of collagen as well as its susceptibility to enzymes and increase its mechanical strength (Light and Bailey 1980).

Because it is neither crosslinked nor tightly aggregated, newly synthesized collagen is still soluble; it is extractable in cold salt solution (Piez 1967). As the collagen becomes older, and thus more aggregated and crosslinked, extraction requires dilute acid and eventually is impossible even with acid. While soluble collagen is primarily molecular collagen, it will contain some fibrils. Acid-extracted collagen will generally contain a greater proportion of

aggregates than salt-extracted collagen, but substantially less than non-extractable collagen (Piez 1967).

If collagen is heated above its denaturation temperature, its helical conformation is disrupted. The resulting random coil structure is called gelatin; the individual polypeptides are unraveled although still linked by any covalent crosslinks. This denaturation occurs within a narrow range of temperature which suggests that the stability of the triple helix is the result of many reinforcing bonds, each of which is relatively weak (von Hippel 1967). These stabilizing bonds are the interchain hydrogen bonds formed by the imino acids (proline and hydroxyproline). A strong correlation has been shown between the thermal stability of the collagen molecule and its hydroxyproline content (Burjanadze 1979). The melting temperature of a non-hydroxylated form of collagen was 15°C lower than a hydroxylated form from the same source (Berg and Prockop 1973).

Upon cooling, the chains assume a collagen-like conformation but combine randomly with other chains to form short triple helical segments (Engel 1962). A more regularly ordered structure will form with controlled cooling but the ends of the chains are typically not aligned. The nonhelical ends of the chains, which were cleaved when the molecule was extruded from the cell, are necessary for proper alignment.

Fibril diameter and degree of crosslinking also affect thermal stability. The melting temperature of insoluble collagen fibers is 20°C above that of soluble collagen molecules (Veis 1967). Multiple denaturation transitions have been observed with differential scanning calorimetry of reconstituted collagen which were shown to contain fibrils of differing fibril diameter (Wallace 1986).

Collagen fibrils *in vivo* are hydrated. In physiological saline at neutral pH, type I (e.g. tendon) collagen fibrils contain ~60% water by weight (Nussbaum and Grodzinsky 1981). The water in collagen can be described in terms of two compartments: intrafibrillar water being the water inside the collagen fibril and extrafibrillar water being the water outside. Swelling of a collagen matrix can occur due to increases in both intrafibrillar and extrafibrillar compartments. Measurements of wet rat tail tendon (type I collagen) showed that the volume of a fibril was 55% collagen and 45% (intrafibrillar) water (Nomura 1977). Measurements of type I and type II collagen from the annulus fibrosus and nucleus pulposus of native human intervertebral disk cartilage gave evidence of an increase in lateral separation between type II molecules compared with type I (Grynpas 1980). Using these

measurements and the assumption of cylindrical fibril geometry, type II collagen fibrils were estimated to have 30% more intrafibrillar water volume. Finally combining this data with the rat tail data, it can be calculated that the type II fibril volume consists of 43% collagen and 57% intrafibrillar water. The mechanism for modulation of fibrillar hydration was proposed to be glycosylation of hydroxylysine residues since type II collagen has a high glycosylated hydroxylysine content compared to type I (Grynpas 1980).

B. COLLAGEN MODEL SYSTEMS

The various forms of collagen can be reproduced in model systems. Single, triple-helical **molecules** exist in a solution of acid soluble collagen (Piez 1967). When an acid solution of native collagen is neutralized or when a cold solution of salt-extracted collagen is warmed to body temperature, the collagen molecules spontaneously polymerize to form a gel. This gel is composed of reconstituted **fibrils** which are similar to those found *in vivo* (Gross 1961). Reconstituted fibrils show the same characteristic banding pattern as native fibrils but have larger lateral spacings between molecules (Eikenberry and Brodsky 1980). Native insoluble fibrils are also more thermodynamically stable, i.e. they exhibit a higher melting temperature, than reconstituted fibrils (Russell 1974). Both of these differences are presumably due to the covalent crosslinks which are present in the native fibrils (making it insoluble) but absent in the reconstituted fibrils (which were formed from soluble molecules).

Collagen gels exhibit an aging process similar to that seen in cartilage during which covalent crosslinks are formed. Newly formed gels re-dissolve when cooled but gels left to stand at body temperature become less soluble with time, even in dilute acid (Gross 1961). In one study, reconstituted 0.1% collagen gels incubated at 37°C for 1 hour or less dissolved completely upon cooling to 5°C (Gross 1964). With increasing incubation time, the gels grew more insoluble; after 48 hrs at 37°C, gels were 80% insoluble. The decreased solubility was presumably a result of increased crosslinking.

C. COLLAGEN IN CARTILAGE

In cartilage, collagen makes up 50-60% of tissue dry weight (Heinegard and Oldberg 1989). In articular cartilage, type II collagen is most abundant (80-95%). Other collagens present to varying degrees in cartilage are types IX, XI, X, V, and VI (Mayne 1989, Eyre 1991). Type XI collagen retains its N-terminal propeptide and may play a role in the

regulation of type II collagen fibril diameter (Eyre 1991). However, during the maturation of articular cartilage, type XI collagen contains an increasing proportion of $\alpha 1$ chains from type V collagen. The significance of this change in gene expression is unknown (Eyre 1991). Type IX collagen contains both a proteoglycan and a collagen domain and in cartilage may provide an interface between the type II collagen fibrils and proteoglycans (Eyre 1991). Type X collagen is found primarily in the hypertrophic zone of growth plate cartilage and in the deep calcified layer of mature articular cartilage (Eyre 1991).

Various types of connective tissue differ in their collagen content and degree of collagen crosslinking. Normal adult articular cartilage does not swell when placed in isotonic saline, even when cut into thin (250 μm) slices (Maroudas 1976). The type II collagen in cartilage is extensively cross-linked and swells little; almost none dissolves in dilute acid. In comparison, flexible rat tail tendon collagen, which is predominantly type I collagen, has less-crosslinked fibrils of smaller diameter, swells about 100-fold when hydrated and is completely acid soluble. Among cartilage samples, collagen content and degree of crosslinking also vary with location and age.

D. PERTURBATIONS TO COLLAGEN

With only a slight excess in the number of amino (NH_3^+) groups compared to carboxyl (COO^-) groups (Li and Katz 1976), type I collagen has approximately zero net charge at neutral pH (Bowes and Kenton 1948a, Maroudas 1979). The pK value for carboxyl groups is reported to be around 3.5; the pK for amino groups is around 11 (Bowes and Kenton 1948a). When bath pH becomes sufficiently basic or acidic, collagen fibrils attain a net negative or positive charge, respectively, and intrafibrillar hydration increases due to electrostatic effects. As ionic strength decreases and there are fewer mobile ions to balance the fixed matrix charges, intrafibrillar hydration increases further. This is referred to as osmotic or Donnan swelling (Veis 1967). Fibers decrease in length as they increase in cross-sectional area with a resulting increase in total volume. At pH 2.5, collagen type I is almost 90% water by weight (Nussbaum and Grodzinsky 1981). Maximum swelling occurs at pH 2; at lower pH deswelling occurs (Bowes and Kenten 1948b, Veis 1967).

Changes in bath ionic strength at neutral pH result in minimal changes in collagen hydration (Grodzinsky 1981). However, when bath pH is below 5.0 or above 9.5 and the collagen fibril has a net charge, measurable changes in hydration occur as bath ionic strength

changes (Ripamonti 1980, Grodzinsky 1981). The addition of salt reduces the osmotic swelling by shielding the charges on the collagen molecule.

Changes in bath pH and ionic strength affect both collagen and tissue hydration. At low pH, matrix carboxyl and sulfate groups are protonated. In native cartilage, the loss of negative charge on the proteoglycans results in decreased proteoglycan hydration and therefore, decreased total tissue water. Collagen intrafibrillar hydration increases both due to the development of a net positive charge on the collagen molecule (electrostatic repulsion) and to the loss of proteoglycan charge (decreased osmotic pressure exerted against the collagen fibrils). In trypsin-treated cartilage which has been depleted of proteoglycans, pH affects only the collagen charge and changes in tissue hydration are determined solely by changes in collagen hydration. The net result is increased intrafibrillar hydration and increased total tissue water.

Exposure of cartilage to the protease trypsin results in the removal of proteoglycans and noncollagenous proteins from cartilage. Collagen fibril hydration is affected by the removal of proteoglycans. The intrafibrillar space of collagen is filled with water and ions. In cartilage, proteoglycans are excluded from this intrafibrillar space because of their large size. But due to their abundant negative charge, the proteoglycans exert a large osmotic pressure on the adjacent collagen fibrils. Katz et al (1986) used xray diffraction to show that the lateral spacing of fibrillar collagen in human articular cartilage increased as the concentration of osmotically active solutes (i.e. proteoglycans) in the extrafibrillar space decreased. Equatorial peak position (which is related to average intermolecular spacing of molecules in the fibrils) decreased from ~1.75 nm in samples with low FCD (-0.1 M) to ~1.6 nm in samples with higher FCD (-0.25 M). Therefore, removal of proteoglycans from cartilage by digestion with trypsin results in increased collagen fibril hydration but decreased total tissue water (due to the loss of the water associated with the proteoglycans).

Compression of cartilage leads to a decrease in tissue water content and concomitant increase in the concentration of solid matrix constituents. For native cartilage, compression results in increased collagen and proteoglycan concentrations and therefore, increased tissue fixed charge density. Given the increased FCD, collagen fibril hydration in native cartilage would be expected to decrease with compression. In trypsin-digested cartilage, intrafibrillar water content may decrease due to direct compression of the collagen fibrils. Xray diffraction measurements of native and proteoglycan-free articular cartilage showed that in both types of tissue, molecular packing density increased and (calculated)

intrafibrillar water content decreased with increasing levels of applied compression (Maroudas 1991).

Perhaps in part due to its compact structure, collagen is highly resistant to enzymatic attack. Proteolytic enzymes such as pepsin or pronase selectively cleave the non-triple helical regions of the collagen molecule where the crosslinks are located and are used to extract insoluble collagen (Bornstein and Traub 1979). Once denatured, collagen is highly susceptible to complete digestion by many proteases, including trypsin and pepsin (Bruckner and Prockop 1981). The intact (non-denatured) collagen fibril is degraded by specific enzymes known as collagenases which cleave peptide bonds in the triple helix. Two types of collagenases are known: bacterial and tissue collagenases. The bacterium clostridium histolyticum secretes a variety of collagenases which split the collagen polypeptide chain at over two hundred sites (between X and Gly of the sequence X-Gly-Pro-Y). Collagenases have been found in amphibian and mammalian tissues and are believed to be responsible for regulation of growth and remodeling (Krane 1982). These tissue collagenases act near neutral pH and cleave the collagen molecule at specific locations along the chains. The collagen molecule is typically cleaved into two fragments which readily denature at 37°C; the longer one is 75% of the original length (Harris and Cartwright 1977). However, for complete collagenolysis, intermolecular crosslinks must also be disrupted. Collagenases presumably work in concert with additional enzymes so that molecules at the surface of the fibril become solubilized until eventually the entire fibril is dissolved (Harris and Cartwright 1977).

Interleukin-1ß (IL-1ß) is a cytokine which is believed to play a role in the degradation of articular cartilage in osteo- and rheumatoid arthritis. In vitro and in vivo, IL-1ß induces cells to produce collagenases and proteoglycanases which in turn degrade the tissue extracellular matrix (Hasty 1990, Hardingham 1992, Evans 1991). Treatment of viable cartilage with IL-1ß results in a progressive, dose-dependent release of tissue proteoglycans. In one study, treatment of cartilage explants with IL-1ß resulted in the appearance of an epitope on collagen which could be recognized by a monoclonal antibody (Dodge and Poole 1989). This data suggests that IL-1ß induces a change in the physical structure of the collagen fibril which could compromise the mechanical integrity of the collagen network.

THEORY

MAGNETIZATION TRANSFER

For a brief introduction to general NMR theory, the reader is referred to the theory section in Part I of this thesis. An overview of the theory relevant to the magnetization transfer experiment is presented here. Much of this discussion was taken from recent review articles on magnetization transfer (Balaban and Ceckler 1992, Hajnal 1992) and from original references where indicated.

Magnetization transfer (MT) is the general term used to describe the transfer of magnetization from one species to another. This transfer can occur between protons in bulk water (H_f) which have relatively unrestricted or "free" motion and protons associated with large macromolecules (H_r) which have restricted motion. In one model, a surface layer of water exists next to some macromolecular matrix and water protons communicate with matrix protons via direct chemical exchange or dipole-dipole interaction (Eng 1991).

One experiment used to study MT between two species is called saturation transfer (Wolff and Balaban 1989). This technique was introduced by Forsen and Hoffman (1963) to study chemical exchange rates for systems in which a nuclear species is reversibly transferred between two nonequivalent sites. Consider the chemical reaction A-H $\leftrightarrow$ B-H involving two distinct pools of protons. Briefly, the MT experiment involves the observation of the magnetization of protons from one pool after the saturation of the magnetization of protons in the other pool. Saturation is a state in which there are equal populations of spins in the parallel and antiparallel states and no phase coherence so that the net magnetization vector for that pool of protons is zero. A strong rf field is continuously applied so that one pool of protons is saturated. As magnetization is transferred between the two pools, the net magnetization vector of the other pool decreases (it becomes saturated). The amount of this decrease is a function of the relative concentration and surface chemistry of the protons involved.

In order for the saturation transfer experiment to be useful, it must be possible to saturate one of the pools without affecting the other. In fact, there are two situations in which this condition is met. The first is when two pools of nuclei have different, non-overlapping resonant frequencies. The second is when the two pools have similar resonant frequencies

but the spectrum for one is substantially broader than the other so that a range of frequencies exists over which irradiation would only affect one pool. The latter case is the one which is applicable to cartilage.

For cartilage, two pools of protons are considered: one consisting of the protons in the bulk water and the other consisting of protons on the macromolecules (Figure 13). The restricted macromolecular protons (H_r) exchange magnetization with adjacent water protons which then diffuse and exchange with bulk water protons (H_f). Chemical exchange may also occur between macromolecular and water protons. The water protons have a characteristic relaxation rate, on the order of hundreds of milliseconds, which results in a narrow (10 - 20 Hz) NMR linewidth. The restricted protons, on the other hand, relax quickly; their spectral linewidth is typically very broad (20 - 40 kHz). The protons in the restricted pool are said to be invisible to NMR since they are not detected with conventional NMR pulse sequences due to their very fast T2 relaxation.

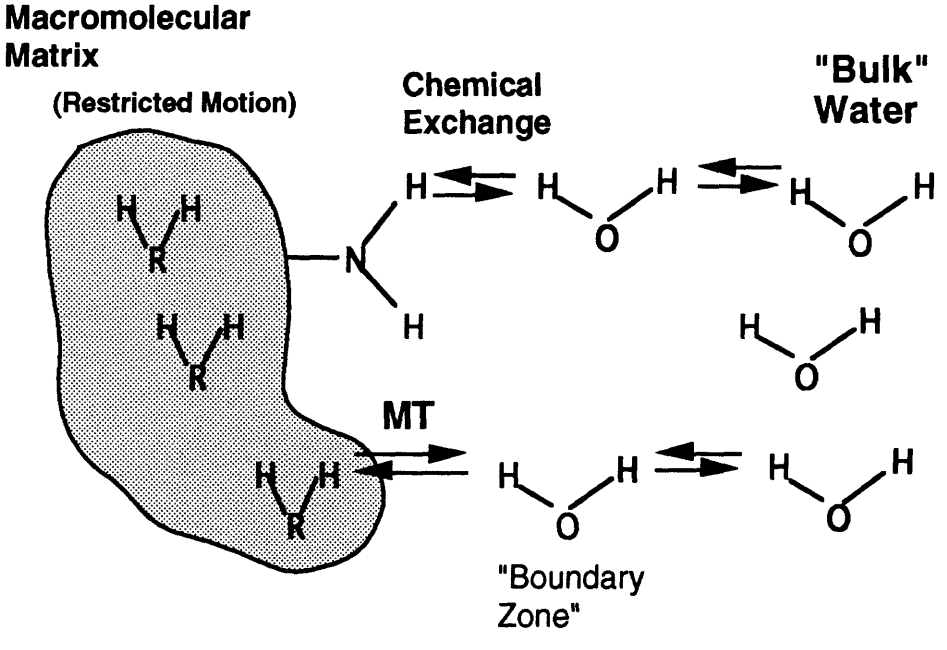

FIGURE 13 Schematic diagram describing water proton magnetization transfer. Note that chemical exchange and diffusion of water to and from the surface layer may contribute to the observed magnetization effect. Figure adapted from Eng 1991.

An rf pulse applied 5 - 10 kHz away from the resonance of the water protons will excite the restricted pool with minimal direct excitation of the unrestricted or water pool (Figure 14). Prolonged excitation at this frequency results in the saturation of the magnetization of the restricted spins. As the magnetization of the restricted pool is saturated, transfer of magnetization between the two pools will result in a decrease in the magnitude of the bulk water (H_f) signal (the one traditionally observed).

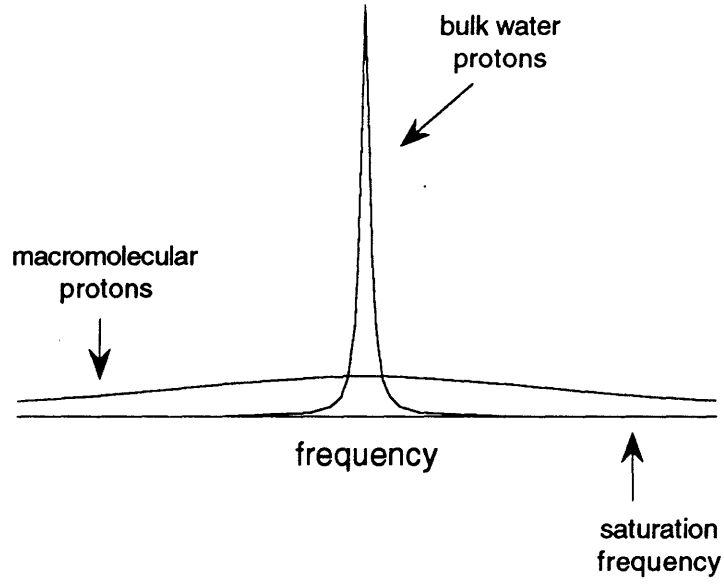

FIGURE 14 Idealized frequency spectra for bulk water protons and for macromolecular protons. The magnetization transfer saturation pulse is directed away from the resonance of the water protons.

Experimentally, the water proton signal, **Mo**, is first measured using a 90 degree pulse. Next, the water proton signal in the presence of saturation of the macromolecular protons, **Ms**, is measured using the following pulse sequence:

$$P_{sat} - 90^{\circ} - \text{acquire} \qquad (21)$$

where P_{sat} is a square rf saturation pulse, directed several kilohertz offset from the resonance frequency. The amount of magnetization transfer is then quantified after Fourier transformation of the two signals (without and with the saturation pulse) by calculating the ratio of spectral area after saturation to that before: Ms/Mo.

Ms is the equilibrium magnetization (for H_f) reached in the presence of continuous saturation of the bound protons. This relative decrease in the water proton signal amplitude (Ms/Mo) depends on the number of protons in the macromolecule and water pools, the rate of exchange of magnetization between the protons in the two pools, and on the T1 relaxation of the bulk water protons. Assuming there is complete saturation of the macromolecular proton pool, Ms/Mo can be expressed as a function of these parameters:

$$\frac{Ms}{Mo} = \frac{1}{1 + k\ T1a} \tag{22}$$

k is the rate constant for magnetization transfer (which is a function of the rate of magnetization exchange between pools and the number of protons in each pool). k has been called a pseudo-first order rate constant because it includes all rate constants involved in the magnetization transfer process (e.g. magnetization exchange, chemical exchange, diffusion). T1a describes the relaxation of the water protons in the absence of exchange.

The process of reaching this new equilibrium is described by the following equation:

$$M(t_{sat}) = (Mo - Ms)\, e^{-(tsat/T1sat)} + Ms \tag{23}$$

where t_{sat} is the length of time for which the saturation pulse is applied, Mo and Ms are the equilibrium magnetizations before and after complete saturation, respectively, and T1sat is the time constant for this process. T1sat is the T1 value of this system in the presence of continuous saturation.

Although Ms/Mo depends on T1a (equation 22), in practice it is difficult to determine T1a since exchange between protons is constantly occurring. However, T1a is related to T1sat:

$$\frac{1}{T1sat} = \frac{1}{T1a} + k \tag{24}$$

T1sat can be directly measured by measuring Ms/Mo for varying saturation pulse lengths and then fitting the data to equation 23 (Hajnal 1992). Alternatively, T1sat can be measured by modifying the inversion recovery sequence (equation 6, Part I) to include a fixed length saturation pulse before the 180° pulse and a variable length saturation pulse during the time delay τ. T1sat is always shorter than T1 measured in the absence of saturation (Balaban and Ceckler 1992). Assuming complete saturation of the macromolecular pool, one can consider Ms/Mo to be a function of k and T1sat:

$$\frac{Ms}{Mo} = 1 - k\,T1sat \qquad (25)$$

Note that Ms/Mo must be between one and zero. For example, in saline or water, Ms/Mo = 1 since there are no macromolecular protons present and pulsing 5 - 10 kHz off resonance will not affect the narrow (20 Hz) water peak.

Recently, magnetization transfer contrast (MTC) imaging has been used to study the human knee. Compared to standard spin echo images, MTC images demonstrated higher contrast/noise ratios for cartilage and synovial fluid with no increase in image acquisition time (Wolff 1991).

Cartilage has been shown to exhibit magnetization transfer; Ms/Mo measured for human articular cartilage is reported to be on the order of 0.2 (Wolff 1991, Ceckler 1992, Kim 1993) compared to 1.0 for synovial fluid (Wolff 1991). In particular, the collagen component of cartilage appears to be the predominant determinant of magnetization transfer in cartilage (Kim 1993). In that study, cartilage samples depleted of proteoglycans exhibited the same degree of magnetization transfer as untreated samples. Proteoglycan monomers in solution (5% w/v) exhibited little magnetization transfer effect while dilute collagen gels (2%) showed significant effect. Based on these results, Kim suggested that collagen is the dominant and perhaps only macromolecular component of cartilage which contributes to the MT effect.

Magnetization transfer may be useful for the determination of collagen content in cartilage and ultimately, the determination of early degradative changes. It is possible that the densely packed fibrils of collagen contain sites of restricted proton motion which will be altered in either concentration or integrity during tissue degradation, such that the observed effect of magnetization transfer will change with increasing degradation.

Correlation times (τ_c) describe the motions associated with the macromolecule-water complex. Studies have shown that correlation times longer than 10^{-9} s are necessary for efficient magnetization transfer (Ceckler and Balaban 1991). Based on MT measurements in aqueous solutions or dispersions of proteins, lipid bilayers, and polymers with varying surface chemistry and dynamic factors, it has been proposed that hydroxyl, amine, or possibly carboxyl groups need to be present on the macromolecular surface for efficient transfer of magnetization (Ceckler 1992). These groups may serve as hydrogen bonding sites, orienting the water proton close to macromolecular protons.

Both collagen and proteoglycans in cartilage contain hydroxyl, amine, and carboxyl groups which might participate in MT. The side chain groups on collagen appear to have sufficiently restricted motion for magnetization transfer to occur. Correlation times with respect to the long axis of the molecule on the order of $\tau_c \leq 10^{-7}$ sec have been reported for chick calvaria collagen, both as fibrils and as molecules in solution (Jelinski 1980). Correlation times of amino acid side chains on the collagen molecule are reported to range from 10^{-3} sec to less than 10^{-9} sec (Torchia 1982). To date, no measurements have been made for amino acid side chains on collagen in articular cartilage (Kim 1993).

Investigation of the molecular motion of glycosaminoglycan chains in cartilage using ^{13}C NMR spectroscopy have shown correlation times on the order of 5×10^{-8} sec (Torchia 1977). The mobility of the glycosaminoglycans was found to be high both in solutions and intact tissue, but highest in solution ($\tau_c \cong 10^{-9}$ sec). The higher concentration of GAG found in tissue increases the probability for interchain interactions, resulting in more restricted motion than would be found in solution. Those studies also showed that the protein portions of the proteoglycan molecule have restricted mobility in contrast to the glycosaminoglycan side chains which are more mobile. It seems possible, therefore, that proteoglycans or other non-collagenous proteins may participate in magnetization transfer.

METHODS

A. NMR METHODS

NMR spectroscopy experiments were performed on an 8.45 tesla Bruker AM Spectrometer (Bruker Instruments, Inc., Billerica, MA), operating at 360 MHz for proton and 95.26 MHz for sodium. Several different NMR experiments were used and are described below. A standard broadbanded probe was used for all experiments, with an rf coil diameter of 10 or 20 mm.

B. NMR EXPERIMENTS

1. ONE PULSE

Spectra were obtained using a 90° pulse sequence with 5T1 between successive excitations to ensure total equilibration of the nuclei before the next pulse (5T1 ≈ 12-16 sec for proton, 100 msec for sodium). The 90° pulse width for proton ranged from 30 to 85 μsec while that for sodium ranged from 15 to 40 μsec, depending on the rf coil used. Typically, the FID signal to noise ratio was improved by averaging 8 FIDs for proton and 3072 for sodium.

Sodium measurements were made as described in Part I. Water content was determined from the proton spectral area. Alternatively, water content was computed as the difference between wet and dry weights (assuming 1 g = 1 mL).

2. T1

Proton T1 was measured using an inversion recovery sequence (see equation 6, Part I). T1 was determined by least squares fit of the data to equation 7 (Part I). There was no evidence of multiple T1 relaxation times for proton.

3. T2

Proton T2 was measured using a Hahn spin-echo experiment (see equation 9, Part I). T2 was determined by least squares fit of the data to equation 8 (Part I). There was no evidence of multiple T2 relaxation times for proton.

4. MT

For each sample, a water proton signal (Mo) was obtained on resonance as described for the one pulse experiment. Resonance area was calibrated to that from a 50 μL sample of water. A second signal (Ms) was then obtained using the saturation transfer experiment (see equation 21). The pulse length used to achieve saturation was at least 5T1 (equal to the time between acquisitions for the one pulse experiment). Methods used for setting and optimization of these parameters are discussed in section F1 below.

C. COLLAGEN MODEL SYSTEM PREPARATIONS

In order to examine the relationship between collagen concentration or state and the magnetization transfer effect, experiments were first performed on model systems of collagen solutions, suspensions, and gels in which collagen content and state could be controlled.

Collagen used in these experiments was of two types, acid-soluble or insoluble, each purchased from Sigma Chemical Company. The purity of these collagens as received from Sigma was not given; no further attempts at purification were made.

Acid-soluble refers to acid-soluble Type I collagen from rat tail tendon (Sigma type VII, C8897). This collagen was prepared by a modification of the extraction method of Bornstein (1958). (Briefly: tendon is dissolved in 1:1000 acetic acid and then freeze dried.)

Insoluble refers to insoluble Type I collagen from bovine Achilles tendon (Sigma type I, C9879). It was prepared by the method of Einbiner and Schubert (1951). (Briefly: tendon is extracted in 3% Na_2HPO_4 to remove soluble proteins, extracted in 25% KCl to remove any proteoglycans, washed with water, dehydrated with alcohol, then air-dried.)

Collagen **solutions** of up to 2% were prepared by dissolving acid-soluble collagen in 1:1000 acetic acid. At concentrations between 1 and 2%, several hours were required for collagen to dissolve; volumes used were too small to enable stirring. Collagen in solution exists primarily as individual molecules.

Hydrated collagen **suspensions** were made by adding water or neutral saline to the dry type I collagen powder (described above), both soluble and insoluble. In these suspensions, collagen was not dissolved but rather in a swollen state. Other investigators have used this same system arguing that it closely represents the native state of collagen since collagen is insoluble but swollen under physiologic conditions (Chien and Wise 1975). Presumably, collagen in suspension exists in whichever state it was after extraction: therefore, it was assumed that suspensions of acid soluble collagen contain predominantly individual molecules (with few fibrils and some crosslinking) while insoluble collagen suspensions contain predominantly fibrils which are extensively crosslinked. Collagen concentrations for suspensions ranged from 1% to 28%.

Collagen **gels** were prepared as follows: Acid-soluble collagen was dissolved in 1:1000 acetic acid. While keeping the solution on ice, appropriate amounts of NaOH and NaCl were added to bring the mixture to neutral pH and 150 mM NaCl. Gelation was then completed by placing the sample in a 37°C incubator or water bath for 10 minutes. Gels were made with collagen concentrations of 0.1% to 2%. At concentrations above 2%, collagen gels become unmanageable. For example, to make a 1% collagen gel, 3.5 mg collagen was dissolved in 350 µL 1:1000 acetic acid and then 3 mg NaCl and 6 µL 1 N NaOH were added. (Note: At 2%, the collagen in acetic acid was so viscous that it made the addition of NaOH and NaCl difficult. The samples were not well mixed and therefore, not homogeneous so the aliquots removed from them for measurement were probably not exactly 2%.) The collagen in gels as described here are similar to native fibrils found *in vivo* (Gross 1961).

Thermal **denaturation** of collagen gels was achieved by placing a centrifuge tube containing the sample in a 55°C water bath for 45 min. The extent of denaturation was not determined. The denatured sample was re-gelled by placing it in an incubator at 37°C for another 15 min. Soluble and insoluble collagen suspensions were also denatured by heating for 30 min at 55°C (soluble) or 70°C (insoluble).

For collagen solutions, gels, and suspensions, collagen concentrations (w/w) were determined as the ratio of collagen (dry weight) to water weight (water weight = total weight minus collagen weight), where 1% collagen equals 1 g collagen per 100 mL water.

D. CARTILAGE PREPARATIONS

Three types of bovine cartilage were used for the NMR experiments: articular cartilage from the femoropatellar joint of adult cows (**adult AC**) and calves (**calf AC**) and epiphyseal cartilage from calves (**calf EP**). Intact foreleg (EC) and hindleg (calf AC) knee joints from 1 to 2 week old calves were obtained immediately after slaughter from A. Arena (Hopkinton, MA); adult bovine hindleg (adult AC) knee joints were obtained frozen from City Packing (Boston, MA). Cartilage was harvested from the femoropatellar groove (AC) or distal ulna (EC) according to previously established techniques to yield plane-parallel disks 0.8 to 2 mm thick and 6.4 to 9.6 mm (1/4 to 3/8 in) diameter (Gray 1988, Sah 1990). Unless otherwise indicated, calf AC was used and tissue was stored at -20°C until later use. For one experiment, additional cartilage samples were used from the calf meniscus and calf metacarpal joint (AC).

A few measurements were made on human cartilage samples, both normal and pathologic. Normal adult articular cartilage was harvested from the femoropatellar groove (FP); pathologic specimens were obtained from the femoral head (FH). FP samples were from previously frozen cadaveric specimens; FH samples were from post-operative joints of patients undergoing hip replacement surgery. Permission for studies on human samples was obtained from the Committee on Clinical Investigations of Beth Israel Hospital. Individual disks of cartilage were obtained by scoring the cartilage with a 7 mm diameter dermal punch and then dissecting the cartilage away from the underlying cortical bone. Universal precautions were observed when handling human specimens. Samples were stored at -20°C until study.

At least two hours before an experiment (in most cases, overnight), disks were thawed (if frozen) and equilibrated at room temperature (or 4°C if equilibrated overnight) in the desired bathing solution. Baths were at least 10 mL per disk which is approximately 100 times the volume of the sample. Unless otherwise indicated, solutions were 150 mM NaCl, 1 mM Tris at pH 8. After equilibration, each sample was taken out of its bathing solution, blotted dry, weighed, and placed in a capped NMR tube.

Various perturbations to the cartilage were performed in order to examine the response of MT to changes in matrix composition. These perturbations included compression, enzymatic degradation, and interleukin-1ß treatment.

Compression Cartilage samples used for compression were typically 5 mm in diameter and 2 mm in thickness. Samples were placed in a specially designed NMR-compatible device which allowed radially unconfined compression between two impermeable platens (Hartman 1991). The degree of compression was established by adjusting the spacing between the platens. Control studies confirmed that insignificant NMR signal was obtained from the compression device. After a new displacement was applied, the sample holder (constraining the sample) was placed in a stirred bath for at least 90 min. Before NMR measurements were made, the sample holder was removed from the bath and thoroughly blotted dry, including the edges of the sample.

Trypsin Cartilage was depleted of proteoglycans and noncollagenous proteins by exhaustive trypsin digestion. Samples were bathed at 4°C overnight in saline containing 25 mg/mL trypsin (lyophilized porcine, from Gibco Laboratories). Cartilage was typically removed from the trypsin solution and bathed in fresh saline for at least one hour before being used in an NMR experiment.

IL-1ß Freshly harvested epiphyseal cartilage samples were cultured in media containing human recombinant IL-1ß (kindly supplied by Dr. Lee Gehrke of MIT). Cartilage was maintained in standard organ culture throughout the experimental period, as the effectiveness of IL-1ß requires viable cells. Culture media consisted of Dulbecco's Modified Eagle's Medium supplemented with 1% fetal calf serum, 0.1 mM nonessential amino acids, 20 µg/mL ascorbate, 100 U/mL penicillin, and 100 µg/mL streptomycin. Each day, the tissue was removed from culture, blotted dry with sterile filter paper, and placed in a sterile NMR tube for NMR measurements which were made at room temperature. Each sample was returned to fresh media after completion of the measurements.

E. CHEMICAL ANALYSIS

Collagen content was determined by hydroxyproline analysis. Samples were first lyophilized and dry weights were obtained. Samples were then hydrolyzed. Each sample was placed in a separate glass tube and 1 mL of 6 N constant boiling HCl (Pierce Chemical

Company) was added. The solution was degassed by freeze pump thawing (three times) and then the apparatus was sealed under vacuum. Samples were heated at 110°C for 24 hours and then transferred to individual test tubes (rinsed with 250 mL distilled water). Finally, the solvent was removed under vacuum (leaving a brown oil).

Amino acid analysis was performed in the laboratory of Dr. Melvin Glimcher at Children's Hospital with the technical assistance of Ms. Marie Torres. Collagen content was determined from the amount of hydroxyproline residues present in each sample according to the following equation:

$$\text{total collagen} = 10^{-3}\,(\text{vol})\,(\text{dilution})\,(10\ \text{hyp})\,(\text{MRW}) \qquad (26)$$

where **total collagen** is in mg/sample, **vol** is the sample volume in mL, **hyp** is the number of hydroxyproline residues in nmol/mL, and **MRW** is the collagen mean residue weight in g/mol. The term (10 hyp) equals the number of residues in collagen and comes from the assumption that there are 100 hyp residues per 1000 collagen residues (Hauschka and Reid 1978). MRW was assumed to be 111 g/mol (including the weight of oxygen to obtain pre-hydrolysis collagen content).

EXPERIMENTAL PROTOCOLS

A. CHARACTERIZE EXPERIMENTAL PARAMETERS

1. SATURATION PULSE LENGTH, POWER, AND FREQUENCY OFFSET

The first set of experiments were designed to characterize the MT experiment and choose the MT experimental parameters: saturation pulse length, power, and frequency offset. To determine whether this characterization changed with different collagen conditions, experiments were carried out on insoluble collagen suspensions and on cartilage samples. The ultimate goal was to achieve complete saturation of the macromolecular protons with minimal direct saturation of the water protons, in order to maximize the amount of magnetization transfer (minimize Ms/Mo).

Ms/Mo was measured in collagen suspensions and cartilage samples as the length of the saturation pulse varied (typically from 0.15 to 7.2 sec) or as the power of the saturation pulse varied (typically from 5 to 40 μT). Furthermore, to determine whether saturation pulse length and power combined to produce a maximum MT effect, Ms/Mo was measured as pulse length was varied for several different power levels. In addition, to examine the relationship between offset frequency and time for saturation, Ms/Mo was measured in cartilage as saturation pulse length varied for offset frequencies of 10, 20, and 25 kHz.

To characterize the frequency response of the magnetization transfer effect, Ms/Mo was measured in NaCl, collagen suspensions and cartilage samples as the frequency offset of the saturation pulse varied from 500 Hz to 50 kHz. To observe the relationship between the offset frequency and applied power of the saturation pulse, Ms/Mo was also measured in cartilage as a function of offset frequency at several saturation pulse power levels.

2. OTHER EXPERIMENTAL PARAMETERS

To examine the MT effects of freezing samples after harvesting, Ms/Mo was measured in articular cartilage samples before and after freezing. Cartilage was harvested and immediately stored at 4°C in a sealed tube (no bathing solution). 48 hrs later, each sample was equilibrated in 150 mM NaCl and Ms/Mo was measured 2 or 3 times, returning sample to its bath in the refrigerator for 60 min between measurements. Samples were then frozen

for 90 min and then for 60 hrs, after which times Ms/Mo was again measured twice with 60 min refrigeration between measurements.

To determine the effect of temperature on the MT measurement, Ms/Mo was measured for 10% and 20% insoluble collagen suspensions and for cartilage as the temperature inside the probe varied from 17°C (room temperature) to 35°C.

B. DEPENDENCE OF MT ON COLLAGEN CONCENTRATION

The second set of experiments was designed to evaluate the relationship of MT to collagen concentration. Collagen concentration was varied using model systems, trypsin digested cartilage under compression, and intact cartilage with varying collagen content.

1. MODEL SYSTEMS

To first examine MT as a function of the concentration of molecular collagen, Ms/Mo was measured in 0.1%, 1% and 2% (w/w) collagen solutions (acid soluble collagen). Ms/Mo was also measured for soluble collagen suspensions, which were assumed to contain primarily molecular collagen, with concentrations ranging from 1% to 10% (w/w). Ms/Mo was then measured in collagen gels with concentrations varying from 0.1% to 2% (w/w). Collagen gels were assumed to contain fibrils which, though similar to those found *in vivo*, lack the extensive crosslinking.

To next examine MT as a function of fibrillar collagen concentrations, with concentrations on the order of those found *in vivo*, Ms/Mo was measured for insoluble collagen suspensions of varying concentration. These insoluble suspensions were assumed to contain primarily highly crosslinked, fibrillar collagen. Aliquots of 150 mM NaCl (pH 8 with 1 mM Tris buffer) were added to insoluble collagen to make suspensions with concentrations ranging from 1% to 28% (w/w).

2. CARTILAGE

Extensive trypsin digestion of cartilage yields a relatively pure collagen matrix. Thus, one way to examine the degree to which the MT effect is a function of native crosslinked fibrillar collagen concentration is to measure the change in Ms/Mo in response to controlled compression of trypsin-digested cartilage. Several cartilage samples were depleted of GAG

and other noncollagenous protein by overnight trypsin digestion. Initial measurements of Ms/Mo were made. Measurements were repeated after each of several progressively larger compressions; tissue was bathed for at least 15 min in buffered 150 mM NaCl between each compression.

Another way to examine the relationship between the MT effect and native crosslinked collagen concentration is to study various types of cartilage since collagen concentration varies with age and source of cartilage. Ms/Mo was measured for samples of calf cartilage (epiphyseal, femoropatellar AC, metacarpal AC, and meniscal) and adult cartilage (femoropatellar AC). Samples were later analyzed for collagen content by hydroxyproline analysis.

C. DEPENDENCE OF MT ON COLLAGEN STRUCTURE AND/OR STATE

The next set of experiments were designed to specifically evaluate the dependence of MT on the structure and/or state of the collagen (molecular, fibrillar, crosslinked, denatured).

We were first interested in examining any difference between MT in collagen molecules and in collagen fibrils. Although collagen solutions are known to contain collagen molecules, it was difficult to obtain concentrations higher than 1%. Therefore, data (described above) for 1% to 10% soluble suspensions were compared to data (also described above) for insoluble suspensions of equal concentration. It was assumed that soluble suspensions contained primarily collagen molecules and that insoluble suspensions contained collagen fibrils.

Next, we were interested in evaluating the role of the triple helical structure of the collagen molecule in the MT process. Therefore, we examined the effect of heat denaturation which results in the loss of the triple helix. Ms/Mo was first measured in collagen gels before and after thermal denaturation and again when the denatured samples had re-gelled. To more closely follow the denaturation process, Ms/Mo was measured periodically for a 5% soluble collagen suspension as temperature increased from 19°C (room temperature) to 40°C; soluble collagen is known to denature near 37°C (Burjanadze 1979). Ms/Mo was also measured in 1%, 5%, and 10% soluble and insoluble collagen suspensions before and after thermal denaturation.

D. MT FOR DETECTION OF CARTILAGE DEGRADATION

Finally, we were interested in determining the specificity with which MT can be used to evaluate cartilage degradation. After having studied normal bovine cartilage samples (above), we then perturbed the samples to impact collagen structure and mimic tissue pathology. Finally, we evaluated normal and pathologic human cartilage specimens.

1. MIMIC TISSUE PATHOLOGY

a. Loss of proteoglycans with trypsin

Since proteoglycans are lost during degeneration of cartilage, we were interested in studying the impact of their loss on MT in cartilage. We studied the contribution of proteoglycans and noncollagenous proteins to magnetization transfer in cartilage by measuring MT before and after trypsin digestion of cartilage. After exposure to trypsin, total tissue water decreases due to the loss of the charges proteoglycans which are abundantly hydrated. Loss of proteoglycans also decreases the osmotic pressure on collagen, thus increasing intrafibrillar water content.

Articular cartilage samples were equilibrated in 150 mM NaCl, 1 mM Tris. Ms/Mo was measured for each sample; sodium content was measured for some samples. Samples were then placed in baths with trypsin added. Two samples were returned to their NaCl baths as controls. After three to five hours at room temperature, Ms/Mo (and sodium content) were again measured in each of the samples. FCD was calculated from sodium data to determine loss of GAG (Lesperance 1992).

To investigate the consequences of prolonged exposure of cartilage to trypsin, Ms/Mo and sodium were measured for several cartilage samples before and after one to four hours in trypsin and again after 16 or 21 hours in trypsin.

b. Cartilage at low pH

Changes in bath pH affect collagen hydration and structure as well as overall tissue hydration. At low pH, matrix carboxyl and sulfate groups are protonated. In native cartilage, the loss of negative charge on the proteoglycans results in decreased proteoglycan hydration and therefore, decreased total tissue water. Collagen intrafibrillar hydration

increases both due to the development of a net positive charge on the collagen molecule (electrostatic repulsion) and to the loss of proteoglycan charge (decreased osmotic pressure exerted against the collagen fibrils). In trypsin-treated cartilage which has been depleted of proteoglycans, pH affects only the collagen charge. The net result is increased intrafibrillar hydration and increased total tissue water.

To investigate the effect of low pH on MT, articular cartilage samples were equilibrated for 90 min in 150 mM NaCl at pH 8 (buffered with 1 mM Tris). Ms/Mo was measured for each sample. Several of the samples were then sequentially bathed for >90 min in 150 mM NaCl at pH 4, and 2 (titrated with HCl) and finally in their original pH 8 bathing solution. The remaining samples were bathed in their original pH 8 solution for an equivalent total time. Ms/Mo was measured after each bath. This experiment was also repeated on trypsin-digested samples in order to eliminate the changes due to the proteoglycans and isolate the effect of pH on the collagen component of cartilage.

To more specifically examine the contribution of osmotic forces to magnetization transfer at low pH, the varying pH experiment was repeated in an abbreviated form in the presence of 0.5 M NaCl. With higher concentrations of salt, the forces experienced by adjacent matrix charges are less. An excess of positively charged sodium ions (i.e. greater than the fixed charge density) can effectively shield the negative charges on the GAG. Higher salt concentration would also be expected to shield any net positive charge developed on the collagen molecule at low pH, thus minimizing changes in fibril hydration. Samples were sequentially equilibrated (for 90 min) in 0.5 M NaCl at pH 8 then pH 2, and finally back to pH 8. Ms/Mo was measured after each equilibration.

c. Enzymatic degradation of collagen

In order to evaluate the potential use of the MT technique for the detection of cartilage changes as might be seen in pathologic states, we were interested in determining the relationship between the MT effect and collagen degradation. We exposed living cartilage to collagenase and other metalloproteinases indirectly by incubating samples with IL-1ß. To study the resulting effect on MT, Ms/Mo was measured for six samples cultured in media containing 0, 10, or 100 ng/mL IL-1ß. In addition to Ms/Mo, sodium was measured for each sample. FCD calculations from sodium measurements were used to track GAG loss and thus, verify IL-1ß effectiveness.

2. CLINICAL SPECIMENS

Finally, for preliminary examination of the relationship between MT and cartilage degradation in human tissue, Ms/Mo was measured for both normal and pathologic samples.

RESULTS

All averaged results are presented as mean ± SD. Statistical analysis involving comparison of samples before and after experimental treatment or between two groups was performed using Student's t test, either paired or unpaired, respectively. Collagen concentrations are expressed as percents (w/w), where 1% equals 1 g collagen per 100 mL water.

A. CHARACTERIZE EXPERIMENTAL PARAMETERS

Characterization of the MT experimental parameters was an iterative process since saturation pulse length, power, and offset frequency simultaneously affect the MT process.

1. SATURATION PULSE LENGTH, POWER, AND FREQUENCY OFFSET

Ms/Mo measured as a function of saturation pulse length at several saturation pulse power levels is shown in Figure 15 for 10% insoluble collagen suspension and for cartilage. Ms/Mo decreases with increasing pulse length. It takes a significant amount of time for the system to reach its new equilibrium due to the slow rate of exchange of magnetization between macromolecular and bulk water protons (Balaban and Ceckler 1992). One way to quantify the speed at which Ms/Mo decays (as in Figure 15) and enable objective comparison of the different curves is to assume an exponential fit for the data and calculate time constants (as in equation 23). In this case, with Ms/Mo versus saturation pulse length, the time constant represents T1sat (Hajnal 1992). Data for this and subsequent experiments (which measured Ms/Mo as a function of varying saturation pulse length) were fit to a single exponential to determine values for T1sat (see Table 3). At higher saturation power, Ms/Mo decreases more rapidly with increasing pulse length (T1sat decreases) and reaches a smaller final value. However, the change in Ms/Mo becomes less as power increases; presumably Ms/Mo is approaching a minimum value.

Figure 16 shows Ms/Mo versus saturation pulse length in cartilage at several different offset frequencies. T1sat was also calculated for these data (Table 4). Ms/Mo decreases more rapidly and reaches a smaller final value as saturation is directed closer to the resonant frequency.

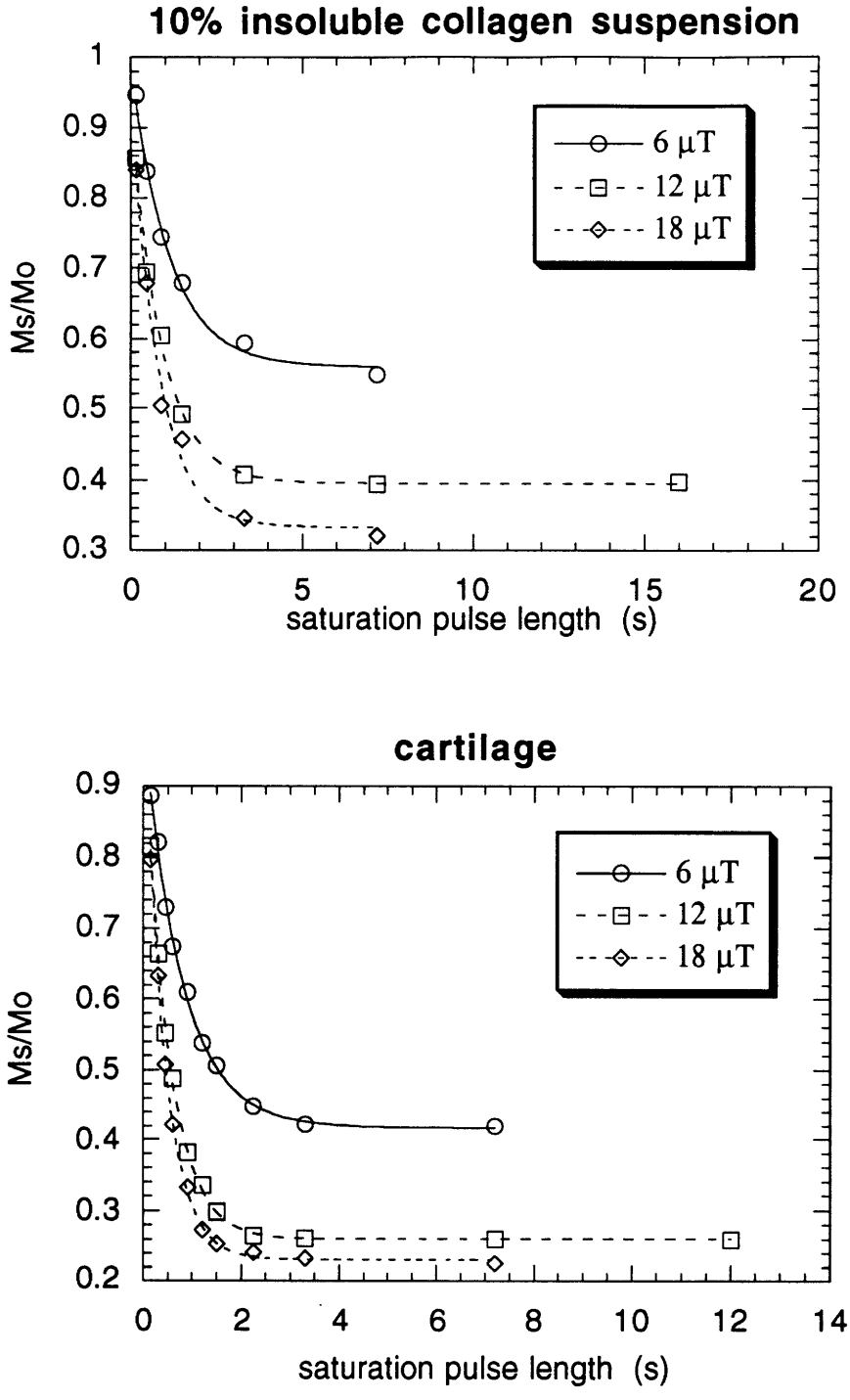

FIGURE 15 Ms/Mo versus saturation pulse length for varying levels of saturation power in 10% insoluble collagen suspension (at 6 kHz offset) and cartilage (at 10 kHz offset). Data are fit to a single exponential using equation 23.

Table 3 T1sat measured in 10% insoluble suspension (at 6 kHz offset) and cartilage (at 10 kHz offset) for varying saturation power (see Figure 15).

saturation power	10% suspension T1sat (sec)	cartilage T1sat (sec)
6 μT	1.11	0.78
12 μT	0.88	0.50
18 μT	0.80	0.42

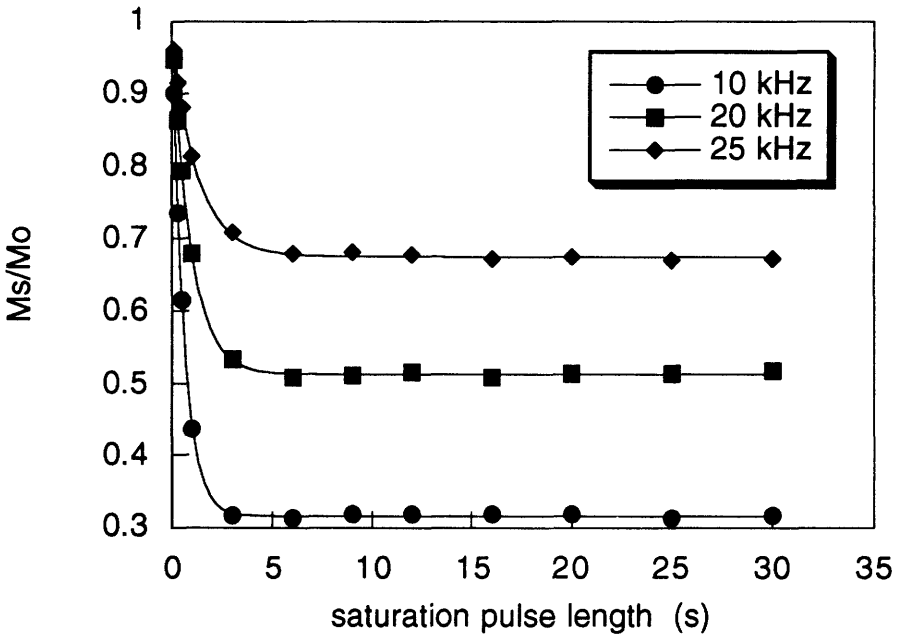

FIGURE 16 Ms/Mo versus saturation pulse length for varying offset frequencies in cartilage at 12 μT saturation power. Lines plotted are for data fit to a single exponential (equation 23).

Table 4 T1sat measured in cartilage for varying offset frequencies at 12 μT saturation power (see Figure 16).

offset frequency	T1sat (sec)
10 kHz	0.58
20 kHz	0.94
25 kHz	1.30

Table 5 lists data for two cartilage samples in which T1sat was measured using both the varying pulse length method and a modified inversion recovery sequence in the presence of saturation. Saturation power and frequency offset were kept constant throughout. The values for T1sat calculated using both methods are comparable. T1 (without saturation) was also measured for each sample. T1 was considerably longer than T1sat (using either method), consistent with theoretical predictions. In the presence of saturation, the system relaxes with the shorter time constant T1sat. Ms/Mo values measured with saturation pulse lengths on the order of 5T1sat were identical to those measured with saturation pulse lengths of 5T1. However, the pulse saturation length was chosen to be 5T1 (at least 10 sec). T1 measured on cartilage samples was consistently around 1.8 sec, for a variety of experimental conditions (except increasing temperature for which T1 increases are expected and were observed; data shown in Table 8). T1sat was much more variable under different experimental conditions; for example, T1sat values in tables 3, 4, and 5 range from 0.4 to 1.3 sec. The more conservative estimate of relaxation time based on T1 ensured complete longitudinal relaxation between data acquisitions and maximum saturation for the applied power.

Table 5 T1sat and T1 measured in cartilage. T1sat is measured using two different techniques (varying saturation pulse length and modified inversion recovery).

sample	varying length T1sat (sec)	modified IR T1sat (sec)	T1 (sec)
A	0.37	0.41	1.80
B	0.50	0.52	1.83

Shown in Figure 17 is the relationship between Ms/Mo and applied saturation pulse power for several collagen suspensions and cartilage samples. For each sample, data are plotted relative to its value for Ms/Mo at 12 μT. Ms/Mo decreases with increasing saturation power, apparently approaching some minimum value. However, increased power output means increased power deposition in the sample and potentially, increased tissue heating. Therefore, to lessen tissue heating and enable comparison of our results to those of other investigators, the power level used in subsequent experiments was 12 μT, as published in previous reports (e.g. Kim 1993). The power setting for our system (per cent of maximum output) was determined, using the saturation pulse for excitation, by that power necessary to produce a 180° flip angle with a saturation pulse width of 1 msec (such that the saturation power equals 12 μT; see equation 5, Part I).

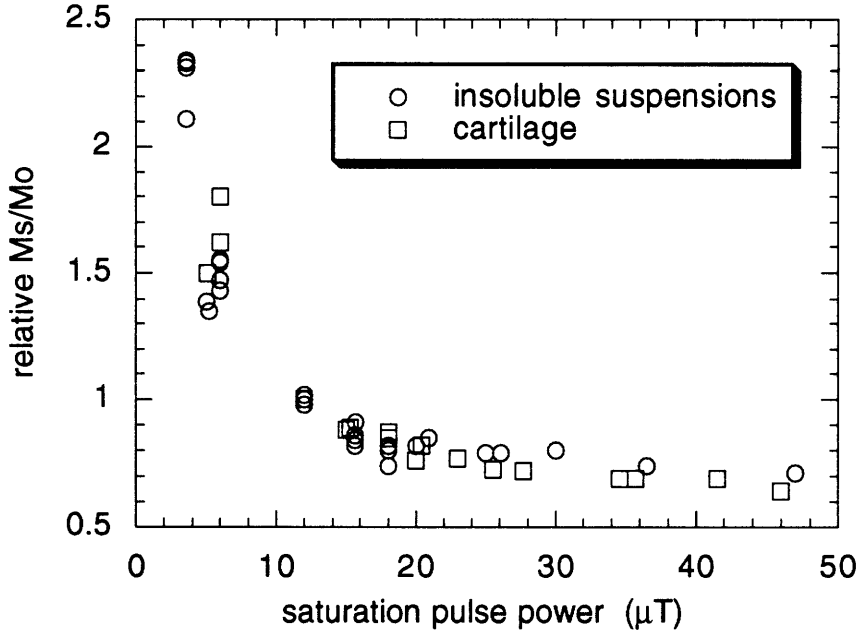

FIGURE 17 Ms/Mo versus saturation pulse power for collagen suspensions and cartilage. Data for each sample are plotted relative to the average value for that sample at 12 μT.

The relationship between Ms/Mo and frequency offset for saline solution, 20% fibrillar collagen suspension, and cartilage are illustrated in Figure 18. Saline has a narrow bandwidth, i.e. saturation at offset frequencies greater than 1 kHz does not decrease the signal. The decrease in signal below 1 kHz is due to the direct saturation effects of the MT pulse on the bulk water. Cartilage and collagen, on the other hand, are similar to each other but distinctly different from the saline in their frequency response. Between 50 and 1 kHz, the signal is gradually decreased due to indirect saturation of the water through magnetization transfer from macromolecular protons. Below 1 kHz, there is a steep decrease in Ms/Mo due to direct saturation of tissue water in addition to the indirect saturation from magnetization transfer.

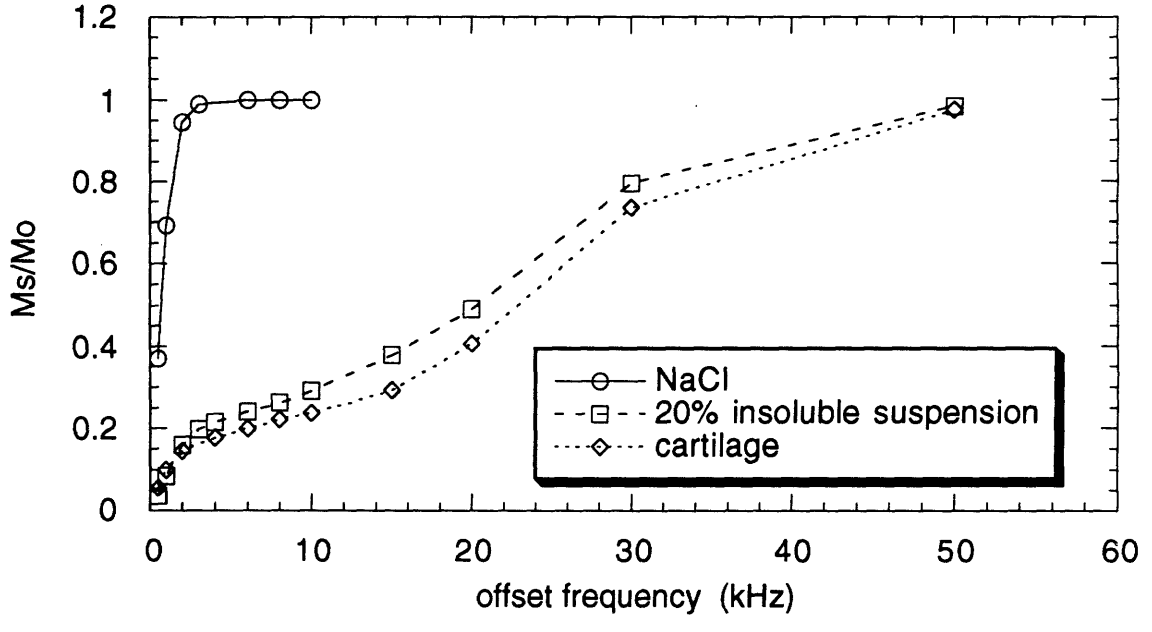

FIGURE 18 Ms/Mo versus offset frequency in NaCl solution, 10% insoluble collagen suspension and cartilage at 12 μT saturation power.

Theoretically there would be a range of offset frequencies in which irradiation would completely saturate the restricted proton pool without affecting the bulk water pool. However, the shape of these curves indicate that the amount of saturation achieved is a function of offset frequency. For constant power, saturation is less effective as the offset increases from the center frequency of the macromolecular proton spectrum. The optimal frequency offset would give maximal saturation of macromolecular protons with minimal direct saturation of the water protons. Visual inspection of these and many other frequency response curves revealed a "plateau" region between 5 and 10 kHz where Ms/Mo increased only slightly with increasing offset frequency. Therefore, we chose this region (specifically, 5 or 6 kHz) to be the optimal frequency offset since saturation of macromolecular protons was achieved without significant direct saturation of water.

Balaban and Ceckler (1992) theoretically calculated an optimal offset frequency for generating image contrast based on the difference between idealized water proton (T1 = 2 sec, T2 = 20 msec) and macromolecular proton (T1 = 2 sec, T2 = 100 μsec) signals. For a 12 μT saturation field, their theoretical optimal frequency range was between 8 and 18 kHz. However, while many studies have been performed using 10 kHz offset (e.g. Fralix 1991, Ceckler and Balaban 1991, Ceckler 1992, Kim 1993), Balaban and Ceckler (1992) have begun to perform studies with much smaller frequency offsets (~1 kHz) and smaller saturation power (0.1 - 1 μT). As Figure 19 illustrates, smaller frequency offsets are more efficient with regard to power. For example, to obtain Ms/Mo = 0.2 with 9 kHz offset requires 20 μT of power, at 6 kHz offset the power requirement is reduced to 15 μT, and at 4 kHz offset, the power necessary to obtain the same value for Ms/Mo is only 12 μT. While it may be possible to obtain clinically useful images with significant contrast using smaller frequency offsets, the resulting absolute value of Ms/Mo probably contains a significant contribution from direct saturation of the bulk water. Therefore, interpretation of the data with regard to the contribution from the macromolecular protons would not be straightforward.

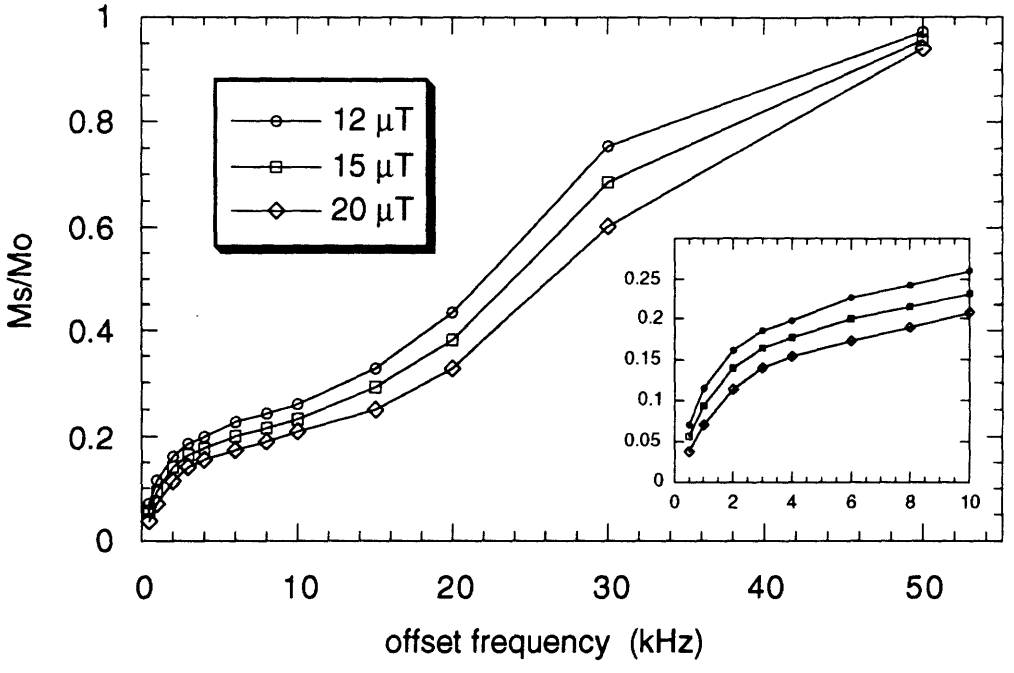

FIGURE 19 Ms/Mo measured in cartilage as a function of offset frequency for several different saturation pulse power levels. Inset shows detail of 0 to 10 kHz data corresponding to discussion in text.

For a few samples, Ms/Mo was measured for both positive and negative frequency offsets. The results for one cartilage sample are shown in Figure 20. The frequency response was symmetric with respect to the resonant frequency of the sample. This shows that the frequency spectrum of the macromolecular protons is centered around that of the water protons and also demonstrates that the resonant frequency was properly identified. Therefore, the saturation transfer experiment could be performed with either positive or negative frequency offsets.

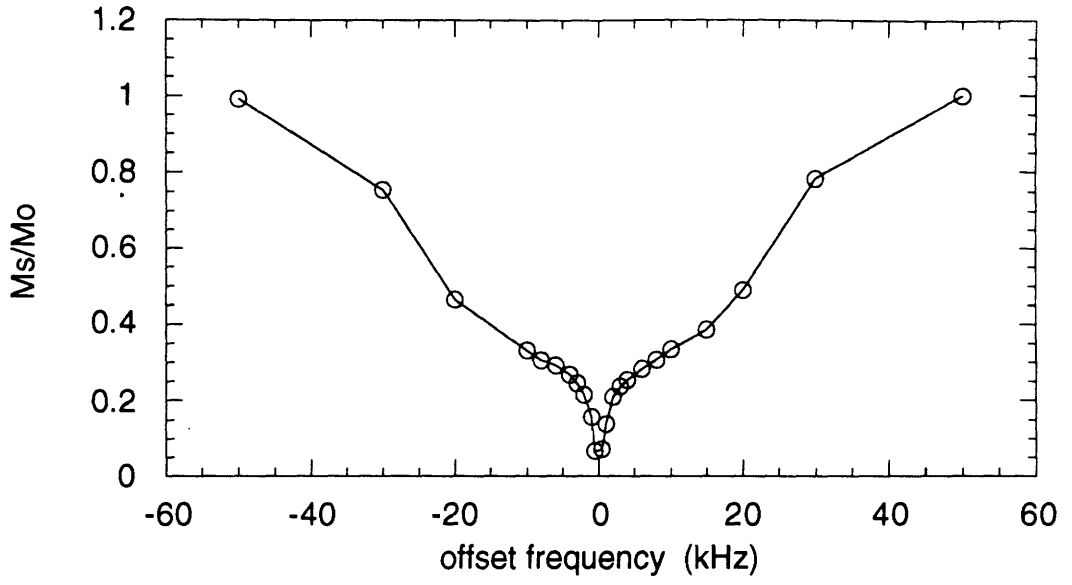

FIGURE 20 Ms/Mo measured in cartilage as a function of both positive and negative offset frequency (with respect to the resonant frequency) at 12 μT power.

The frequency response curves in Figures 18 and 20 have shapes similar to those obtained for cartilage by other investigators using the same saturation power (Morris and Freemont 1992, Kim 1993). The curves of Figure 20 also resemble frequency response curves obtained for agar gels with varying saturation pulse power (Henkelman 1993).

Summary of experimental parameters Saturation pulse length was chosen to be at least 5T1 (typically 12 sec for cartilage, 16 sec for collagen model systems), saturation pulse power was 12 μT (set with 1 msec 180 degree pulse), and frequency offset was 6 kHz. All experiments were performed at room temperature unless otherwise stated.

2. OTHER EXPERIMENTAL PARAMETERS

Ms/Mo measured for cartilage samples (n = 4) before and after freezing are shown in Table 6. Ms/Mo did not change significantly after freezing ($p > 0.05$).

Table 6 Ms/Mo measured in cartilage before and after freezing. Numbers in parentheses indicate the number of repeated measurements on each sample.

sample	Ms/Mo before freezing	Ms/Mo after freezing
1	0.29 ± 0.008 (n = 3)	0.32 ± 0.006 (n = 2)
2	0.28 ± 0.008 (n = 3)	0.29 ± 0.01 (n = 2)
3	0.28 ± 0.004 (n = 2)	0.30 ± 0.012 (n = 3)
4	0.29 ± 0.001 (n = 2)	0.29 ± 0.004 (n = 3)

To evaluate the repeatability of the Ms/Mo measurement, the above measurements were used to calculate coefficients of variance. For measurements made on the same day, the average coefficient of variance was 2.2% ± 1.1% (n = 8); for measurements made on the same and different days, the average coefficient of variance was 4.1% ± 2.1% (n = 4). For this same group of samples over all measurements on the same and different days, the average variation for proton areas was less than 2% (COV = 1.8% ± 0.4%) and the average variation for wet weights was less than 1% (COV = 0.2% ± 0.1%).

To illustrate the relationship of temperature to MT, Figure 21 shows Ms/Mo measured in 10% and 20% insoluble collagen suspensions and cartilage as a function of temperature. Ms/Mo decreases as the sample temperature increases. The decrease in Ms/Mo with increasing temperature most likely reflects an increased rate of interaction between macromolecular and water protons (due to increased molecular motion). The slope of the regression line plotted though the 10% collagen suspension data is approximately four times that for the cartilage sample and approximately twice that for the 20% collagen suspension. The difference in the slopes may be a function of the different initial values for Ms/Mo.

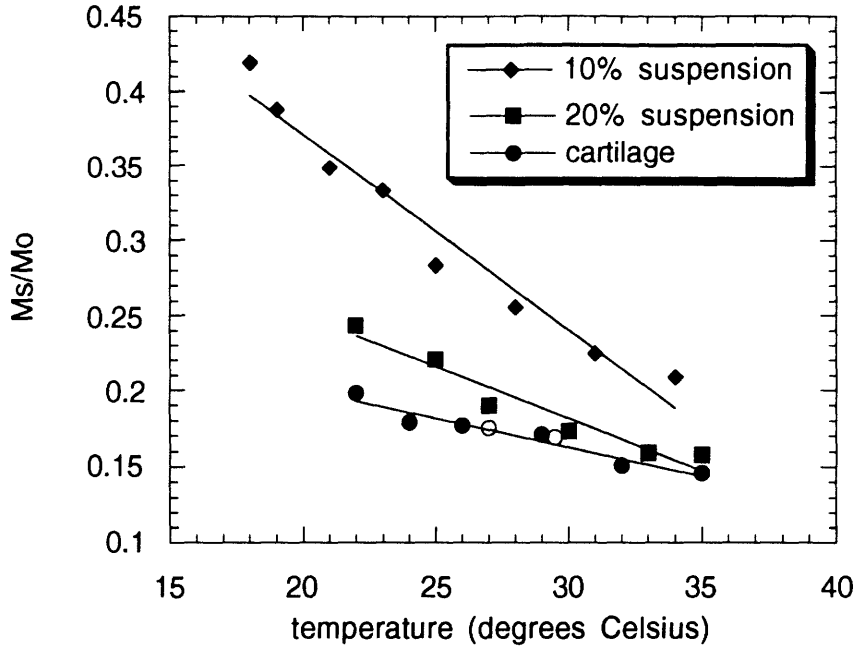

FIGURE 21 Ms/Mo measured for varying sample temperature in insoluble collagen suspensions and cartilage (at 6 kHz offset). Open symbols represent data obtained for one sample while it was cooling after being heated.

B. DEPENDENCE OF MT ON COLLAGEN CONCENTRATION

1. MODEL SYSTEMS

Figure 22A shows Ms/Mo measured for acid soluble collagen solutions, soluble collagen suspensions and collagen gels, with collagen concentrations ranging from 0.1 to 10%. In these preparations, collagen exists predominantly as individual molecules (soluble suspensions and solutions) or as newly formed fibrils with little or no crosslinking (gels). Ms/Mo decreases (MT increases) with increasing collagen concentration.

Shown in Figure 22B is data for insoluble collagen suspensions, with collagen concentrations ranging from 1 to 28%. For these suspensions which contain highly crosslinked fibrils, Ms/Mo also decreased with increasing collagen content. The decrease was nonlinear; at higher concentrations (those near physiologic values), the change in Ms/Mo for a given change in concentration was smaller than at low concentrations.

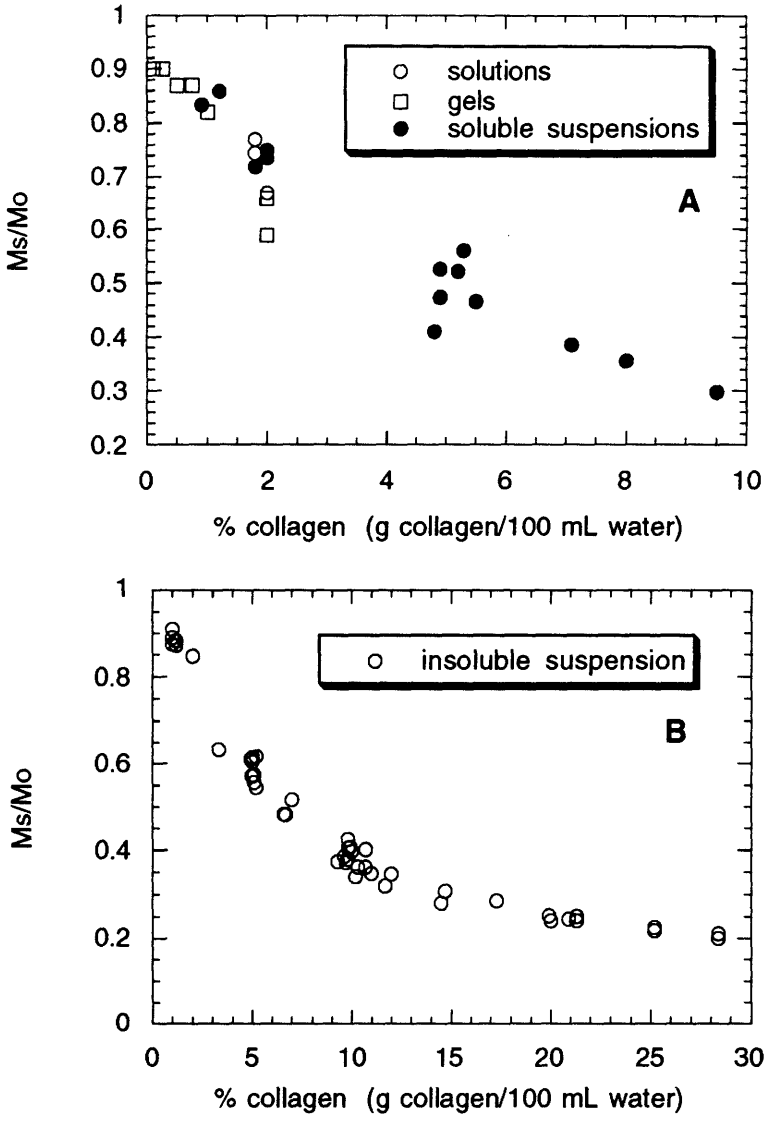

FIGURE 22 Ms/Mo versus collagen concentration for A) collagen solutions, collagen gels, and soluble collagen suspensions and for B) insoluble collagen suspensions.

A subset of these insoluble suspensions (3, 7, 11, and 20%) was studied at several offset frequencies, in order to determine whether saturation frequency affected the ability to discriminate between samples of varying collagen concentrations. As shown in Figure 23, the difference in Ms/Mo among these samples was greatest between 2 and 10 kHz (which included our 6 kHz setting); the difference between samples decreased on either side of this region. This is not surprising since in the limit as frequency approached zero or infinity (more practically, the edge of the macromolecular proton spectrum around 50 kHz), Ms/Mo must be equal for all samples. That is, Ms/Mo equals zero at resonance where water is directly saturated and it equals one at high frequencies where the macromolecules are unaffected by the saturation pulse. In model systems containing collagen up to physiologic concentrations, therefore, the MT effect is strongly dependent on collagen concentration.

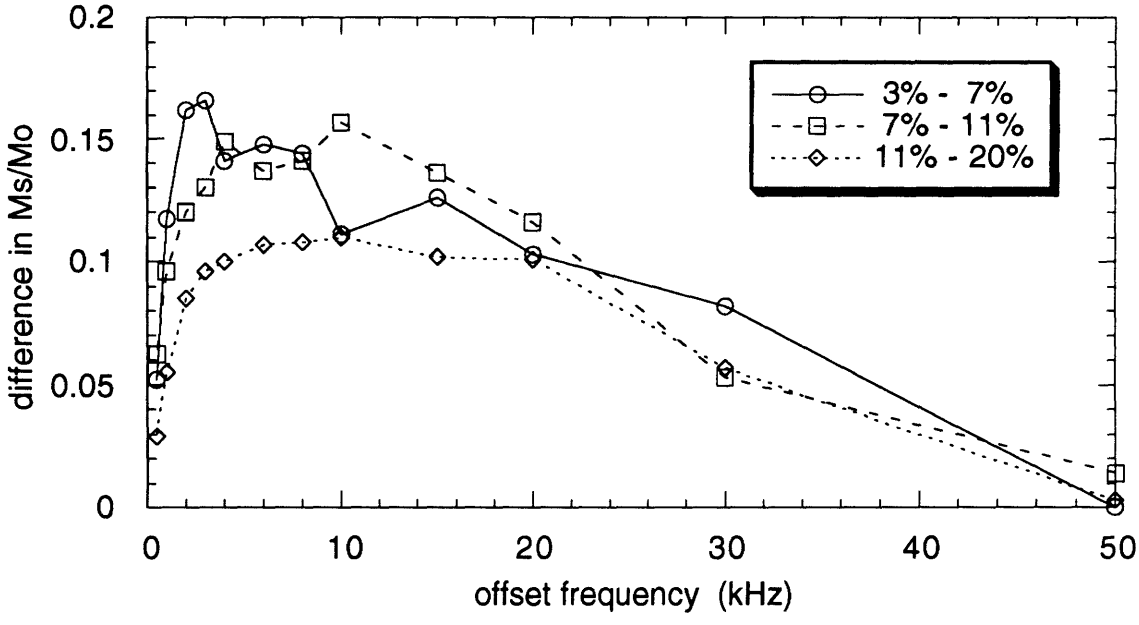

FIGURE 23 Difference in Ms/Mo between collagen suspensions of varying concentration as a function of offset frequency (at 12 μT saturation power). Each line represents difference taken between two suspensions, as indicated in the legend.

2. CARTILAGE

Shown in Figure 24 is Ms/Mo measured for trypsin-digested cartilage compressed by increasing amounts. Collagen concentrations are estimated for trypsin digested samples by assuming that the final dry weight of the sample is due only to collagen and then dividing this by measured tissue water content at each level of compression. Data from insoluble collagen suspensions is included for comparison. As compression increases, tissue water is extruded and collagen becomes more concentrated. Ms/Mo decreases slightly as trypsin-digested cartilage is compressed and the collagen concentration increases.

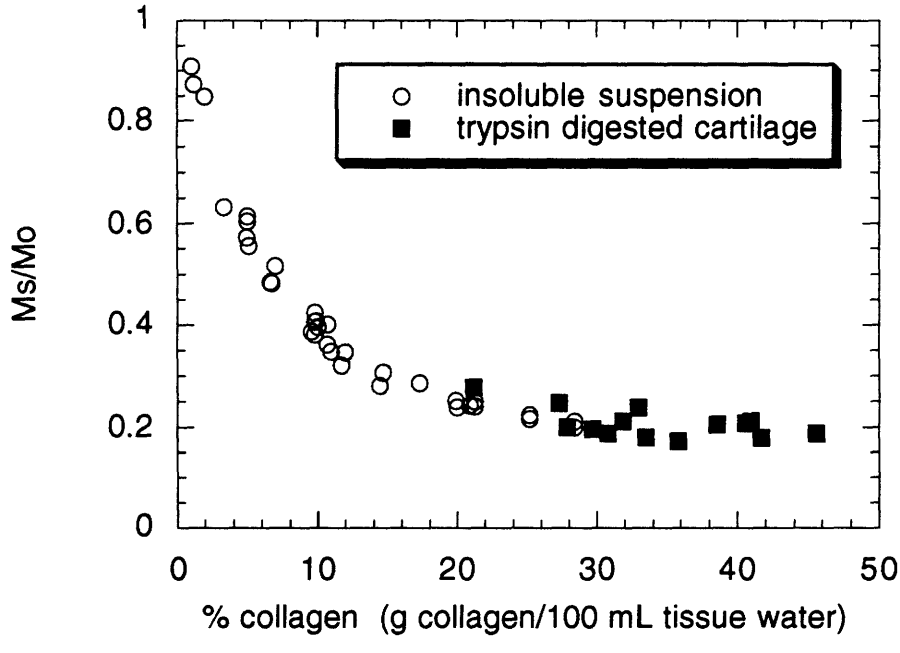

FIGURE 24 Ms/Mo as a function of collagen content in trypsin digested cartilage under compression. Collagen content was assumed from dry weight. For comparison, data for insoluble suspensions are included.

Ms/Mo measured for different types of cartilage (Figure 25A) also roughly correlated with collagen content as measured by hydroxyproline analysis. However, tissue specific differences were evident, suggesting that structural differences have a non-negligible effect on MT. Both adult articular (FP) and calf meniscal cartilage had similar collagen contents (which were higher than the other calf cartilages), but the meniscal cartilage had lower Ms/Mo than the adult articular. There were also differences in Ms/Mo among the femoropatellar, epiphyseal, and metacarpal calf cartilages. Figure 25B compares these results to those for insoluble suspensions. For the cartilage with higher collagen concentration, Ms/Mo values are on the order of those for the suspensions. Ms/Mo values for cartilage with lower collagen content are lower than for suspensions of equal concentration.

Determination of collagen content by hydroxyproline analysis is a relatively labor intensive process. Since collagen is the predominant solid component in cartilage, dry weight may be a sufficient predictor of collagen content. Figure 26 shows the relationship between dry weight and collagen content (as determined by hydroxyproline analysis), expressed as percent per tissue water. Least squares linear regression analysis of this data results in the equation:

$$\frac{\text{dry wt}}{\text{tissue water}} = 1.0\left(\frac{\text{collagen content}}{\text{tissue water}}\right) + 12.4 \qquad (26)$$

($r^2 = 0.954$, $n = 15$). The nonzero y intercept is consistent with the fact that collagen does not account for the entire tissue dry weight. To check the validity of this regression equation, the fraction of collagen per dry weight can be calculated and compared to the literature values of 50% - 60%. Using this equation, 10 - 30 g/dL of collagen would represent 45% - 70% of tissue dry weight which is reasonably close to the literature values and suggests that estimation of collagen content from dry weights is an acceptable alternative to hydroxyproline analysis.

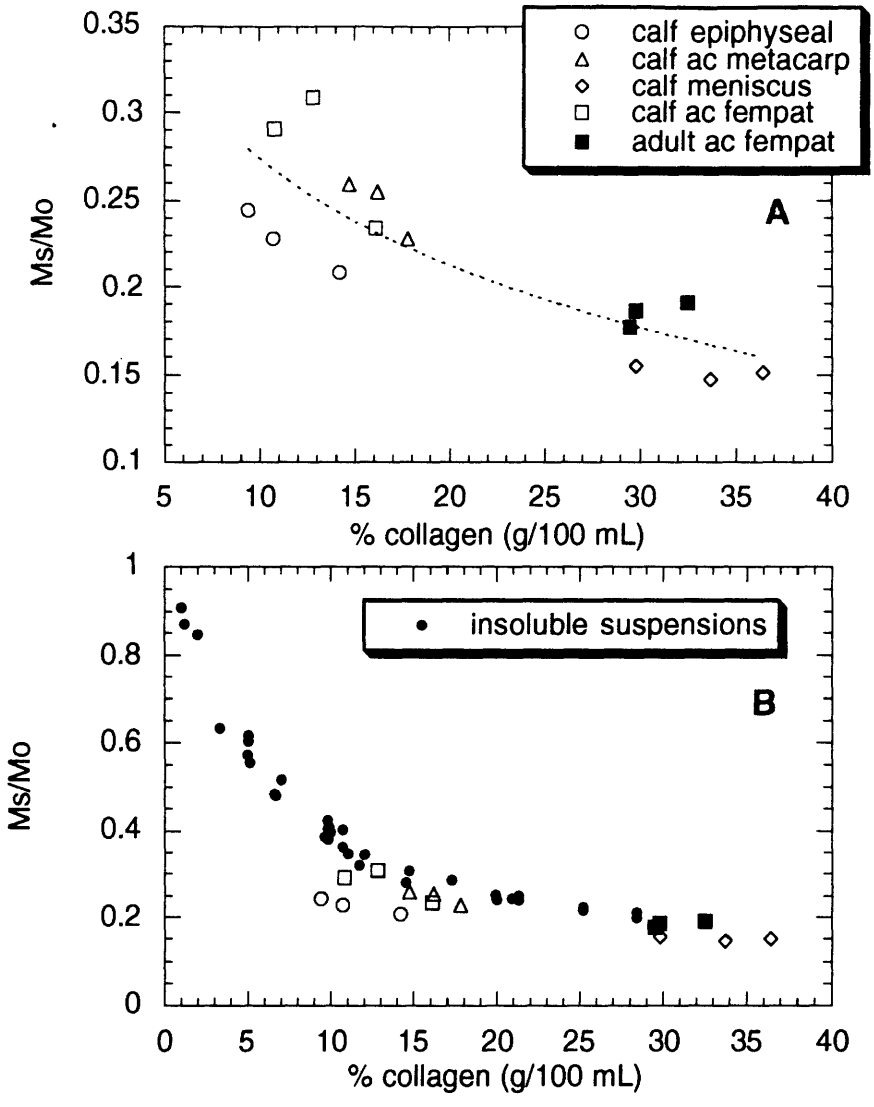

FIGURE 25 A) Ms/Mo measured for different types of cartilage (n = 15). Dotted line is logarithmic regression line: Ms/Mo = 0.48 - 0.2 log [collagen], $r^2 = 0.704$. B) Data for insoluble suspensions are included for comparison.

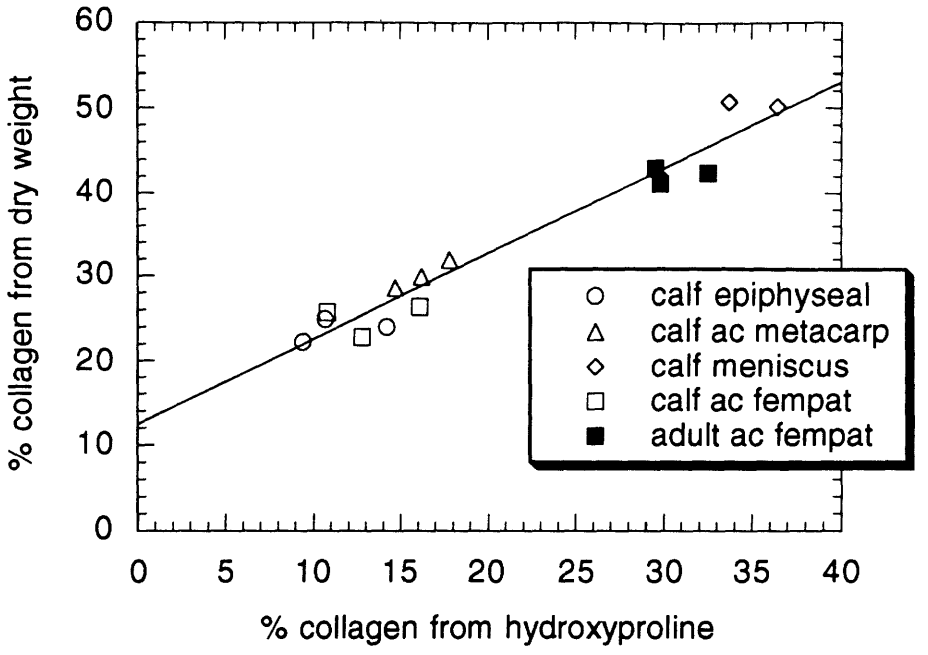

FIGURE 26 Estimation of collagen content from dry weights versus collagen content determined from hydroxyproline analysis. Linear regression line is plotted through data: $y = 1.0\ x + 12.4$ ($r^2 = 0.954$, n = 15).

C. DEPENDENCE OF MT ON COLLAGEN STRUCTURE AND/OR STATE

We were first interested in comparing the MT effect for collagen molecules to that for collagen fibrils. Therefore, we compared Ms/Mo measured for soluble suspensions (which were assumed to contain primarily molecular collagen) to Ms/Mo measured for insoluble collagen suspensions. The data are plotted together in Figure 27. Logarithmic regression lines of the form $y = a + b \log x$ are fit (least squares) separately for the soluble and insoluble suspensions. The equations are:

$$\textbf{Ms/Mo} = 0.875 - 0.552 \log [\textbf{soluble}] \quad (r^2 = 0.936,\ n = 14) \qquad (27)$$

$$\textbf{Ms/Mo} = 0.917 - 0.513 \log [\textbf{insoluble}] \quad (r^2 = 0.977,\ n = 46) \qquad (28)$$

Ms/Mo was ~20% less for soluble collagen than for insoluble collagen suspensions of comparable concentration. To give an indication of the statistical significance of this difference, the inset of Figure 27 shows average data from 1, 5, and 10% suspensions with standard deviations. The data for 5% suspensions are significantly different with $p < 0.05$ ($p < 0.11$ for 1% suspensions; 10% suspensions could not be compared with t test because there was insufficient soluble data). We suspect the difference in Ms/Mo may be due to structural differences between the two types of collagen. Another possible explanation could be bias in the determination of collagen content from weight since commercial preparation methods for the two types differ. However, hydroxyproline analysis of both soluble and insoluble collagen has shown similar purity for the samples, making this explanation unlikely. Results of this analysis are presented in the Discussion.

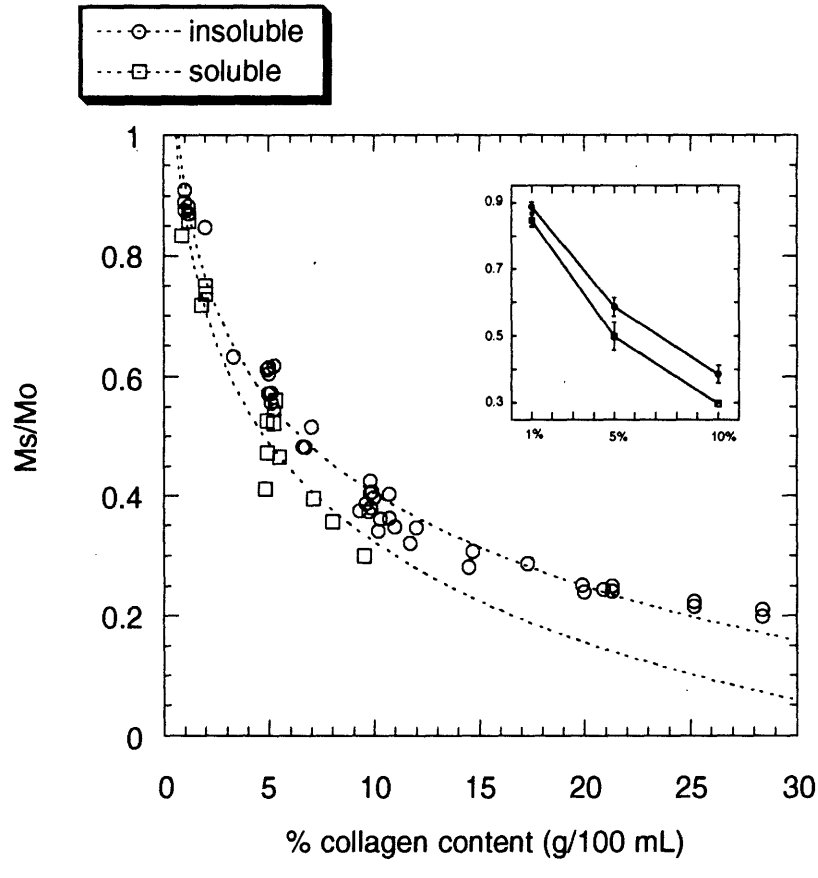

FIGURE 27 Ms/Mo for soluble and insoluble collagen suspensions. Each data set is fit to a logarithmic regression line (see equations 27 and 28). Inset shows mean and standard deviations for data from 1, 5, and 10% suspensions.

We next evaluated the contribution of the triple helix to magnetization transfer. Ms/Mo measured for two collagen gels before and after heating are shown in Table 7. The MT effect is irreversibly lost with the denaturation of collagen (loss of triple helix) in these dilute gels.

Table 7 Ms/Mo measured in dilute collagen gels before and after thermal denaturation and again after re-gelling.

	Ms/Mo		
% collagen	gel	denatured	re-gelled
0.75	0.86	0.99	1.0
1.0	0.85	0.99	1.0

Figure 28 shows Ms/Mo measured periodically in two 5% acid soluble collagen suspensions as the samples were heated. Ms/Mo initially decreased as temperature increased, most likely reflecting an increased rate of interaction between macromolecular and water protons. There was a dramatic increase in Ms/Mo when the collagen was heated beyond its denaturation point (where triple helical structure is lost). Upon cooling, some triple helix will be reformed. Figure 28 also includes several values for Ms/Mo measured in the samples as temperature decreased. The observed decrease in Ms/Mo was presumed to reflect renaturation. However, since Ms/Mo does not return to its original value, renaturation may be incomplete. While the collagen to gelatin transition is reversible, complete return to the native molecular state is only achieved in the special circumstance where all three constituent chains are covalently crosslinked (von Hippel 1967).

In order to evaluate the sensitivity of Ms/Mo for detection of structural changes compared to T1 (on which many clinical images are based), T1 was measured for one of the above samples at the start of the experiment while the sample was at room temperature (21°C), again near the denaturation temperature (37°C), and then after the sample had returned to room temperature (21°C). These data are listed in Table 8. T1 increased with increasing temperature and then decreased to its original value when the sample temperature decreased. However, a slight increase in Ms/Mo persisted, presumably indicative of a persisting denatured collagen fraction. Although with data obtained for only one sample

the results are inconclusive, they are interesting because they suggest that Ms/Mo may be a more sensitive indicator of structural changes than T1.

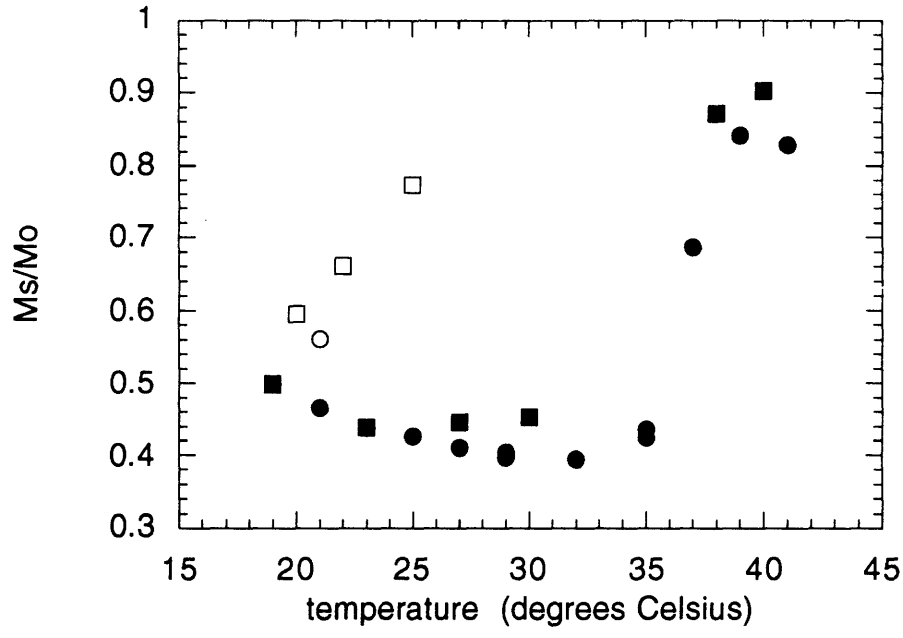

FIGURE 28 Ms/Mo as a function of temperature in two 5% soluble collagen suspensions. Ms/Mo was measured while temperature was increased (filled symbols) and then while samples were allowed to cool (open symbols). Measurements were taken at each temperature after sample was allowed to reach equilibrium (> 10 min).

Table 8 Ms/Mo and T1 measured in 5% soluble collagen suspension as a function of temperature (n/m = not measured).

temperature	Ms/Mo	T1 (sec)
21°C	0.47	2.45
37°C	0.67	4.03
21°C	0.56	2.48

Figure 29 compares Ms/Mo measured in both soluble and insoluble collagen suspensions before and after thermal denaturation (heated 30 min at 55°C and 70°C, respectively). Ms/Mo is increased (magnetization transfer effect is decreased) for all samples after heating, consistent with earlier results. The increase in Ms/Mo after heating is proportionally greater for soluble collagen suspensions than for insoluble, presumably due to more complete separation of soluble collagen into discrete α chains. Although the sample temperature was undoubtedly increased when Ms/Mo was measured after denaturation relative to the initial temperature, the effect on Ms/Mo due to temperature alone would be to decrease Ms/Mo.

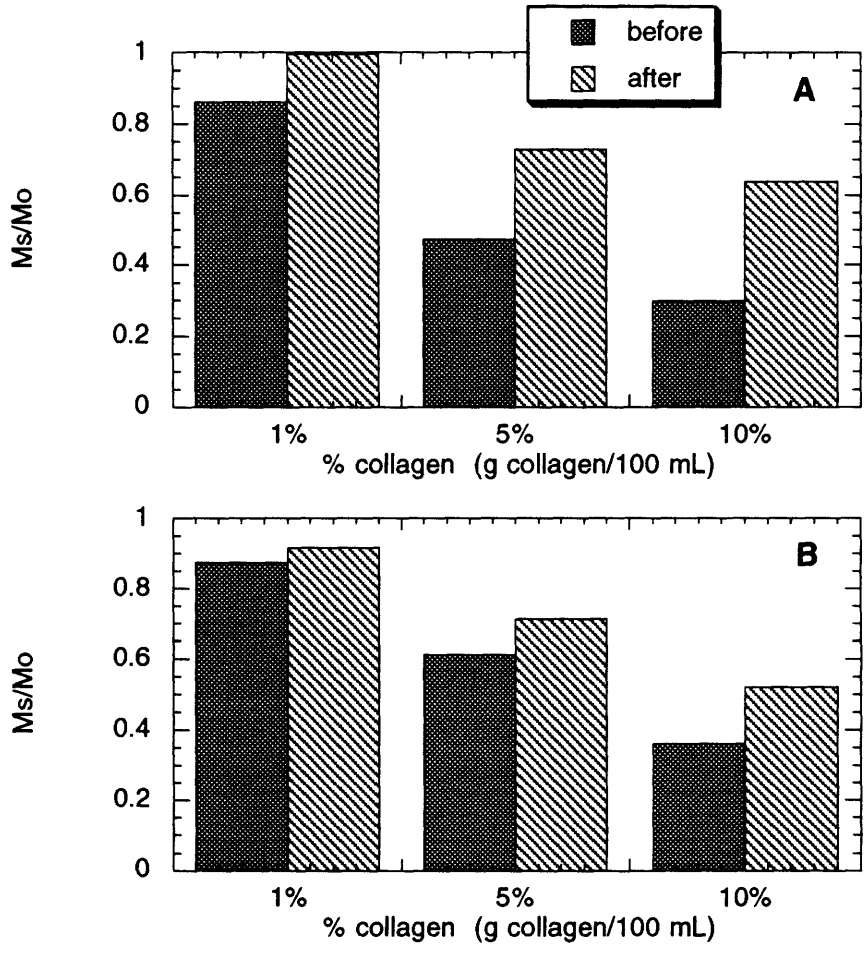

FIGURE 29 Ms/Mo in A) soluble and B) insoluble collagen suspensions before and after heating (n = 1 for each concentration) to 55°C (soluble) or 70°C (insoluble).

Ms/Mo consistently increased after heating of collagen gels and suspensions sufficient to cause thermal denaturation. Collectively, these results indicate that the triple helical structure of collagen is important for the observation of magnetization transfer.

D. MT FOR DETECTION OF CARTILAGE DEGRADATION

1. MIMIC TISSUE PATHOLOGY

a. Loss of proteoglycans with trypsin

Figure 30 shows Ms/Mo, wet weight, water content and fixed charge density (FCD) measured for cartilage after (three to five hr) trypsin digestion, normalized to values measured in the same sample before trypsin. (A value of one indicates no change.) Data for control (undigested) samples are also shown. Ms/Mo significantly increased in trypsin-digested samples compared to controls. Ms/Mo after trypsin was 1.15 ± 0.12 relative to initial values ($n = 14$, $p < 0.01$). Wet weight also decreased significantly after trypsin digestion ($p < 0.05$). The ratio of wet weights after trypsin digestion to those before was 0.92 ± 0.02 ($n = 11$) compared to 1.01 ± 0.01 for controls. Presumably the decreased wet weights were due to the decreased swelling pressure after glycosaminoglycan depletion and also to the actual loss of solid matrix. Tissue water fraction (defined as water/wet weights) increased slightly (~3%), however, absolute tissue water content (defined by proton area) decreased significantly after trypsin digestion. The ratio of water content after trypsin to that before was 0.94 ± 0.03 ($n = 14$, $p < 0.001$). FCD decreased significantly after exposure to trypsin ($p < 0.05$), but not in controls. These results are consistent with earlier reports that magnetization transfer in cartilage is dominated by the collagen component (Kim 1993). Only a small change in Ms/Mo was observed after nearly complete removal of proteoglycans from cartilage (evidenced by the small FCD after trypsin digestion).

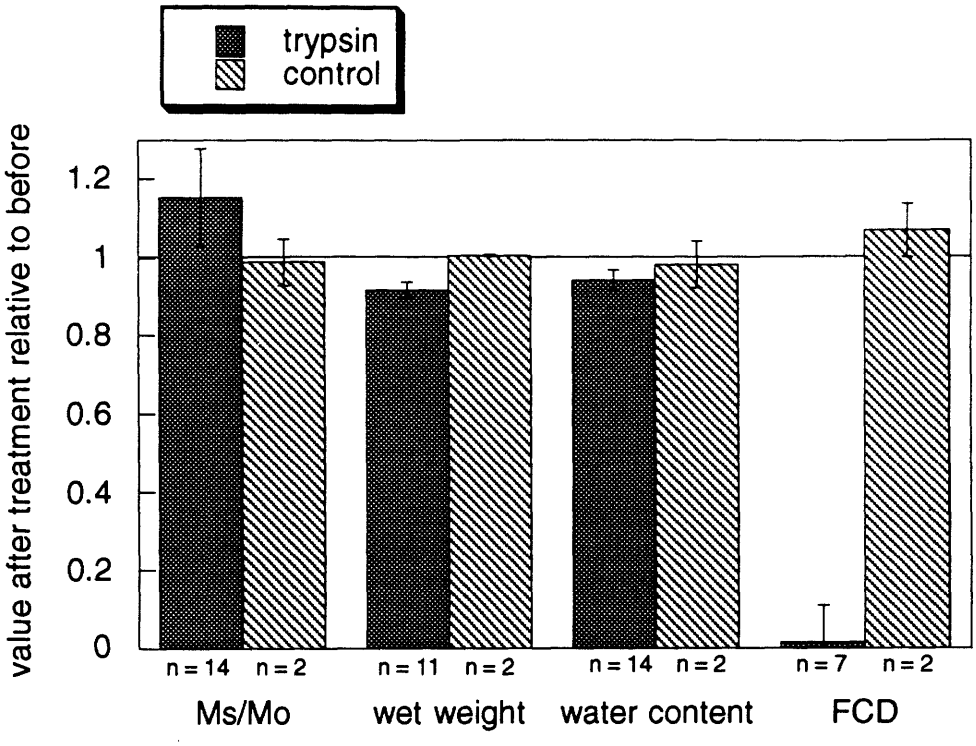

FIGURE 30 Ms/Mo, wet weight, water content, and FCD in cartilage after treatment with saline containing trypsin (trypsin) or saline alone (controls) relative to initial values. Data from 3 and 4 hr time points in Figure 31 are included.

Prolonged exposure of cartilage to trypsin resulted in only a slight increase in Ms/Mo compared to shorter periods of exposure (Figure 31). Measurements of Ms/Mo after 16 or 21 hours in trypsin were 0.28 ± 0.03 compared to measurements from 1 to 4 hours in trypsin 0.29 ± 0.03 ($p < 0.05$). Between two and four hours were needed for sufficient removal of proteoglycans to eliminate the net negative charge (FCD) on cartilage (Figure 31). The final slight positive charge is assumed to be due to the slight excess of positively charged amino groups (compared to the negatively charged carboxyl groups) found on collagen (Li and Katz 1976).

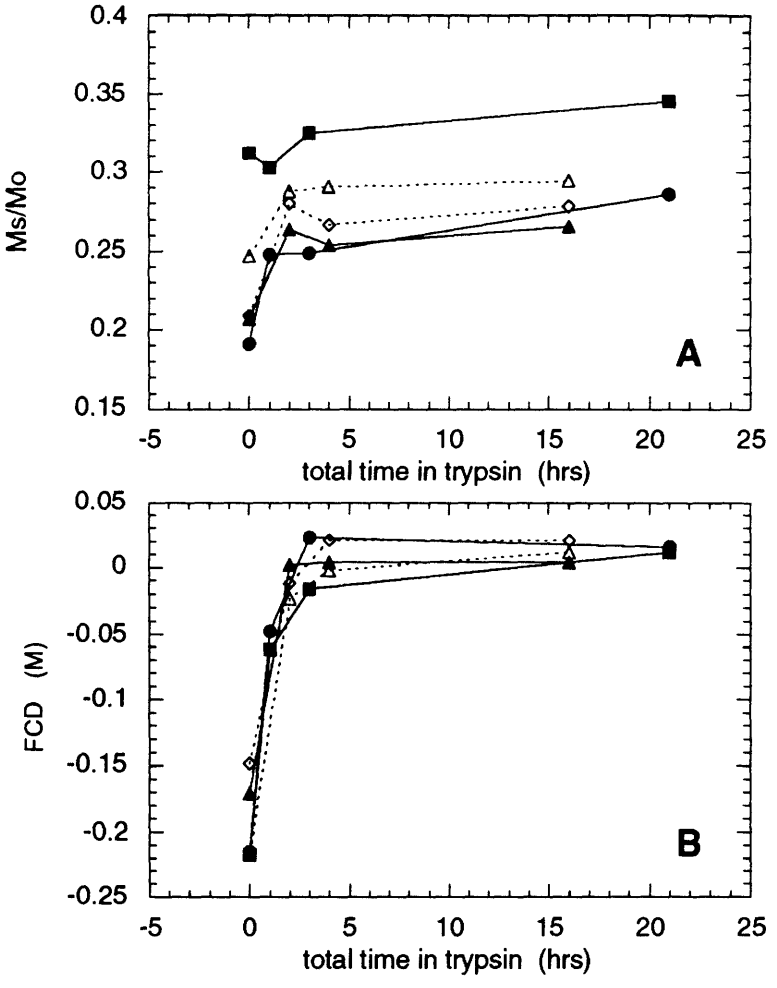

FIGURE 31 A) Ms/Mo and B) FCD measured at several time points for cartilage (n = 5) bathed in saline containing trypsin. Solid and open symbols represent two different experiments.

The increase in Ms/Mo after trypsin digestion is difficult to explain in terms of collagen concentration. Since absolute tissue water content decreased after trypsin (due to the loss of the abundantly hydrated proteoglycans), this implies that collagen concentration increased after trypsin digestion (assuming no collagen is lost). Figure 32 illustrates this with collagen concentrations calculated for several cartilage samples before and after trypsin digestion (using the dry weight of the trypsinized cartilage as a measure of collagen

content, assumed to be constant throughout, and tissue water measured before and after). Data from insoluble suspensions (Figure 22B) are included for comparison. Despite the apparent increases in collagen concentration with trypsin digestion (which would be expected to decrease Ms/Mo), Ms/Mo increased after trypsin digestion.

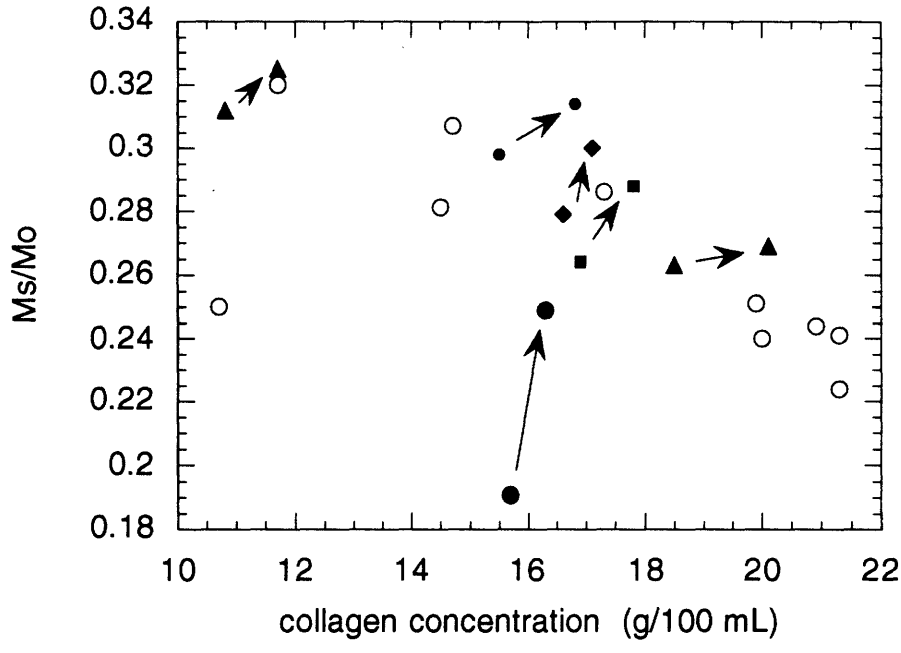

FIGURE 32 Collagen concentration in cartilage (filled symbols) before and after trypsin digestion. Arrow points from Ms/Mo before trypsin to that measured after. Data from insoluble suspensions (open symbols) is included for comparison. Cartilage collagen concentration is calculated from dry weight after trypsin digestion (assumed to be entirely collagen) divided by tissue water before and after trypsin, where it is assumed that no collagen is lost with trypsin.

However, there may be a modest loss of collagen with trypsin digestion due to the presence of damaged collagen which is sensitive to proteolytic cleavage. While early electron microscopic studies of human dermis showed that normal collagen structure did not change after exposure to 10 mg/mL trypsin at 37°C (for a "suitable period"), they also showed that amorphous material and non-striated strands (possibly arising from the mechanical breakdown of collagen) were all digested away (Tunbridge 1952). Later, Harris (1972) and Manahan and Mandl (1968) studied canine articular cartilage and bovine Achilles

tendon, respectively, and showed that 5% of total sample collagen was lost after 24 hours incubation in 1 mg/mL trypsin. In another study on bovine articular cartilage, less than 1% of collagen content (as measured by hydroxyproline) was lost after 24 hr at 25°C in 1 mg/mL trypsin (Schmidt 1990). Harris suggested that there "may be a population of collagen molecules in cartilage susceptible to trypsin treatment." If collagen was lost during trypsin digestion, calculation of collagen concentration for earlier time points can not be made as we did by assuming constant collagen content (based on final sample dry weight). However, examination of Ms/Mo as a function of concentration for insoluble suspensions (Figure 22B) suggests that losses on the order of 25% would be necessary to explain a 15% increase in Ms/Mo.

It is possible that the increased Ms/Mo observed with trypsin is a function of increased fibril hydration. Loss of proteoglycans from the tissue results in decreased swelling pressure exerted on collagen, thus increasing intrafibrillar water content. However, conflicting results were observed when fibril hydration was increased at low pH (results discussed below).

An alternative explanation for the increase in Ms/Mo after trypsin may be that non-collagenous molecules (removed by trypsin) contribute to the MT effect seen in cartilage, either directly or indirectly. However, neither isolated proteoglycan monomers nor chondroitin sulfate in solution exhibit MT. Measurement of 5% (w/v) chondroitin sulfate solution revealed no MT effect: Ms/Mo = 1.0 (n = 1). Published results for proteoglycan monomer in solution (5% w/v) also showed no MT effect: Ms/Mo = 0.96 ± 0.002 (Kim 1993). Nevertheless, it is possible that it is the interaction between proteoglycans (or GAG sidechains like chondroitin sulfate) and the collagen fibril network which contributes to the MT effect observed in cartilage.

b. Cartilage at low pH

Figure 33A shows Ms/Mo measured for trypsin-digested (n = 8) and native cartilage samples (n = 12) bathed sequentially for 90 min in 0.15 M NaCl at pH 8, 4, 2, and then back to pH 8. Figure 33B shows wet weights (normalized to initial value after pH 8 bath) for the same trypsin-digested and native cartilage samples as in Figure 33A. Wet weights provide an indication of tissue swelling.

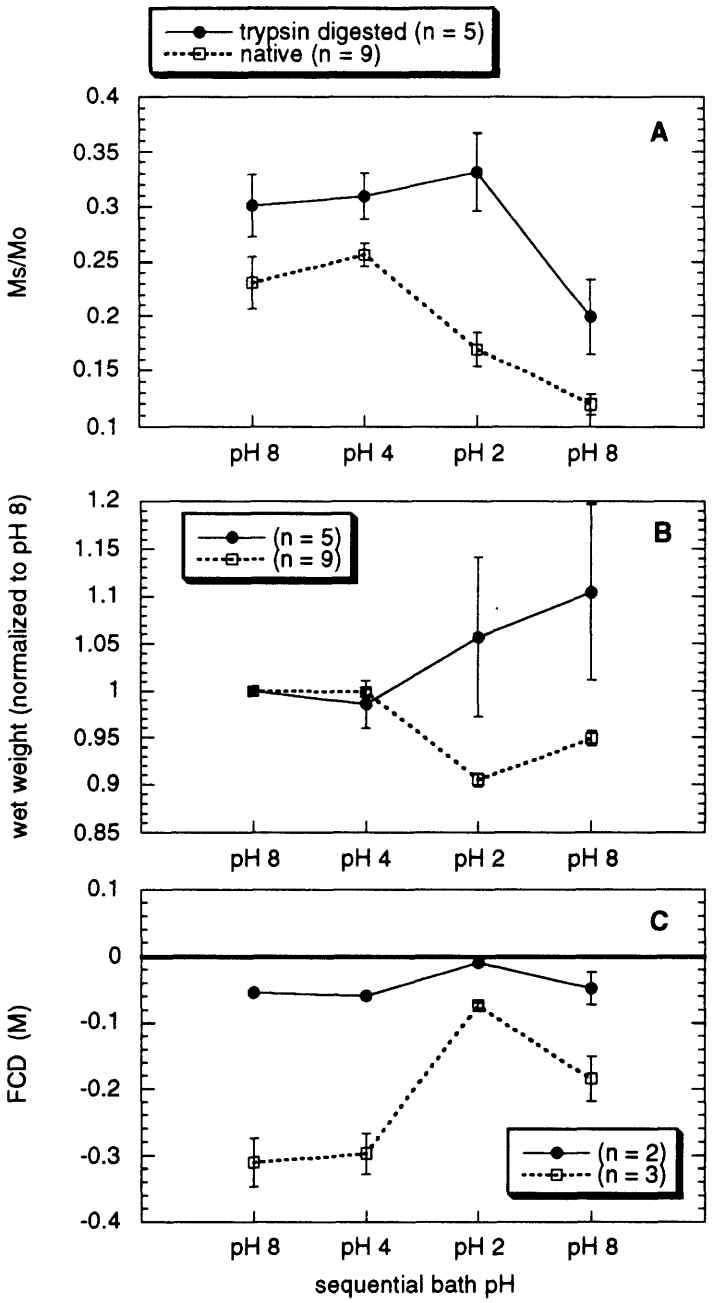

FIGURE 33 A) Ms/Mo, B) wet weight, and C) FCD (calculated from sodium) for native and trypsin-digested cartilage bathed in 0.15 M NaCl at varying pH. Wet weights are normalized for each sample to value at original pH bath.

In native cartilage, Ms/Mo increased slightly between pH 8 and pH 4, then decreased considerably when samples were moved from pH 4 to pH 2 and decreased further upon return to pH 8 (Figure 33A). Ms/Mo in the final pH 8 bath was only ~60% of the original pH 8 value. No further change in Ms/Mo was seen in several samples which were kept at pH 8 for a prolonged period (36 hr, data not shown). Wet weights decreased by ~10% as pH dropped from 8 to 2 and then recovered half of this decrease upon return to pH 8 (Figure 33B). The decreased wet weight at low pH was presumably due to the decreased hydration and swelling pressure of the glycosaminoglycans after titration of their negative charges. The decrease in Ms/Mo for native samples at pH 2 might therefore be explained by increased collagen concentration relative to the decreased tissue water. However, judging from data for trypsin-digested cartilage under compression (Figure 24), Ms/Mo values of 0.15 (as seen in native samples at pH 2) were seen for cartilage with approximately 30% collagen; collagen concentrations for these samples were estimated to be one the order of 15%. Although total tissue water decreases at low pH, collagen fibril hydration is expected to increase at pH 2 due to the development of a net positive charge on the collagen molecule. The decrease in Ms/Mo seen at pH is in contrast to the increased Ms/Mo seen when fibril hydration increased after trypsin digestion (discussed above).

In trypsin digested samples, Ms/Mo increased slightly between pH 8 and pH 2 but then decreased substantially when returned to pH 8 (Figure 33A). Like native cartilage, Ms/Mo in the final pH 8 bath was only ~60% of the original pH 8 value. No further change in Ms/Mo was seen in several samples which were kept at pH 8 for a prolonged period (36 hr, data not shown). For trypsin-digested cartilage, the average normalized wet weight was slightly increased at pH 2 and then further increased when returned to pH 8 (Figure 33B). However, error bars demonstrate the wide variability of wet weights for trypsin digested samples. The results were dominated by two of the eight samples for which wet weights increased by 15 and 20% at pH 2 and pH 8, respectively (relative to initial pH 8 values). Wet weights for the remaining samples either increased slightly (~4% at pH 2 and then ~8% at pH 8) or remained constant. The variation in tissue swelling may be due to differences in the degree of crosslinking of collagen within the samples. Where observed, the increase in wet weight at pH 2 was most likely due to measurably increased fibril hydration (due to net excess positive charge on the collagen molecule) and the resulting increased total tissue water. However, when fibril hydration was varied by making insoluble collagen suspensions with saline at low pH, no significant change in Ms/Mo was observed (Table 9).

Table 9 Ms/Mo measured for ~10% insoluble collagen suspensions made with 0.15 M NaCl at varying pH

% collagen (w/w)	9.8	10.3	10.0	10.4	10.3
pH	7	6	5	3	2
Ms/Mo	0.43	0.38	0.42	0.38	0.43

At pH 2, trypsin digested cartilage samples were observed to change color from opaque white to translucent. The transformation began at the outer edge of the sample and proceeded radially toward the center, making a progressively larger ring around the sample until the entire disk was relatively clear. This transformation was complete within 30 min. These results are similar to those reported for bovine corium (dermis) exposed to low pH (Veis 1967).

For several of the samples, sodium measurements were also obtained so that fixed charge density (FCD) could be followed (Lesperance 1992). Figure 33C shows FCD for native (n = 3) and trypsin digested (n = 2) cartilage at varying bath pH. For native tissue, FCD becomes significantly less negative as the charge groups on proteoglycans become titrated around pH 2. After return to pH 8, in this case for over 36 hours, only ~50% of the original charge is measured. Some proteoglycans may have been lost from the tissue during the course of this experiment, particularly during its time in the pH 2 bath. For trypsin digested cartilage, the initial charge is slightly negative. This may be due to incomplete removal of the proteoglycans or due to offset in the FCD calculation from error in calibration of the sodium measurements. After bathing at pH 2, almost no charge is detected but the original charge is restored upon return to pH 8.

One question raised by the results of Figure 33 is whether the further decrease in Ms/Mo observed in native cartilage when returned to pH 8 is merely an artifact of insufficient equilibration time at pH 2. In other words, given longer time at pH 2, perhaps Ms/Mo would have reached the value ultimately seen upon return to pH 8. In order to test this hypothesis, Ms/Mo was measured for native and trypsin digested cartilage initially bathed in 0.15 M NaCl at pH 8 and then after 2 hr and overnight in pH 2 and finally 36 hr in bath at pH 8. Results are shown in Figure 34. Ms/Mo in native cartilage decreased after 2 hr at pH 2, then increased after overnight equilibration and again decreased when cartilage was

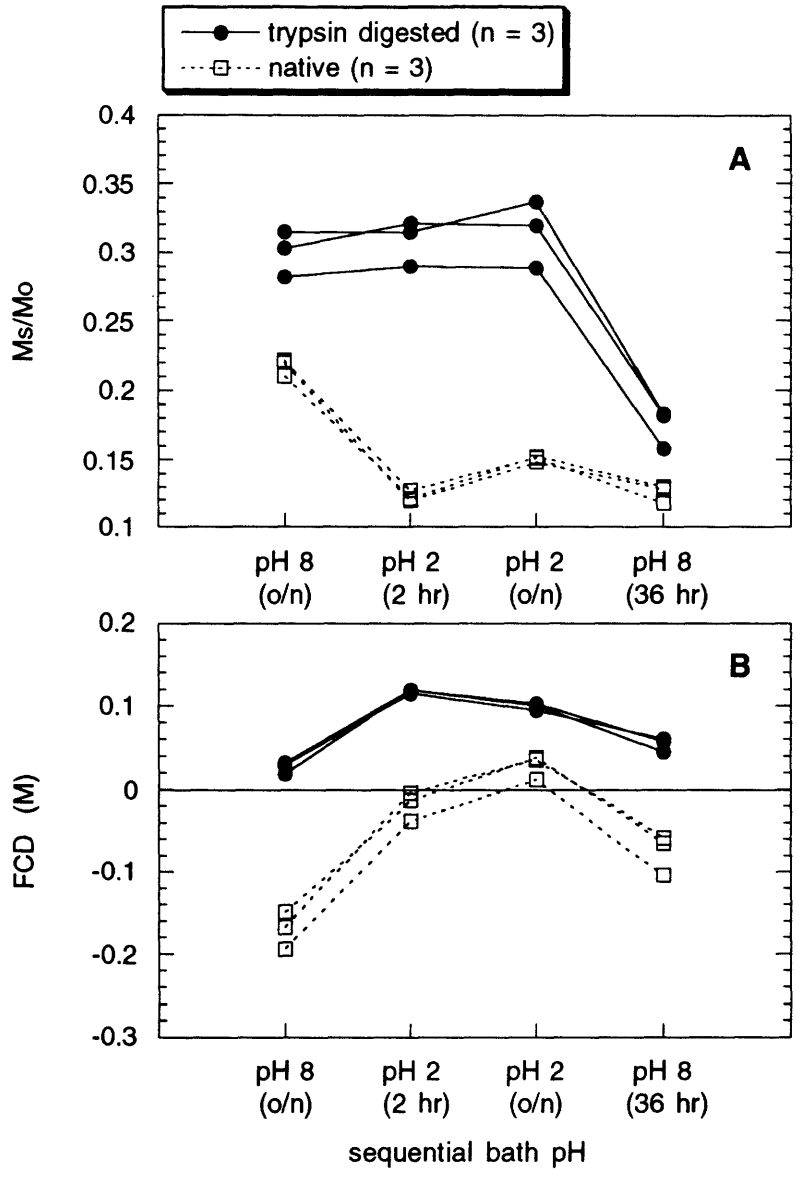

FIGURE 34 A) Ms/Mo and B) FCD for native and trypsin-digested cartilage with prolonged exposure to pH 2 bath. Measurements were made after initial pH 8 bath and then after 2 hr and overnight (o/n) at pH 2, and finally after 36 hr at pH 8.

returned to pH 8 (Figure 34A). For trypsin digested cartilage, Ms/Mo did not change at pH 2 but then decreased when samples were returned to pH 8. These results clearly demonstrate that it is the transition from pH 2 to pH 8 (and not the pH 2 bath itself) which is responsible for the observed decrease in Ms/Mo. It is interesting that the increase in Ms/Mo observed in native cartilage samples is accompanied by the development of a net positive charge (Figure 34B). However, while substantial positive FCD is measured in trypsin digested cartilage at pH 2, no change in Ms/Mo is seen.

To further examine the contribution of fibril hydration and osmotic forces to Ms/Mo measured at low pH, the varying pH experiment was repeated in the presence of higher salt concentration. Figure 35 shows the results for native (n = 3) and trypsin digested cartilage (n = 3) bathed for 90 min each in 0.5 M NaCl baths at pH 8, pH 2, and pH 8. Compared to Figure 33, Ms/Mo for native cartilage is relatively constant throughout this experiment with a slight decrease when returned to pH 8. Ms/Mo for trypsin digested cartilage at high salt decreased slightly at pH 2 (although it increased for one sample) compared to a slight increase in Ms/Mo with lower salt. As in the low salt experiment, Ms/Mo decreased substantially when trypsin-digested samples were returned to pH 8.

c. Enzymatic degradation of collagen

Figure 36 shows sodium and MT data for cartilage cultured with IL-1ß. Sodium concentration was calculated using water content determined by proton spectral area. Data are shown relative to controls and to their values on day zero of culture. Normalization to controls eliminates any effects of day to day variations in temperature. Actual values for controls were relatively stable throughout the culture period.

The data of Figure 36 illustrate that, as shown for cartilage before and after trypsin digestion, the loss of GAG can be monitored using sodium NMR. However, the time scale for GAG loss is substantially longer with IL-1ß than for trypsin studies (data for time course of trypsin digestion is shown in Part I, Figure 9). In contrast to the increased Ms/Mo observed when cartilage was depleted of proteoglycans by exposure to trypsin, incubation in IL-1ß led to a progressive decrease in Ms/Mo. Although the Il-1ß treated samples lost water as the tissue matrix was depleted during culture, hydration, calculated from the ratio of water content to wet weight, increased when comparing the end point of the experiment (day nine) to the initial time point (day zero). Increased hydration suggests

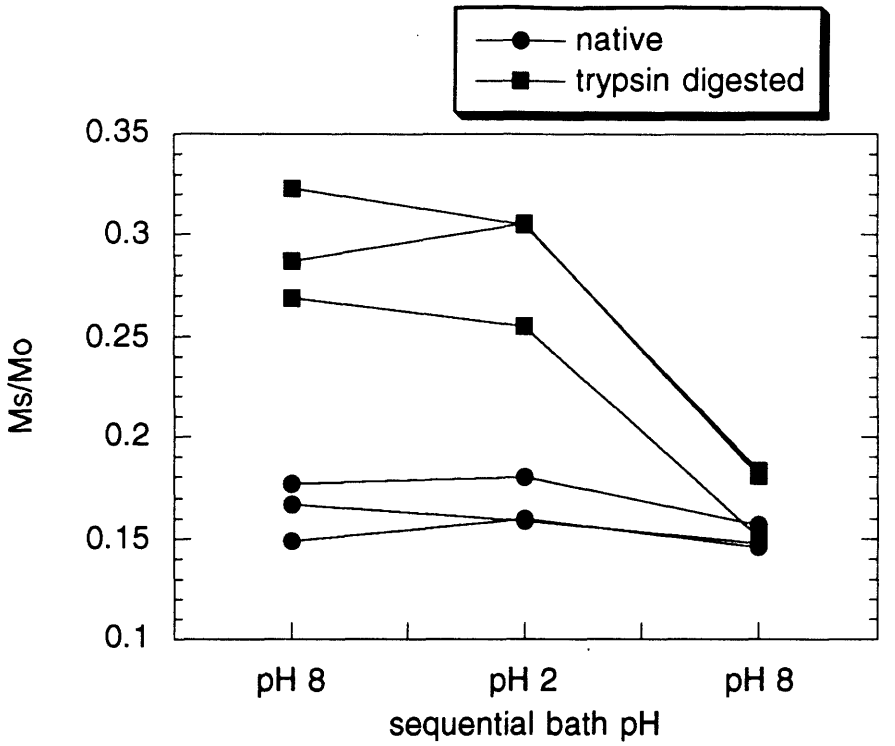

FIGURE 35 Ms/Mo in native and trypsin digested cartilage bathed sequentially (90 min each) in 0.5 M NaCl at pH 8, pH 2, and then returned to pH 8.

that the remaining matrix constituents became less concentrated and thus, Ms/Mo would be expected to increase. Therefore, the observed decrease in Ms/Mo is apparently not due to changes in collagen concentration and could be the result of a structural change in the collagen. The decrease in Ms/Mo observed with IL-1ß is consistent with data from an earlier experiment in which Ms/Mo was measured in cartilage only at the end of eight days in culture. Ms/Mo for samples exposed to IL-1ß was decreased slightly compared to controls ($p < 0.1$). Ms/Mo for samples cultured with IL-1ß (10 or 30 ng/mL) was 0.28 ± 0.04 ($n = 15$) compared to 0.32 ± 0.06 for controls ($n = 8$).

2. CLINICAL SPECIMENS

Ms/Mo measured for samples from visually fibrillated femoral head articular cartilage was 0.16 ± 0.01 ($n = 4$); Ms/Mo for samples from normal appearing human femoropatellar articular cartilage was 0.11 ± 0.01 ($n = 2$). As an estimate of collagen content, the ratio of dry weight to water volume was 32.2 ± 4.0 for the fibrillated femoral head cartilage

compared to 31.3 ± 0.1 for femoropatellar cartilage. It is notable that Ms/Mo measured for these samples is considerably lower than that measured for bovine articular cartilage (for which typically Ms/Mo ≈ 0.25).

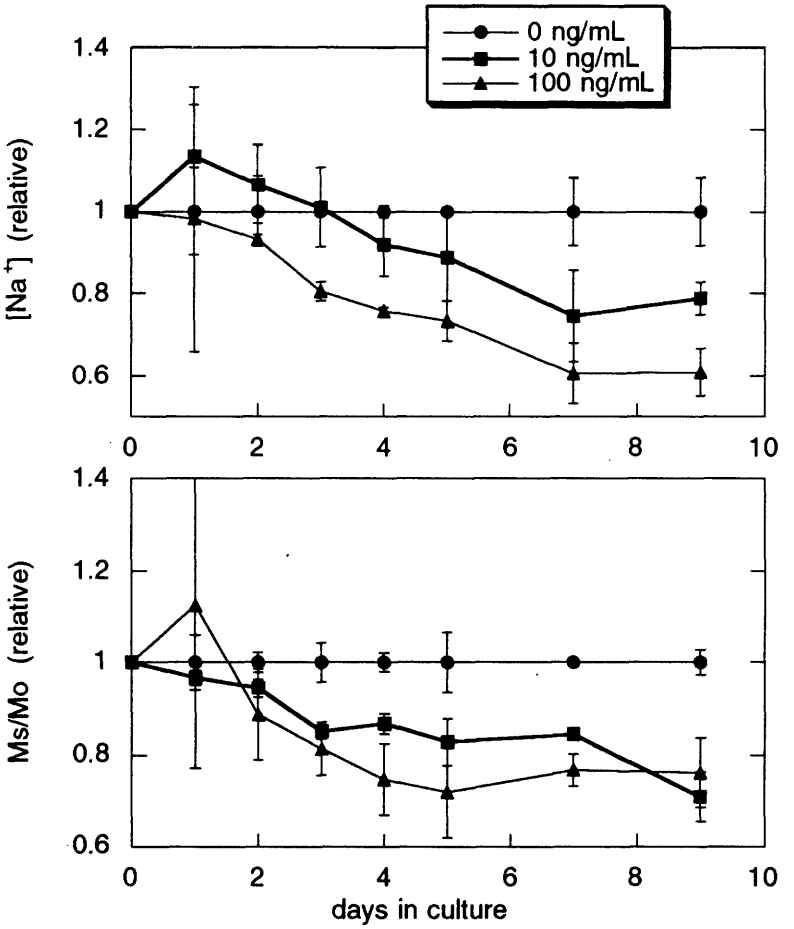

FIGURE 36 Sodium concentration and Ms/Mo for samples exposed to IL-1ß: (●) controls, 0 ng/mL (n = 2); (■) 10 ng/mL (n = 2); and (▲) 100 ng/mL (n = 2) IL-1ß. Data are shown relative to controls and to their values on day 0 of culture. Normalization to controls minimizes effects of day to day variations in temperature.

DISCUSSION

A. SPECIFIC AIMS

The goal of this work has been to evaluate the magnetization transfer technique for the noninvasive and nondestructive determination of collagen content and/or structure in cartilage. Specifically, we wanted to (1) characterize the MT experimental parameters, (2) examine the dependence of MT on collagen concentration or content, (3) examine the dependence of MT on collagen structure and/or state, and (4) determine the specificity with which MT can be used to evaluate cartilage degradation in intact cartilage samples.

1. CHARACTERIZATION OF EXPERIMENTAL PARAMETERS

We have characterized the parameters for the MT experiment in collagen suspensions and cartilage. Our results are consistent with those of other investigators studying cartilage and other systems (e.g. Morris and Freemont 1992, Wolff and Balaban 1989). Ms/Mo decreases with increasing saturation pulse length (Figure 15), increasing saturation power (Figure 17), and with decreasing offset frequency (Figure 18).

After characterization of the parameters, subsequent experiments were performed with a 12 μT saturation pulse of 6 kHz offset and length at least 5T1. The parameters chosen were not necessarily those which gave the maximum MT effect (minimum Ms/Mo). We were interested in obtaining maximal saturation of the macromolecular protons with minimal direct saturation of the water protons. Therefore, the offset frequency was chosen to be far enough from the water to avoid direct effects and yet close enough to provide substantial MT effects. We were also concerned with ultimately using this technique for *in vivo* measurements. Therefore, power settings needed to be kept low to avoid tissue heating. (Clinical pulse sequences must meet guidelines for power deposition set by the US Food and Drug Administration.) Furthermore, we were interested in comparing our results to those of other investigators. For these reasons, we chose the power setting to be that used in earlier MT reports (12 μT). Altering the saturation power level did not change results in terms of comparison between samples.

The frequency spectrum for the MT effect (i.e. plot of Ms/Mo versus offset frequency, as in Figure 18) gives an indication of the efficiency of power transfer to the macromolecular

protons. As discussed in the results section, recent MT imaging studies are being performed with smaller frequency offsets and reduced power levels for the same image contrast. We may consider similarly decreasing our frequency offset and saturation pulse power. However, the minimum frequency offset for which water will not be directly saturated depends on the linewidth of the water spectrum. The water spectrum for these explanted cartilage samples has a linewidth which is substantially wider than that for pure saline. Furthermore, the spectral width can vary from sample to sample. This could result in sample to sample variation when measuring Ms/Mo. Samples with larger spectral widths would experience more direct saturation of the water which would result in decreased Ms/Mo. Direct saturation of water would complicate the interpretation of the significance of Ms/Mo in terms of the macromolecular protons. At 6 kHz offset, direct saturation was assumed to be minimal for our samples, even with significant sample to sample variability. A more careful study of the variation in proton spectral width for cartilage samples will have to be conducted before moving the offset frequency any closer toward resonance.

It also may be of interest to perform continued studies with Ms/Mo measured in various samples as a function of offset frequency (as in Figures 18 and 20). The two proton pool is probably a simplification for any tissue, cartilage being no exception. The diagram in Figure 37 gives a hypothetical picture of a proton spectra in tissue which is a superposition of the spectra for three distinct pools. It is conceivable that irradiation at specific offset frequencies could selectively affect one macromolecular pool, perhaps one which may be responsible for the changes seen with pathologic states. Furthermore, recent studies suggest that the shape of the frequency spectrum (i.e. Ms/Mo versus offset frequency) may provide additional information about molecular structure. (A plot of 1-Ms/Mo versus frequency would look similar to Figure 37.) Preliminary data presented by both Bryant (1993) and Ceckler (1993) has shown that the shape of the frequency spectra varies depending on the molecular motion of the macromolecules; rigid structures have broad and Gaussian-shaped frequency spectra while flexible structures have narrow and Lorentzian-shaped spectral width.

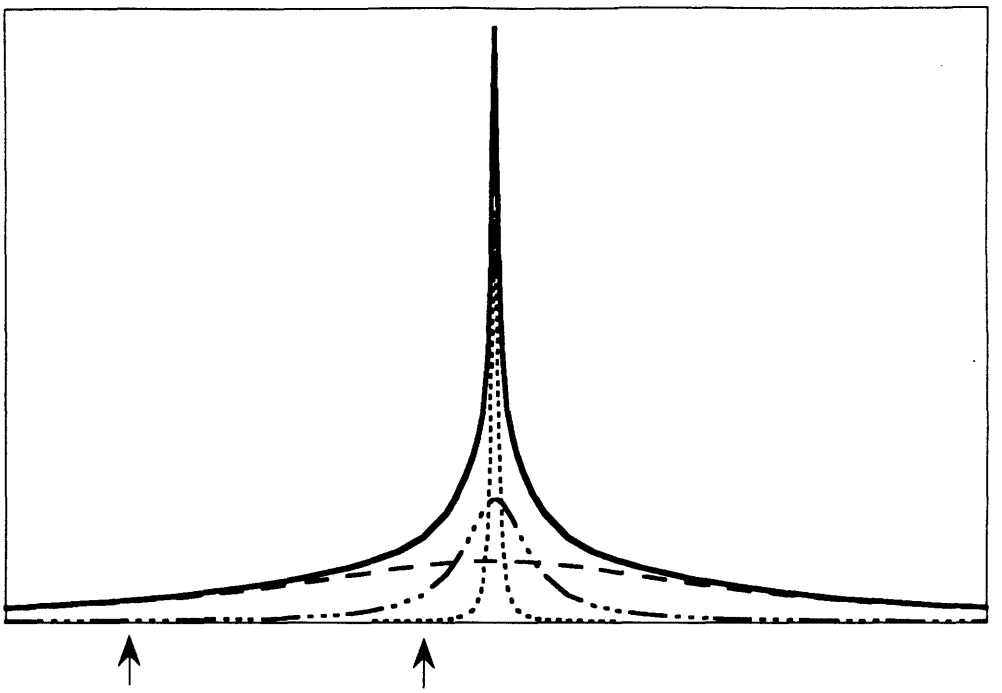

FIGURE 37 Proton NMR spectrum shown as a hypothetical superposition of distinct spectral components, each representative of a different population of protons.

We chose the saturation pulse length to be at least 5T1 which is significantly longer than it has to be for maximal MT. To shorten the experiment and to lessen the total tissue power deposition, saturation pulse length could be chosen based on T1sat which for cartilage is significantly shorter than T1. However, T1sat varies for cartilage (on the order that Ms/Mo varies) while T1 varies little. Therefore, a shorter saturation pulse length may produce non-uniform saturation in different samples, unless T1sat is measured for each sample and saturation pulse length is set accordingly (e.g. 5T1sat). Further studies on the MT effect in normal versus pathologic cartilage are necessary in order to determine whether either uniform or maximal saturation is necessary to discern differences between the samples.

2. DEPENDENCE OF MT ON COLLAGEN CONCENTRATION

We have shown that the MT effect is dependent on collagen concentration (Figure 22). Ms/Mo in insoluble collagen suspensions decreases logarithmically with increasing collagen concentration. Over the range of concentrations on the order of those found *in vivo* (10-20%), the magnitude of Ms/Mo changes little. Ms/Mo decreases by 0.1 (from

0.8 to 0.7) as collagen concentration increases from 1.7 to 2.6%. (Values for Ms/Mo were calculated from logarithmic regression equation 28.) In contrast, a decrease in Ms/Mo of 0.1 (from 0.25 to 0.15) is observed when collagen concentration increases from 19 to 30%. However the changes in Ms/Mo are similar throughout the measured range of concentrations when expressed as percentages (which is characteristic of the logarithmic relationship). At a collagen concentration of 20%, to increase or decrease Ms/Mo by 5%, collagen concentration must decrease or increase by 5%. Ms/Mo also decreased with increasing collagen concentration for collagen solutions, collagen gels, and soluble collagen suspensions (Figure 22) and for trypsin digested cartilage (where dry weight is assumed to be purely collagen) in which collagen concentration was varied by compressing the samples (Figure 24). In addition, Ms/Mo measured in different types of cartilage decreased with increasing collagen concentration determined biochemically from hydroxyproline analysis (Figure 25). However, as predicted from the suspension results, MT was not very sensitive to changes in collagen concentration for those cartilage samples which have relatively high collagen contents.

Our results for collagen suspensions and cartilage of varying collagen content suggest that under the conditions of these experiments, Ms/Mo is probably not a sensitive enough indicator for the quantification of collagen concentration in cartilage. Certainly the development of a nondestructive technique for the determination of collagen concentration would be of interest for the study of cartilage and other tissues, both for clinical diagnosis and as a research tool. However, the collagen content in osteoarthritic tissue is similar to that found in normal tissue (when normalized to dry weight) and differences in collagen concentration (due to increased tissue water) are small, on the order of 5% (Venn and Maroudas 1977). Therefore, the detection of collagen structural changes may ultimately prove more useful for the early diagnosis of cartilage degradation. The differences in Ms/Mo seen between soluble and insoluble suspensions and among various types of cartilage with similar collagen content suggest that structural differences have a non-negligible effect on MT and may provide the basis for the discrimination of cartilage degradation.

The relative insensitivity of MT to changes in collagen concentrations in the range of those seen in cartilage may, rather than diminishing the potential usefulness of the MT technique, actually help the interpretation of MT studies in the presence of cartilage degradation. If Ms/Mo varies minimally with large changes in collagen concentration, then differences in Ms/Mo between samples or within the same sample over time must be attributed to factors

other than concentration (e.g. structural changes, changes in the interaction between macromolecular and water protons).

3. DEPENDENCE OF MT ON COLLAGEN STRUCTURE AND/OR STATE

Ms/Mo for soluble collagen suspensions was found to be ~20% less than for insoluble suspensions (Figure 27). This difference may be due to structural differences between the two types of collagen: insoluble collagen has highly crosslinked fibrils while soluble collagen contains predominantly collagen molecules (discussed further below). However, another reason for the observed difference in Ms/Mo may be bias in the determination of collagen content from weight since commercial preparation methods for the two types differ. In other words, equal amounts of each type of collagen (by weight) do not actually contain equal amounts of collagen (determined, for example, by hydroxyproline analysis). The data in Figure 27 were fit to logarithmic regression lines. These expressions can be combined to determine the amount of insoluble collagen which would be necessary to obtain the Ms/Mo value seen for the same concentration of soluble collagen (or vice versa). The relationship thus obtained is:

$$[\text{insoluble}] = 1.2 * [\text{soluble}]^{1.1} \qquad (29)$$

We can then use this relationship to determine the error in weight determination which would have to be present in order to explain the discrepancy in Ms/Mo between soluble and insoluble suspensions. Doing so, we find that 15% insoluble collagen gives the same Ms/Mo as 10% soluble while 7% insoluble collagen yields the same Ms/Mo as 5% soluble collagen. Assuming the soluble collagen had no contaminants, the insoluble collagen would have to contain 25% to 45% contaminants (by weight) to bring the two curves together between 1% and 10% (soluble) collagen concentration. In order to estimate the purity of the collagen, samples of each type were sent for hydroxyproline analysis (as described for cartilage samples). Collagen was weighed and then placed directly into hydrolysis tubes. One sample of pure hydroxyproline was included as were several pieces of trypsin digested cartilage samples. Results of the analysis are shown in Table 10.

Table 10 Results of hydroxyproline analysis on soluble (n = 2) and insoluble (n = 2) collagen and trypsin digested cartilage (n = 3). Hydroxyproline sample was also included for reference. Dry weights were measured before analysis. Protein and collagen content are from amino acid analysis. Percents collagen per protein, and protein and collagen per dry weight were calculated.

sample	dry wt (mg)	protein (mg)	collagen (mg)	$\frac{\text{collagen}}{\text{protein}}$	$\frac{\text{protein}}{\text{dry wt}}$	$\frac{\text{collagen}}{\text{dry wt}}$
soluble	2.20	1.86	1.67	89.8	84.5	75.9
collagen	1.01	0.92	0.83	90.2	91.0	82.2
insoluble	2.06	1.65	1.54	93.3	80.1	74.8
collagen	0.82	0.59	0.52	88.1	71.9	63.4
hypro	1.8	1.39*	--	--	77.2	--
trypsin	5.7	4.99	4.42	88.6	87.5	77.5
digested	6.7	5.00	4.54	90.8	74.6	67.8
cartilage	6.0	4.81	4.15	86.3	80.2	69.2

*All identified as hydroxyproline.

Results of amino acid analysis on the samples included total protein content per sample, total collagen content per sample, and percent collagen per residue. Total collagen content was determined assuming a mean residue weight of 111 based on type II collagen (see equation 26). Mean residue weight for type I collagen is not substantially different (109). The percent collagen gives an indication of the purity of the sample since this number comes from the ratio of sample amino acids which would be found in collagen to total sample amino acid content and is therefore independent of losses in sample volume during analysis. Soluble and insoluble collagen have approximately the same fractional collagen content relative to total protein (~90%). The ratios of protein and collagen content per dry weight were calculated from the analysis data and known dry weights. The difference between total protein content and dry weight may represent sample loss during the analysis procedure. However, it may also be due to non-protein components of the sample. For the soluble and insoluble collagen samples, between 10 and 30% of the original sample weight is unaccounted for by protein. The wide variability of the data suggest that random sample losses must contribute. This is further supported by the case of hydroxyproline, where the difference between protein content and dry weight must represent sample loss

(23%). It is impossible to tell without further biochemical analysis which fraction of this is due to non-protein components. Therefore, definite conclusions about the purity of the soluble and insoluble collagen used in these experiments can not be drawn at this time.

Throughout these experiments, trypsin digested cartilage was assumed to represent a relatively pure collagen matrix. Results from hydroxyproline analysis (Table 10) of trypsin digested cartilage suggest that there is a nontrivial fraction of noncollagenous proteins remaining in the cartilage sample (11.4% ± 2.3%, n = 3, from ratio of collagen to protein) which are insensitive to proteolysis by trypsin. However, the results for trypsin digested cartilage are not substantially different from those for samples of soluble and insoluble collagen, casting more suspicion on the analysis procedure than on the purity of the trypsin digested cartilage.

The similar fraction of collagen to total protein seen in this analysis for soluble and insoluble collagen makes it improbable that differences in collagen content per measured weight account for the observed difference in Ms/Mo found for soluble versus insoluble collagen. Therefore, structural dissimilarity seems more likely to account for the differences. We had presumed that the insoluble collagen contained highly crosslinked fibrils while soluble collagen contained predominantly individual collagen molecules rather than fibrils. In fact, the exact composition and structure of the acid soluble collagen are uncertain. Discussion with the supplier (Sigma) revealed that the collagen was dissolved in weak acetic acid prior to freeze drying. We had assumed that it maintained its molecular structure as it dried. However, if fibrils had formed upon drying or when hydrated in suspensions, they would be expected to be minimally crosslinked. In contrast, the insoluble collagen fibrils must be extensively crosslinked since it is crosslinking which makes the collagen insoluble (Tanzer 1973).

Since completion of the experiments measuring Ms/Mo in soluble and insoluble suspensions, the suspensions have been examined under electron microscopy. Small amounts of each type of collagen were added to phosphate buffered saline and then sonicated to obtain a more homogeneous dispersion. Samples were then examined under electron microscopy at 60,000X magnification. Soluble suspensions were found to contain fibrils (Figure 38). These fibrils were of small diameter (20-30 nm) and were frequently without apparent banding patterns. The non-banded fibrils were typically also curved. While these results confirm the presence of fibrils in the soluble collagen suspensions, they do not preclude the presence of collagen molecules. Collagen molecules are too small to be

observed with this level of magnification. Insoluble collagen suspensions were found to contain characteristically banded fibrils with diameters of approximately 100 nm (Figure 39). The clear globules seen in the photograph were not identified and may be an artifact of the EM staining procedure (Jon Come, personal observation). Due to the non-uniform dispersion of collagen in these suspensions, no attempt was made to either quantitatively or qualitatively estimate the apparent density of fibrils seen with EM.

Presumably the structural difference which makes soluble collagen suspensions exhibit more MT than insoluble suspensions involves the solubility of the collagen. To see whether Ms/Mo would decrease in insoluble collagen suspensions if the collagen became soluble, we exposed several insoluble suspensions to pepsin. Pepsin is a proteolytic enzyme used to extract collagen from tissues. It cleaves collagen in the crosslink-containing non-helical regions of the molecule, thereby turning insoluble fibrils into soluble molecules (Bornstein and Traub 1979). The triple helical region resists proteolysis, provided the sample is kept at temperatures which are well below the denaturation temperature of collagen. Ms/Mo was measured immediately after hydrating two 5% insoluble collagen suspensions with pepsin (5% w/v in 0.1 N HCl) and again after 7 hr. Ms/Mo showed no change in these samples after 7 hr (ratio of Ms/Mo after pepsin to that before was 0.99 ± 0.02; raw data shown in Table 11). These preliminary results suggest that solubilizing insoluble collagen is not sufficient to make Ms/Mo for insoluble collagen suspensions equal to that for soluble collagen suspensions.

Table 11 Ms/Mo in collagen suspensions hydrated with pepsin or trypsin. Data also included for suspensions made with control solutions (0.15 M NaCl, 0.15 M NaCl pH 2, or 0.1 N HCl)

preparation	solvent added	Ms/Mo immediately	Ms/Mo after 7 hr
10% insoluble	0.15 M NaCl	0.37 ± 0.01 (n = 2)	
10% insoluble	5% pepsin in 0.1 N HCl	0.57	0.55
5% insoluble	0.15 M NaCl	0.59 ± 0.03 (n = 2)	
5% insoluble	0.15 M NaCl, pH 2	0.60	
5% insoluble	5% pepsin in 0.1 N HCl	0.69 ± 0.01 (n = 2)	0.69 ± 0.01
5% insoluble	25 mg/mL trypsin	0.66 ± 0 (n = 2)	0.66 ± 0.03
5% insoluble	0.1 N HCl	0.78 ± 0.01 (n = 2)	

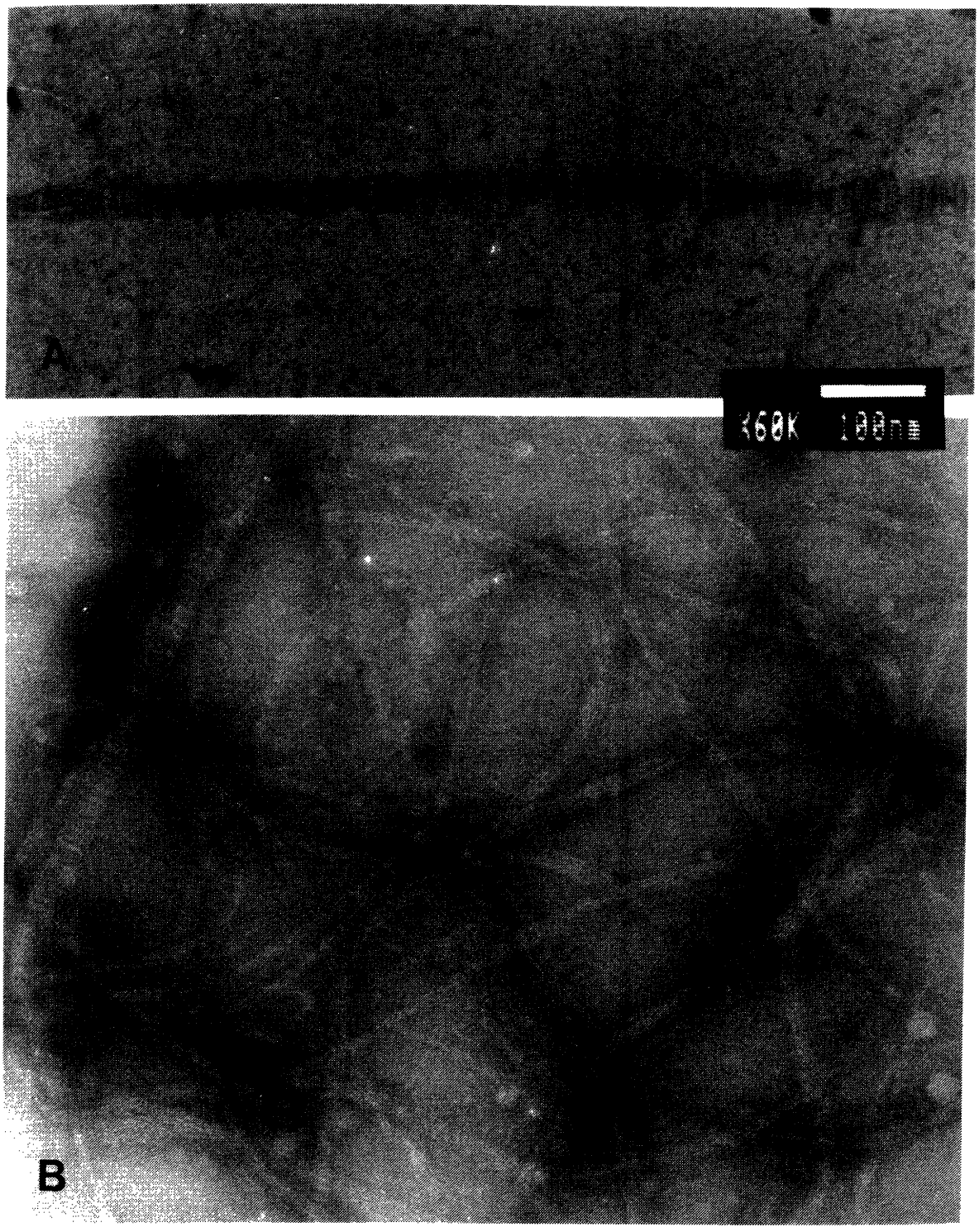

FIGURE 38 Electron microscopy of acid soluble collagen suspended in phosphate buffered saline (60,000X magnification). Fibrils are present; fibril diameter approximately 20-30 nm. Some fibrils exhibit characteristic banded pattern (A), others do not (B). Molecules may be present but would not be visible at this magnification.

FIGURE 39 Electron microscopy of insoluble collagen suspended in phosphate buffered saline (60,000X magnification). Fibrils exhibit characteristic banded pattern; fibril diameter approximately 100 nm.

In order to explain the difference in Ms/Mo observed between soluble and insoluble collagen suspensions, further studies are needed to characterize the two types of collagen and to examine the state of the insoluble collagen after pepsin or other enzymatic digestion (e.g. electron microscopy to rule out the presence of fibrils).

While Ms/Mo in cartilage decreased slightly with increasing collagen concentration, differences were evident among samples which were taken from different sites but which had similar collagen content, suggesting that structural differences have a non-negligible effect on MT. Ms/Mo for trypsin digested cartilage is on the order of that seen for suspensions, suggesting that MT effects for type II collagen may be similar to those for type I. However, the possibility must be considered throughout this discussion that the observed magnitude of Ms/Mo is due to a summation of effects which may be either additive or subtractive (i.e. opposing). For example, the similar Ms/Mo seen for cartilage samples when compared to collagen suspensions with the same collagen concentration may be a result of opposing effects which cancel each other. Hypothetically, type I collagen could exhibit less MT than type II but collagen woven into a tight network in cartilage might exhibit more MT than the same collagen fibrils in suspension. The net result would therefore be no difference in MT.

We have shown that an intact triple helix is important for MT. Loss of the collagen triple helix with thermal denaturation of dilute collagen gels and soluble collagen suspensions resulted in substantially increased Ms/Mo. The incomplete loss of MT in soluble and insoluble suspensions after heating (Ms/Mo < 1) may be due to incomplete denaturation. The denaturation of acid soluble collagen has been shown to proceed in two steps or phases (Engel 1962). Phase I denaturation happens quickly (within 15 min at 38°C) and involves collapse of the helical backbone. Phase I denaturation has been detected by decreased optical rotation, specific viscosity, and radius of gyration. Phase II denaturation occurs much more slowly (on the order of two hours at 38°C) and involves the disentanglement of the α chains. Phase II denaturation was detected only by decreased molecular weight of the denaturation products (and not by further changes in optical rotation or specific viscosity). The samples in our study were heated at a higher temperature but for less than an hour and therefore may have undergone only Phase I denaturation. (Attempts at heating longer than 30-45 min resulted in loss of sample water which interfered with measurement of Ms/Mo.) Perhaps some degree of residual chain association is sufficient to allow magnetization transfer. This hypothesis is further supported by the proportionately larger increase in Ms/Mo seen for soluble suspensions after heating compared to insoluble

suspensions (Figure 29). Denaturation of the soluble collagen presumably results in more individual α chains compared to the highly crosslinked insoluble collagen.

MT in denatured collagen was examined further by measuring Ms/Mo in several gelatin solutions. Gelatin is a general term referring to denatured (unfolded) collagen. However, commercial preparations may be heterogeneous since gelatin can refer to degraded collagen, including fragments of the molecule (Bornstein and Traub 1979). Ms/Mo for one 10% (w/w) preparation of gelatin was 0.90; Ms/Mo for two 5% samples were 0.92 and 0.96. Further studies are necessary to determine whether experimental conditions can be found for which MT in collagen suspensions disappears completely.

4. MT FOR DETECTION OF CARTILAGE DEGRADATION

We have demonstrated measurable changes in MT when cartilage is subjected to perturbations which mimic aspects of tissue pathology such as treatment with enzymes and exposure to low pH. Moreover, these changes were not explained by changes in collagen concentration. They may be attributable to changes in structure and/or fibril hydration (although changes in fibril hydration with trypsin and low pH produced conflicting results, as described below).

Ms/Mo increased significantly in trypsin-digested samples compared to controls (Figure 30). At first glance, the observed increase in Ms/Mo appears to be different from results reported by Kim (1993). In that paper, Kim stated that "the proteoglycan depleted cartilage samples exhibited the same degree of magnetization transfer as the untreated cartilage." In fact, Kim's results are similar to ours. Data included in their paper show that Ms/Mo measured for intact cartilage was 0.189 ± 0.030, while Ms/Mo measured in cartilage after removal of proteoglycans with chondroitinase II or trypsin was 0.201 ± 0.007 or 0.214 ± 0.010, respectively (mean ± SEM, n = 3). The mean of Ms/Mo measured for their trypsin digested samples is 13.2% higher than that for intact samples. Although no mention is made of statistical analysis, these differences appear to be statistically insignificant (using Student's t distribution with mean and SEM provided). Unlike our study, however, these were not paired data (i.e. the same sample before and after) which makes the interpretation more difficult since we have shown sample-to-sample variation on the order of 10%.

The increase in Ms/Mo with trypsin was not explained by changes in collagen concentration. In fact, collagen concentration apparently increased after trypsin digestion due to decreased tissue water content (Figure 32). The MT effect may be a function of fibril hydration. The observed increase in Ms/Mo could be due to the increased intrafibrillar water after removal of proteoglycans with trypsin. Alternatively, it is possible that non-collagenous molecules which are removed by trypsin contribute to the MT effect seen in cartilage, either directly or indirectly (e.g. through their interactions with collagen). Although neither chondroitin sulfate nor monomer proteoglycans in solution exhibit MT, they may have some MT effect when incorporated into the cartilage matrix. In cartilage, the collagen network physically entraps the proteoglycans. Furthermore, small proteoglycans such as decorin and fibromodulin can bind to the collagen fibril (Eyre 1991). When proteoglycans are bound to collagen, or trapped by the fibrillar matrix, sufficient motional restriction may exist for some protons to participate in the MT process. It is also possible that some of the quantitatively minor collagens which regulate fibril formation (e.g. type IX, Eyre 1991) are degraded by trypsin and lost from the matrix, resulting in decreased type II fibril integrity and decreased MT (increased Ms/Mo).

To study possible changes in MT due to direct effects of trypsin on the collagen molecule or fibril, we directly exposed insoluble collagen suspensions to trypsin. Ms/Mo was measured immediately and at 7 hr after hydrating the collagen with saline containing 25 mg/mL trypsin. Ms/Mo showed no change after 7 hr in trypsin, suggesting that direct effects of trypsin are not responsible for the observed increase in Ms/Mo seen for cartilage after trypsin digestion (ratio of Ms/Mo after 7 hr with trypsin to that before was 1.0 ± 0.04, $n = 2$). Raw data from this experiment is included in Table 11. While no explanation has yet been determined, it is interesting to note that Ms/Mo measured for suspensions hydrated with trypsin and pepsin was higher than normal (with 0.15 M NaCl). Further studies will be directed at exploring the reason for this difference.

Biochemical analysis (including studies of protein separation to quantitate minor collagen components) on cartilage before and after trypsin digestion should provide information about the composition of cartilage after exposure to trypsin. Hydroxyproline analysis of the bathing solution would give an estimate of collagen lost from the matrix although, as discussed earlier, we would not expect to see more than 5% loss over a 24 hr digestion period. In order to visualize structural changes which might occur with trypsin, techniques providing higher resolution than standard electron microscopy will be necessary.

Exposure of cartilage to low pH in 0.15 M NaCl revealed some differences in behavior for native versus trypsin-digested cartilage (Figure 33). Ms/Mo for native cartilage began to decrease at pH 2 and decreased further when returned to pH 8 while Ms/Mo for trypsin-digested cartilage did not decrease until return of the tissue to the original pH 8 bath. Collagen fibril hydration is expected to increase in both native and trypsin-digested cartilage at pH 2 due to the development of a net positive charge on the collagen molecules. However, it seems unlikely that fibril hydration alone is responsible for the magnitude of Ms/Mo observed in cartilage since conflicting results were seen with increased fibril hydration due to removal of GAG by trypsin (increased Ms/Mo) compared to increased fibril hydration at low pH (Ms/Mo increased slightly in trypsin digested samples but decreased in native samples). Furthermore, when fibril hydration was varied by making insoluble collagen suspensions with saline at low pH, no significant change in Ms/Mo was observed.

The results for trypsin-digested cartilage (i.e. Ms/Mo is approximately constant until returned to pH 8) suggest that some structural change is occurring to the collagen molecule or fibril at pH 2 which is then futher modified when the tissue is returned to pH 8, resulting in an enhancement of the magnetization transfer effect. However, the fact that Ms/Mo decreases in native tissue at pH 2 while Ms/Mo for trypsin-digested cartilage does not suggests that the interaction between proteoglycans and collagen (possibly via charge) must contribute to the measured value of Ms/Mo.

Maximum swelling of collagen fibrils has been observed at pH 2 due to the net positive charge developed on the molecules (Bowes and Kenten 1948a). However, this swelling is supposed to be completely reversible when the excess charge is removed by adjusting the pH back to the isoelectric point or by shielding the charges with excess salt (Veis 1967). Ms/Mo did not return to initial values when samples were returned to pH 8; however, neither did wet weights. Therefore, it is unclear whether fibril hydration decreased as expected when samples were returned to pH 8, making it difficult to draw conclusions on the relationship of fibril hydration to Ms/Mo. In a study on bovine tendon, thermal denaturation (measured by differential scanning microcalorimetry) occurred at room temperature for 0.15 M NaCl below pH 3.1, compared to ~60°C for 0.15 M NaCl or water between pH 4 and pH 10 (Hellauer and Winkler 1975). It was hypothesized that the lowering of the denaturation temperature was due to ionic disorganization of the water associated with the collagen molecule and also to electrostatic repulsion. However, the

decrease in Ms/Mo at pH 2 is in contrast to the increased Ms/Mo observed with thermal denaturation of soluble collagen.

To more specifically examine the contribution of osmotic forces and fibril hydration to Ms/Mo measured at low pH, the varying pH experiment was repeated in an abbreviated form in the presence of 0.5 M NaCl (Figure 35). Higher salt concentration was expected to shield any net positive charge developed on the collagen molecule at low pH, thus minimizing changes in fibril hydration. Ms/Mo in native cartilage was approximately constant from pH 8 to 2 and back to 8 while trypsin-digested cartilage exhibited behavior similar to that seen at lower salt.

Careful comparison of the results for native cartilage in Figures 33 and 35 reveals a difference in the initial pH 8 value of Ms/Mo. Ms/Mo for native cartilage in 0.15 M NaCl is approximately 0.22 while that for samples in 0.5 M NaCl is around 0.17. In native tissue, increased ionic strength would be expected to increase collagen fibril hydration and decrease total tissue hydration due to the shielding of negative charges on the proteoglycans by excess mobile cations (Na^+). These changes are similar to those expected in 0.15 M NaCl at low pH; where the net charge on the proteoglycans is reduced by protonation of the anionic sites. Interestingly, the value of Ms/Mo seen for native cartilage in 0.15 M NaCl at pH 2 is approximately 0.16 which is nearly equal to the value seen at pH 8 in high salt. When native samples were returned to pH 8 baths, Ms/Mo decreased further for samples in 0.15 M NaCl to around 0.12 but only decreased slightly for samples in 0.5 M NaCl. It is conceivable that the higher salt concentration would influence whatever molecular rearrangements are occurring upon return to pH 8. These results suggest that for native cartilage, the interactions of proteoglycans with adjacent molecules may influence the amount of MT. Moreover, the observed changes in Ms/Mo with varying pH may be due to changes in the interactions of proteoglycans with the matrix. However, the interpretation becomes more difficult when considering that the complete removal of proteoglycans with trypsin resulted in the opposite effect: an increase in Ms/Mo.

For trypsin digested cartilage, the magnitude of Ms/Mo seen in 0.15 M and 0.5 M NaCl at pH 8 is similar. However, at pH 2, Ms/Mo for trypsin digested cartilage in 0.15 M NaCl increased slightly while that for samples in 0.5 M NaCl decreased slightly. Since there are no proteoglycans in trypsinized cartilage, no difference would be expected for fibril hydration at pH 8 in 0.15 M NaCl compared to 0.5 M. However, at pH 2, fibril hydration would be expected to increase for samples in 0.15 M NaCl due to the development of a net

positive charge on the collagen molecules but would not change for samples in 0.5 M due to the shielding of the positive charges by the excess salt (Cl^-). These results suggest that fibril hydration may exert some subtle influence on the amount of MT observed in cartilage.

Taken together, the results for experiments in which cartilage was exposed to trypsin and bathed at low pH suggest that the net charge on the proteoglycans plays a substantial role in the observed MT phenomenon. They further suggest that contributions to the measured Ms/Mo value may be made by both collagen fibril hydration and the interaction between the proteoglycans and collagen matrix.

The mechanism underlying the changes in Ms/Mo for both native and trypsin-digested cartilage at pH 2 and when returned to pH 8 will have to be studied further. It is particularly interesting that MT is enhanced (Ms/Mo decreased) in this experiment and in the IL-1ß experiment, making it unlikely that degradation or denaturation (of the type seen with thermal denaturation of collagen where Ms/Mo increased) is responsible. Furthermore, since Ms/Mo for soluble collagen suspensions was decreased relative to insoluble suspensions of the same concentration, the enhancement of MT seen with low pH and IL-1ß raises the possibility that some degree of solubilization of the collagen fibril occurs under these experimental conditions and is responsible for the increased MT effect. It may be of interest to perform assays for endogenous metalloproteinases which might be activated at low pH and then continue working at pH 8. High resolution microscopic evaluation of both native and trypsin-digested tissue at low pH may provide information about structural changes, such as disordering of the collagen fibril, which may occur when exposed to low pH.

The data on exposure of cartilage to IL-1ß suggest that measurable decreases in Ms/Mo occur with increased time of exposure and that MT is enhanced in a dose dependent fashion. These experiments need to be repeated for more samples and for different levels of IL-1ß. Ms/Mo should be measured at several offset frequencies in order to determine whether there are saturation frequencies for which differences among samples exposed to different amounts of IL-1ß would be accentuated. In order to further isolate the effects of IL-1ß on collagen, cartilage which has been depleted of proteoglycans by trypsin digestion could be cultured with IL-1ß. Given the temperature dependence of MT, measurements of Ms/Mo in future experiments involving cell culture conditions should be performed at 37°C when possible.

In addition, exposure of cartilage to other enzymes which affect collagen may reveal information about the sites responsible for MT. For example, stromelysin has been shown to cleave collagen types II, IX, X, and XI in cartilage (Wu 1991). Measurement of Ms/Mo before and after the selected cleavage of minor types of collagen may allow elucidation of specific structural changes responsible for changes in Ms/Mo.

B. GENERAL CONCLUSIONS AND DISCUSSION

Much of the evaluation of the MT technique has been performed on model systems and it is important to consider the applicability of these model systems to cartilage. Collagen gels initially seemed to be the ideal model system for studying collagen in cartilage since the fibrils formed in gels are almost indistinguishable from those found *in vivo*. However, the newly formed fibrils in collagen gels are not highly crosslinked as are the collagen fibrils in cartilage. Furthermore, gels can only be made in concentrations up to 2% and collagen in cartilage is present at concentrations of 10-20% (weight per tissue water). In order to increase the concentration of collagen under study, we made collagen suspensions. In fact, this model system may be most applicable to cartilage. It was possible to obtain concentrations on the order of those which found in cartilage which appeared homogeneous throughout. Moreover, collagen was insoluble in these suspensions as it is insoluble in tissue. However, these suspensions were made with type I collagen while cartilage contains predominantly type II collagen. A more ideal model system could be constructed with suspensions made from type II collagen extracted from native tissue. Unfortunately, nondegradative extraction from cartilage yields little collagen since it is highly crosslinked. Therefore, the model system described here may be the most appropriate for the majority of experiments.

During our evaluation of collagen concentration in various types of cartilage, we compared estimates of collagen content based on hydroxyproline analysis with those based on dry weights. Obtaining wet and dry weights is experimentally straightforward. On the other hand, hydroxyproline analysis is considerably labor intensive and the accuracy of results is not guaranteed. Estimates of collagen content based on dry weight may be sufficient for studies on MT in cartilage.

Our data have shown that the temperature at which the MT experiment is performed will have an impact on the observed results (Figure 21). Absolute values for Ms/Mo are dependent on the temperature. Decreases on the order of 25% (0.2 to 0.15) were observed

when cartilage was heated from room to body temperature. Therefore, comparison of data obtained for samples at different temperatures would be difficult since temperature effects could intensify or cancel out effects due to other processes. Although absolute values for Ms/Mo will change with temperature, trends will presumably be preserved provided the temperature is kept constant throughout an experiment. It is also notable that at higher temperatures, the sensitivity to differences in concentration decreases (Figure 21). The percent change in Ms/Mo for a given change in concentration will be smaller at higher temperatures. Therefore, this implies that measurable differences in Ms/Mo seen at higher temperatures are likely to be due to large differences in concentration, or to factors other than concentration.

Changes seen with temperature and with varying experimental conditions from day to day suggest that a reference standard be developed to which results can be compared or normalized. Agar gels exhibit substantial MT effect and have been used in many studies evaluating the MT phenomenon (e.g. Ceckler 1992). Crosslinked bovine serum albumin gels may be a more appropriate tissue phantom than agar gels (Koenig 1993, Mendelson 1991). In one study, the frequency response (as in Figure 18) measured for 2% agar gels was shown to differ from that seen in fresh rat muscle while that for 24% thermally crosslinked bovine serum albumin gels did not (Mendelson 1991). However, results of a more recent study suggest that the Gaussian lineshape seen for agar is similar to that seen for tissue (Henkelman 1993). Both types of gel are easily produced; exact concentrations can be determined after use by drying the samples. In order to choose an appropriate reference standard, both types of gels should be characterized in terms of their MT response and compared to the tissue under study (e.g., collagen suspensions or cartilage).

Changes in T1 were seen with increased temperature. However, T1 returned to its room temperature value when the sample cooled. Changes in Ms/Mo after thermal denaturation persisted after the temperature had returned to normal. Therefore, the MT technique seems to be more sensitive to structural changes than T1. Consequently, MT images would potentially provide structural information which is above and beyond the anatomical information currently supplied by T1-weighted images. MT images should also provide more information than proton density images, since Ms/Mo varied as a function of collagen concentration and relative changes in collagen concentration would be expected to be greater than relative changes in water concentration. A change from 10% collagen to 20% collagen by weight is a doubling in collagen concentration but the accompanying change in water content from 90% to 80% represents only an 11% decrease.

Spectroscopic and imaging studies using magnetization transfer have reported results in terms of both Ms/Mo and the (pseudo) rate constant k (e.g. Eng 1991, Hajnal 1992, Wolff 1991). We have consistently reported our results in terms of Ms/Mo. In some studies we did measure T1sat and were therefore able to calculate k by rearranging equation 25 derived earlier in the theory section:

$$k = \frac{1}{T1sat}\left(1 - \frac{Ms}{Mo}\right) \tag{30}$$

Figure 40 shows both Ms/Mo and k as a function of collagen concentration for insoluble collagen suspensions. Ms/Mo increases with increasing collagen concentration while k decreases. The slopes of the two curves are opposing but relative trends are preserved. However, over the range of 3 to 20%, the relative change in k (+700%) is substantially greater than that in Ms/Mo (-60%). Figure 41 shows Ms/Mo and k for several samples from the experiment in which cartilage was exposed to low pH. Over the course of this experiment, Ms/Mo decreases by 50% while k increases by 165%. Again, the slopes of the two curves are different but the relative trends are the same.

It has been shown that images based on k have significantly greater contrast than Ms/Mo images (Eng 1991). In this study of the kidney, the fractional difference between cortex and medulla was greater in terms of k (3.8:1) than in terms of Ms/Mo (1.6:1). However, T1sat images must first be obtained in order to calculate k which considerably increases the total imaging time. Furthermore, while the magnitude of contrast was greater with k images, the pattern was consistent with Ms/Mo images of the same tissue (Eng 1991). The results in figures 40 and 41 agree with these imaging results. Fractional increases in k are greater than those in Ms/Mo. Since calculation of k did not appear to provide further insight into either of these two diverse experiments, the additional time required to measure T1sat does not seem justified. Furthermore, calculation of k using equation 30 depends on the assumption that the entire pool of macromolecular protons is completely saturated. Using a two pool model to fit their data, Henkelman (1993) has shown that this assumption is not valid for agar gels. It remains to be shown whether the assumption is invalid for other tissues. Interpretation of data based on direct measurement of Ms/Mo involves no such assumptions.

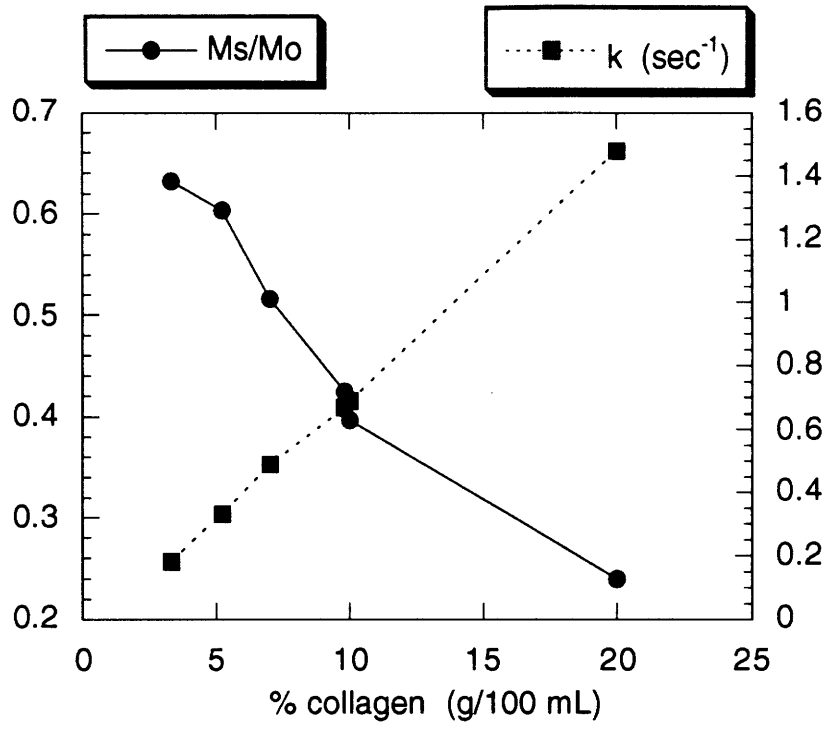

FIGURE 40 Ms/Mo and k versus collagen concentration for insoluble collagen suspensions. Values for k were calculated using equation 30.

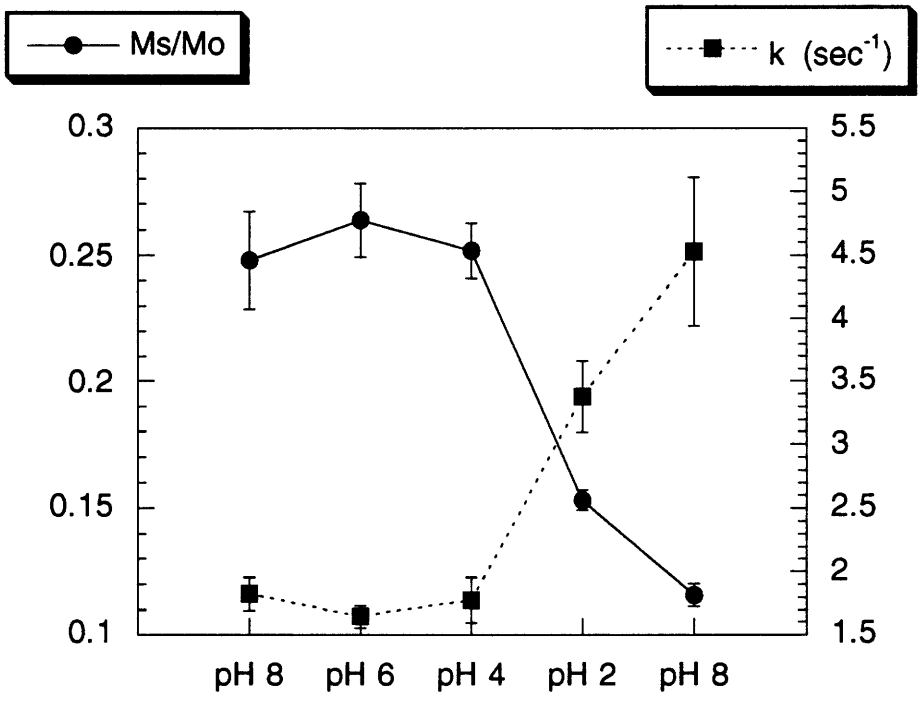

FIGURE 41 Ms/Mo and k for cartilage samples (n = 3) bathed in 150 mM NaCl baths of pH 8, 6, 4, 2, and then back to pH 8. Equation 30 was used to calculate k.

C. SUMMARY

We have shown that the MT effect is dependent on collagen concentration in collagen suspensions, with an approximately logarithmic relationship. However, at concentrations on the order of those seen *in vivo*, the magnitude of Ms/Mo varies little. In addition, we have demonstrated that factors other than concentration affect the MT signal in collagen suspensions. For example, Ms/Mo was ~20% greater for highly crosslinked insoluble collagen suspensions than for soluble suspensions of equal collagen content. Ms/Mo also varied among cartilage from different sources with similar collagen content. We have shown that an intact triple helix is important for MT. Loss of the collagen triple helix with thermal denaturation of soluble collagen suspensions resulted in substantially increased Ms/Mo. Furthermore, treatment with enzymes or low pH led to measurable differences in Ms/Mo which are not explained by differences in collagen concentration. They may be attributable to changes in collagen structure, proteoglycan charge, and/or collagen fibril hydration (although changes in fibril hydration with trypsin and low pH produced conflicting results).

Since changes in collagen structural integrity, collagen and proteoglycan concentrations, and fibril hydration all occur with degenerative diseases such as osteoarthritis, further studies are warranted to investigate more fully the mechanism for MT observed in cartilage. Specifically, future efforts should be directed at examining the differences in Ms/Mo seen for soluble versus insoluble collagen suspensions, cartilage before and after trypsin digestion, cartilage bathed in low pH solutions, and cartilage exposed to IL-1ß.

In future studies, results obtained from spectroscopic studies should be extended to an imaging mode. Magnetization transfer images of joints could be obtained prior to scheduled arthroscopy or joint replacement surgery and followed up with biochemical and histologic examination of tissue composition and structure. Ultimately, the technique may be useful for the study of progressive changes in cartilage structure and function in animal models of cartilage degeneration.

SUMMARY

In the first half of this work, NMR was used to nondestructively measure multiple ions in cartilage under both physiologic and non-physiologic conditions. Specifically, sodium NMR was used to measure sodium content in cartilage from which fixed charge density (FCD) was calculated, giving an estimate of proteoglycan content. Proteoglycan content determined by NMR was consistent with that determined biochemically. The sodium NMR technique is sufficiently sensitive to detect normal variations in FCD. Changes in tissue sodium content and FCD were observed when cartilage was exposed to baths of differing salt composition, pH, or ionic strength. FCD was also observed to increase when cartilage was compressed and decrease when cartilage was depleted of proteoglycans by exposure to trypsin.

In the second half of this work, magnetization transfer (MT) was used to study the collagen component of cartilage. The magnetization transfer effect (quantified as Ms/Mo) was shown to be dependent on collagen concentration in a model system of collagen suspensions, with an approximately logarithmic relationship. In addition, it was demonstrated that factors other than concentration affect the magnetization transfer process in collagen and cartilage. For example, Ms/Mo was ~20% greater for highly crosslinked insoluble collagen suspensions than for soluble suspensions of equal collagen content. Ms/Mo also varied among cartilage from different sources with similar collagen content. Data showed that an intact triple helix is important for MT; loss of the collagen triple helix with thermal denaturation resulted in substantial increases in Ms/Mo. Furthermore, treatment with enzymes or low pH led to measurable differences in Ms/Mo which are not explained by differences in collagen concentration. They may be attributable to changes in matrix charge, structure, and/or fibril hydration (although changes in hydration with trypsin and low pH produced conflicting results). Since changes in collagen structural integrity, collagen and proteoglycan concentrations, and fibril hydration all occur with degenerative diseases like osteoarthritis, further studies are warranted to investigate more fully the mechanism for MT observed in cartilage.

The sodium and magnetization transfer data demonstrate that the NMR experiment is a versatile technique for studies of cartilage matrix constituents, specifically the proteoglycan and collagen components. The nondestructive nature of the NMR studies provides the powerful capability of conducting kinetic or sequential studies on the same specimen (or

patient). Moreover, while these techniques were developed on well-controlled *in vitro* systems, they can be directly applied to the *in vivo* clinical setting. A multiparametric approach including sodium and magnetization transfer NMR experiments should provide the unprecedented opportunity to nondestructively monitor the progression of matrix destruction during the early stages of arthritis and to evaluate the efficacy of preventive and therapeutic interventions.

REFERENCES

Antonopoulos 1964 Antonopoulos CA, Gardell S, Szirmai JA, de Tyssonsk ER. Determination of glycosaminoglycans from tissues on the microgram scale. *Biochim Biophys Acta* **83**:1-19.

Baker 1985 Baker DG, Schumacher HR, Wolf GL. Nuclear magnetic resonance evaluation of synovial fluid and articular tissues. *J Rheumatol* **12**:1062-1065.

Balaban and Ceckler 1992 Balaban RS, Ceckler TL. Magnetization transfer contrast in magnetic resonance imaging. *Mag Res Quarterly* **8**(2):116-137.

Berg and Prockop 1973 Berg RA, Prockop DJ. The thermal transition of a non-hydroxylated form of collagen. Evidence for a role for hydroxyproline in stabilizing the triple-helix of collagen. *Biochem Biophys Res Comm* **52**(1):115-120.

Bitter and Muir 1962 Bitter T, Muir H. A modified uronic acid carbazole reaction. *Anal Biochem* **4**:330-334.

Bornstein 1958 Bornstein MB. Reconstituted rat-tail collagen used as substrate for tissue cultures on coverslips in maximow slides and roller tubes. *Lab Invest* **7**(2):134-137.

Bornstein and Traub 1979 Bornstein P, Traub W. The chemistry and biology of collagen. In *The Proteins*, 3rd Ed, Vol IV, Neurath H, Hill RL, eds. Academic Press, New York, pp. 411-632.

Boustany 1991 Boustany N. Regulation of chondrocyte biosynthesis in epiphyseal cartilage: The role of interstitial pH. M.S. Thesis, Massachusetts Institute of Technology.

Bowes and Kenten 1948a Bowes JH, Kenten RH. The amino-acid composition and titration curve of collagen. *Biochem J* **43**:358-365.

Bowes and Kenton 1948b Bowes JH, Kenten RH. The effect of alkalis on collagen. *Biochem J* **43**:365-372.

Brandt and Kovalov 1991 Brandt KD, Kovalov-St John K. Osteoarthritis. In *Harrison's Principles of Internal Medicine*, Wilson JD, Braunwald E, et al, eds. McGraw-Hill, New York, pp. 1475-1479.

Brodsky 1990 Fibrous proteins: Folding and higher order structure. In *Protein Folding*, Gierasch LM, King J, eds. AAAS, Washington DC, pp. 55-62.

Bruckner and Prockop 1981 Bruckner P, Prockop DJ. Proteolytic enzymes as probes for the triple-helical conformation of procollagen. *Anal Biochem* **110**:360-368.

Bryant 1993 Bryant RG. Paramagnetic effects in magnetic relaxation coupling. Abstract from workshop on Water/Macromolecule Magnetization transfer in MRI, sponsored by SMRI and SMRM, Frederick MD, July 1993.

Burgeson and Nimni 1992 Burgeson RE, Nimni ME. Collagen types: Molecular structure and tissue distribution. *Clin Orthop Rel Res* **282**:250-272.

Burjanadze 1979 Burjanadze TV. Hydroxyproline content and location in relation to collagen thermal stability. *Biopolymers* **18**:931-938.

Burk 1986 Burk DL, Kanal E, Brunberg JA, Johnstone GF, Swensen HE, Wolf GL. 1.5-T surface-coil MRI of the knee. *AJR* **147**:293-300.

Byers 1990 Byers PH. Folding of collagen molecules containing mutant chains. In *Protein Folding*, Gierasch LM, King J, eds. AAAS, Washington DC, pp. 241-247.

Carrington and McLachlan 1967 Carrington A, McLachlan AD. *Introduction to Magnetic Resonance with Applications to Chemistry and Chemical Physics*. Harper & Row, New York.

Ceckler 1992 Ceckler TL, Wolff SD, Yip V, Simon SA, Balaban RS. Dynamic and chemical factors affecting water proton relaxation by macromolecules. *J Mag Res* **98**:637-645.

Ceckler 1993 Ceckler TL. Chemical basis of water macromolecule proton magnetization exchange. Abstract from workshop on Water/Macromolecule Magnetization transfer in MRI, sponsored by SMRI and SMRM, Frederick MD, July 1993.

Ceckler and Balaban 1991 Ceckler TL, Balaban RS. Tritium-proton magnetization transfer as a probe of cross relaxation in aqueous lipid bilayer suspensions. *J Mag Res* **93**:572-588.

Chien and Wise 1975 Chien JCW, Wise WB. A 13C nuclear magnetic resonance and circular dichroism study of the collagen-gelatin transformation in enzyme solubilized collagen. *Biochemistry* **14**(12):2786-2792.

Creighton 1984 Creighton TE. *Proteins: Structure and Molecular Principles*. W. H. Freeman and Company, New York, pp. 194-197.

Dodge and Poole 1989 Dodge RF, Poole AR. Immunohistochemical detection and immunochemical analysis of type II collagen degradation in human normal, rheumatoid, and osteoarthritic articular cartilages and in explants of bovine articular cartilage cultured with interleukin-1. *J Clin Invest* **83**:647-661.

Edelman and Hesselink 1990 Edelman RR, Hesselink JR. *Clinical Magnetic Resonance Imaging*. WB Saunders, Philadelphia.

Eikenberry and Brodsky 1980 Eikenberry EF, Brodsky B. Xray diffraction of reconstituted collagen fibers. *J Mol Biol* **144**:397-404.

Einbiner and Schubert 1951 Einbinder J, Schubert M. Binding of mucopolysaccharides and dyes by collagen. *J Biol Chem* **188**:335-341.

Eisenberg 1983 Eisenberg SR. Nonequilibrium electromechanical interactions in cartilage: swelling and electrokinetics. Ph.D. thesis, Massachusetts Institute of Technology.

Eisenberg and Grodzinsky 1985 Eisenberg SR, Grodzinsky AJ. Swelling of articular cartilage and other connective tissues: Electromechano-chemical forces, *J Orthop Res* **3**:148-159.

Eng 1991 Eng J, Ceckler TL, Balaban RS. Quantitative ^{1}H magnetization transfer imaging *in vivo. Mag ResMed.* **17**:304-314.

Engel 1962 Engel J. Investigation of the denaturation and renaturation of soluble collagen by light scattering. *Arch Biochem Biophys* **97**:150-158.

Evans 1991 Evans CH. The role of proteinases in cartilage destruction. *Agents Actions Suppl* **32**:135-152.

Eyre 1980 Eyre DR. Collagen: Molecular diversity in the body's protein scaffold. *Science* **207**:1315-1322.

Eyre 1984 Eyre DR, Paz MA, Gallop PM. Cross-linking in collagen and elastin. *Ann Rev Biochem* **53**:717-748.

Eyre 1991 Eyre DR. The collagens of articular cartilage. *Sem Arthritis Rheum* **21**(3):2-11.

Farndale 1986 Farndale RW, Buttle DJ, Barrett AJ. Improved quantitation and discrimination of sulfated glycosaminoglycans by use of dimethylmethylene blue. *Biochim Biophys Acta* **883**:173-177.

Farrar 1989 Farrar TC. *Pulse Nuclear Magnetic Resonance Spectroscopy.* Farragut Press, Madison.

Fife 1991 Fife RS, Brandt KD, Braunstein EM, Katz BP, Shelbourne KD, Kalasinski LA, Ryan S. Relationship between arthroscopic evidence of cartilage damage and radiographic evidence of joint space narrowing in early osteoarthritis of the knee. *Arthritis Rheum* **34**:377-382.

Forsen and Hoffman 1963 Forsen S, Hoffman RA. Study of moderately rapid chemical exchange reactions by means of nuclear magnetic double resonance. *J Chem Phys.* **39**(11):2892-2901.

Foy 1989 Foy BD, Lesperance LM, Gray ML, Burstein D. NMR parameters of interstitial sodium in cartilage. *Proc Soc Mag Res Med* p. 1108.

Fralix 1991 Fralix TA, Ceckler TL, Wolff SD, Simon SA, Balaban RS. Lipid bilayer and water proton magnetization transfer: effect of cholesterol. *Mag Res Med* **18**:214-223.

Frank 1987 Frank EH, Grodzinsky AJ, Koob TJ, Eyre DR. Streaming potentials: A sensitive index of enzymatic degradation in articular cartilage. *J Orthop Res* **5**:497-508.

Frank 1990 Frank EH, Grodzinsky AJ, Phillips SL, Grimshaw PE. Physicochemical and bioelectrical determinants of cartilage material properties. In *Biomechanics of Diarthrodial Joints.* Mow VC, Ratcliffe A, Ly-Woo S, eds. New York, Springer-Verlag.

Gray 1988 Gray ML, Pizzanelli AM, Grodzinsky AJ, Lee RC. Mechanical and physicochemical determinants of chondrocyte biosynthetic response. *J Orthop Res* **6**:777-792.

Grodzinsky 1981 Grodzinsky AJ, Roth V, Myers E, Grossman WD, Mow VC. The significance of electromechanical and osmotic forces in the nonequilibrium swelling behavior of articular cartilage in tension. *J Biomech Eng* **103**:221-231.

Grodzinsky 1983 Grodzinsky AJ. Electromechanical and physicochemical properties of connective tissue. *Crit Rev Biomed Engr* **9**(2):133-199.

Gross 1961 Gross J. Collagen. *Sci Am* **204**:121-130.

Gross 1964 Gross J. Thermal denaturation of collagen in the dispersed and solid state. *Science* **143**: 960-961.

Grushko 1989 Grushko G, Schneiderman R, Maroudas A. Some biochemical and biophysical parameters for the study of the pathogenesis of osteoarthritis: a comparison between the processes of ageing and degeneration in human hip cartilage. *Conn Tiss Res* **19**:149-176.

Grynpas 1980 Grynpas MD, Eyre DR, Kirschner DA. Collagen type II differs from type I in native molecular packing. *Biochim Biophys Acta* **636**:346-355.

Gylys-Morin 1987 Gylys-Morin VM, Hajek PC, Sartoris DJ, Resnick D. Articular cartilage defects: detectability in cadaveric knees with MR. *AJR* **148**:1153-1157.

Hajnal 1992 Hajnal JV, Baudouin CJ, Oatridge A, Young IR, Bydder GM. Design and implementation of magnetization transfer pulse sequences for clinical use. *J Comput Assist Tomogr* **16**(1):7-18.

Handley and Lowther 1977 Handley DJ, Lowther DA: Extracellular matrix metabolism by chondrocytes III. Modulation of proteoglycan synthesis by extracellular levels of proteoglycan in cartilage cells in culture. *Biochim Biophys Acta* **500**:132-139.

Harris 1972 Harris ED Jr, Parker HG, Radin EL, Krane SM. Effects of proteolytic enzymes on structural and mechanical properties of cartilage. *Arthritis and Rheum* 15(5):497-503.

Harris and Cartwright 1977 Harris ED Jr, Cartwright EC. Mammalian collagenases. In *Proteinases in mammalian cells and tissues*, Barrett AJ, ed. North Holland Publishing Co, New York, pp. 249-283.

Hartman 1991 Hartman AL. Diffusion coefficient of protons in compressed cartilage. M.S. thesis, Massachusetts Institute of Technology.

Hardingham 1992 Hardingham TE, Bayliss MT, Rayan V, Noble DP. Effects of growth factors and cytokines on proteoglycan turnover in articular cartilage. *Br J Rheumatol* **31**(suppl 1):1-6.

Hasty 1990 Hasty KA, Reife RA, Kang AH, Stuart JM. The role of stromelysin in the cartilage destruction that accompanies inflammatory arthritis. *Arthritis Rheum* **33**(3):388-397.

Hauschka and Reid 1978 Hauschka PV, Reid ML. Timed appearance of a calcium-binding protein containing γ-carboxyglutamic acid in developing chick bone. *Dev Biol* **65**:426-434.

Heinegard 1987 Heinegard D, Inerot S, Olsson S-E, Saxne T. Cartilage proteoglycans in degenerative joint disease. *J Rheumatol* **14**(S14):110-112.

Heinegard and Oldberg 1989 Heinegard D, Oldberg A. Structure and biology of cartilage and bone matrix noncollagenous macromolecules. *FASEB* **3**:2042-2051.

Hellauer and Winkler 1975 Hellauer H, Winkler WR. Denaturation of collagen fibers in NaCl and water of different pH values as studied by differential scanning calorimetric measurements. *Conn Tiss Res* **3**:227-230.

Henkelman 1993 Henkelman RM, Huang X, Xiang Q-S, Stanisz GJ, Swanson SD, Bronskill MJ. Quantitative interpretation of magnetization transfer. *Mag Res Med* **29**:759-766.

Inerot 1991 Inerot S, Heinegard D, Olsson S-E, Telhag H, Audell L. Proteoglycan alterations during developing experimental osteoarthritis in a novel hip joint model. *J Orthop Res* **9**:658-673.

Jelinski 1980 Jelinski LW, Sullivan CE, Torchia DA. 2H NMR study of molecular motion in collagen fibrils. *Nature* **284**:531-534.

Katz 1986 Katz EP, Wachtel EJ, Maroudas A. Extrafibrillar proteoglycans osmotically regulate the molecular packing of collagen in cartilage. *Biochem Biophys Acta* **882**:136-139.

Kaye 1990 Kaye JJ. Arthritis: Roles of radiography and other imaging techniques in evaluation. *Radiology* **177**:601-608.

Kim 1993 Kim DK, Ceckler T, Hascall VC, Calabro A, Balaban RS. Analysis of water-macromolecule proton magnetization transfer in articular cartilage. *Mag Res Med* **29**:211-215.

Koenig 1993 Koenig SH, Brown RD, Ugolini R. Magnetization transfer in cross-linked bovine serum albumin solutions at 200 MHz: A model for tissue. *Mag Res Med* **29**:311-316.

Krane 1982 Krane SM. Collagenases and collagen degradation. *J Invest Derm* **79**:83s-86s.

Kuettner and Kimura 1985 Kuettner KE, Kimura JH. Proteoglycans: An overview. *J Cell Biochem* **27**:327-336.

Lesperance 1992 Lesperance LM, Gray ML, Burstein D. Determination of fixed charge density in cartilage using nuclear magnetic resonance. *J Orthop Res* **10**:1-13.

Li and Katz 1976 Li S-T, Katz EP. An electrostatic model for collagen fibrils. *Biopolymers* **15**:1439-1460.

Light and Bailey 1980 Light ND, Bailey AJ. Molecular structure and stabilization of the collagen fibre. In *Biology of Collagen*, Viidik A and Vuust J, eds. Academic Press, New York, pp. 15-38.

Manahan and Mandl 1968 Manahan J, Mandl I. Primary structure of insoluble tendon collagen. III. Analysis of products of tryptic digestion on native collagen. *Arch Biochem Biophys* **128**:25-33.

Mankin and Lipiello 1971 Mankin HJ, Lipiello L. The glycosaminoglycans of normal and arthritic cartilage. *J Clin Invest* **50**:1712-1719.

Maroudas 1968 Maroudas A. Physicochemical properties of cartilage in the light of ion exchange theory. *Biophys J* **8**:575-595.

Maroudas 1969 Maroudas A, Muir H, Wingham J. The correlation of fixed negative charge with glycosaminoglycan content of human articular cartilage. *Biochim Biophys Acta* **177**:492-500.

Maroudas 1970 Maroudas A. Distribution and diffusion of solutes in articular cartilage. *Biophys J* **10**:365-379.

Maroudas 1973 Maroudas A, Evans H, Almeida L. Cartilage of the hip joint: Topographical variation of glycosaminoglycan content in normal and fibrillated tissue. *Ann Rheum Dis* **32**:1-9.

Maroudas 1976 Maroudas A. Balance between swelling pressure and collagen tension in normal and degenerate cartilage. *Nature* **260**:808-809.

Maroudas 1979 Maroudas A. Physicochemical properties of articular cartilage. In *Adult Articular Cartilage*, Freeman MAR, ed. Pitman, London, pp. 215-290.

Maroudas 1988 Maroudas A, Weinberg PD, Parker KH, Winlove CP. The distributions and diffusivities of small ions in chondroitin sulfate, hyaluronate and some proteoglycan solutions. *Biophys Chem* **32**:257-270.

Maroudas 1991 Maroudas A, Wachtel E, Grushko G, Katz EP, Weinberg P. The effect of osmotic and mechanical pressures on water partitioning in articular cartilage. *Biochim Biophys Acta* **1073**:285-294.

Maroudas and Evans 1972 Maroudas A, Evans H. A study of ionic equilibria in cartilage. *Conn Tiss Res* **1**:69-77.

Maroudas and Thomas 1970 Maroudas A, Thomas H: A simple physicochemical micromethod for determining fixed anionic groups in connective tissue. *Biochim Biophys Acta* **215**:214-216.

Matthews 1953 Matthews BF. Composition of articular cartilage in osteoarthritis: Changes in collagen/chondroitin sulfate ratio. *BMJ* **2**:660-661.

Mayne 1989 Mayne R. Cartilage collagens. *Arthritis Rheum* **32**(3):241-246.

McDevitt and Muir 1976 McDevitt CA, Muir H. Biochemical changes in the cartilage of the knee in experimental and natural osteoarthritis in the dog. *J Bone Joint Surg* **58-B**:94-101.

Meachim and Stockwell 1979 Meachim G, Stockwell RA. The matrix. In: *Adult Articular Cartilage*. Freeman MAR, ed, London, Pitman pp 1-67.

Mendelson 1991 Mendelson DA, Heinsbergen JF, Kennedy SD, Szczepaniak LS, Lester CC, Bryant RG. Comparison of agarose and cross-linked protein gels as magnetic resonance imaging phantoms. *Mag Res Imaging* **9**:975-978.

Miller 1984 Miller EJ. Collagen Chemistry. In *Extracellular Matrix Biochemistry*, Piez KA and Reddi AH, eds. Elsevier, New York, pp. 41-81.

Mink 1988 Mink JH, Levy T, Crues JV. Tears of the anterior cruciate ligament and menisci of the knee: MR imaging evaluation. *Radiology* **167**:769-774.

Morris and Freemont 1992 Morris GA, Freemont AJ. Direct observation of the magnetization exchange dynamics responsible for magnetization transfer contrast in human cartilage *in vitro*. *Mag Res Med* **28**:97-104.

Nomura 1977 Nomura S, Hiltner A, Lando JB, Baer E. Interaction of water with native collagen. *Biopolymers* **16**:231-246.

Nussbaum and Grodzinsky 1981 Nussbaum JH, Grodzinsky AJ. Proton diffusion reaction in a protein polyelectrolyte membrane and the kinetics of electromechanical forces. *J Membrane Science* **8**:193-219.

Phillips 1984 Phillips SL. The determination of charge density in articular cartilage via chemical titration. S.M. Thesis, Massachusetts Institute of Technology.

Piez 1967 Piez KA. Soluble collagen and denaturation components. In *Treatise on Collagen*, Ramachandran GN, ed. Academic Press, New York, pp. 367-439.

Pollak 1990 Pollak AN, Berns D, Kormos D, McDevitt C, Modic M, Moskowitz RW. Sodium magnetic resonance imaging demonstrates intervertebral disc degeneration in human cadaveric spines. *Trans ORS* **15**:252.

Ripamonti 1980 Ripamonti A, Roveri N, Braga D, Hulmes DJS, Miller A, Timmins PA. Effects of pH and ionic strength on the structure of collagen fibrils. *Biopolymers* **19**:965-975.

Rosenberg and Buckwalter 1986 Rosenberg LC, Buckwalter JA. Cartilage proteoglycans. In *Articular Cartilage Biochemistry*, Kuettner KE, Schleyerbach R, Hascall VC, eds. Raven Press, NY, pp. 39-57.

Russell 1974 Russell AE. Effect of pH on thermal stability of collagen in the dispersed and aggregated states. *Biochem J* **139**:277-180.

Sabiston 1987 Sabiston CP, Adams ME, Li DKB. Magnetic resonance imaging of osteoarthritis: Correlation with gross pathology using an experimental model. *J Orthop Res* **5**:164-172.

Sah 1990 Sah RL-Y, Grodzinsky AJ, Plaas AHK, Sandy JD. Effect of tissue compression on the hyaluronate binding properties of newly synthesized proteoglycans in cartilage explants. *Biochem J* **267**:803-808.

Schmidt 1990 Schmidt MB, Mow VC, Chun LE, Eyre DR. Effects of proteoglycan extraction on the tensile behavior of cartilage. *J Orthop Res* **8**:353-363.

Schneiderman 1986 Schneiderman R, Keret D, Maroudas A. Effects of mechanical and osmotic pressure on the rate of glycosaminoglycan synthesis in the human adult femoral head cartilage: an *in vitro* study. *J Orthop Res* **4**:393-408.

Skoog and West 1980 Skoog DA, West DM. *Principles of Instrumental Analysis*. Philadelphia, Saunders College.

Smith 1968 Smith JW. Molecular pattern in native collagen. *Nature* **219**:157.

Slichter 1980 Slichter CP. *Principles of Magnetic Resonance*. Springer-Verlag, New York.

Stockwell and Meachim 1979 Stockwell RA, Meachim G. The chondrocytes. In *Adult Articular Cartilage*, Freeman MAR, ed. Pitman, London, pp. 69-144.

Tanzer 1973 Tanzer ML. Cross-linking of collagen. *Science* **180**:561-566.

Torchia 1977 Torchia DA, Hasson MA, Hascall VC. Investigation of molecular motion of proteoglycans in cartilage by 13C magnetic resonance. *J Biol Chem* **252**(11):3617-3625.

Torchia 1982 Torchia DA. Solid state NMR studies of molecular motion in collagen fibrils. *Meth Enzymol* **82**:174-186.

Tunbridge 1952 Tunbridge RE, Tattersall RN, Hall DA, Astbury WT, Reed R. The fibrous structure of normal and abnormal human skin. *Clin Sci* **11**:315-323.

Urban and Bayliss 1989 Urban JPG, Bayliss MT. Regulation of proteoglycan synthesis rate in cartilage *in vitro*: Influence of extracellular ionic composition. *Biochim Biophys Acta* **992**:59-65.

Urban and Maroudas 1979 Urban JPG, Maroudas A: The measurement of fixed charge density in the intervertebral disc. *Biochim Biophys Acta* **586**:166-178.

Veis 1967 Veis A. Intact collagen. In *Treatise on Collagen*, Ramachandran GN, ed. Academic Press, New York, pp. 367-439.

Venn and Maroudas 1977 Venn M, Maroudas A. Chemical composition and swelling of normal and osteoarthrotic femoral head cartilage. I. Chemical composition. *Ann Rheum Dis* **36**:121-129.

von Hippel 1967 von Hippel PH. Structure and stabilization of the collagen molecule in solution. In *Treatise on Collagen*, Ramachandran GN, ed. Academic Press, New York, pp. 253-338.

Wallace 1986 Wallace DG, Condell RA, Donovan JW, Paivinen A, Rhee WM, Wade SB. Multiple denaturational transitions in fibrillar collagen. *Biopolymers* **25**:1875-1893.

Wolff and Balaban 1989 Wolff SD, Balaban RS. Magnetization transfer contrast (MTC) and tissue water proton relaxation *in vivo*. *Mag Res Med* **10**:135-144.

Wolff 1991 Wolff SD, Chesnick S, Frank JA, Lim KO, Balaban RS. Magnetization transfer contrast: MR imaging of the knee. *Radiology* **179**:623-628.

Wu 1991 Wu J-J, Lark MW, Chun LE, Eyre DR. Sites of stromelysin cleavage in collagen types II, IX, X, and XI of cartilage. *J Biol Chem* **266**:5625-5628.

There it is then.